

FUNCTIONAL CHARACTERIZATION OF PHLOEM-MOBILE LIPID-BINDING  
PROTEINS FOR SYSTEMIC STRESS RESPONSE

By

Amanda Marie Koenig

A DISSERTATION

Submitted to  
Michigan State University  
in partial fulfillment of the requirements  
for the degree of

Genetics – Doctor of Philosophy  
Molecular Plant Sciences – Dual Major

2022

## ABSTRACT

Plant resiliency and survival hinges on rapid, efficient, and synchronized responses to stress and expedient, coordinated execution of developmental processes. The environmental cues are often simultaneous and compounding. The plant must perceive and differentiate these stimuli and subsequently manifest an appropriate and integrated response. Therefore, communication across the whole plant is essential. The vascular system not only transports nutrients, water, and energy, but also serves as an information highway to traffic macromolecular signals. The phloem mobilizes nucleic acids, proteins, hormones, and lipophilic compounds from source to sink for targeted systemic signaling. A handful of phloem-mobile nucleic acids and proteins have been unambiguously linked to stress response and development: for example, *BEL* transcripts for tuber development and Flowering Locus T (FT) as a central regulator of the transition to flowering. However, given the expansive number of macromolecules identified in phloem sap, their functions in long-distance signaling remains an active area of research. Moreover, the presence of lipids and lipid-binding proteins (LBPs) in the hydrophilic environment of the phloem is an anomalous phenomenon that prompts further investigation. In this dissertation, I have elucidated the role of phloem-mobile lipid binding proteins in lipid-mediated long-distance signaling for abiotic stress response. **First**, I surveyed several small lipid-binding proteins previously identified in the phloem. Annexin 1 (ANN1), Major Latex Protein-like Proteins 43 and 423 (MLP43 and MLP423) and Bet v1 Allergen bind neutral and negatively charged phospholipids and predominantly localize to the periphery of the cell. Their genetic expression profiles differ from one another in response to various abiotic stress factors, indicating that they act in distinct mechanisms.

Further, the expression patterns correlate with those of phospholipases that generate phosphatidic acid, a known regulator of stress response. **Second**, I expand upon the function of Phloem Lipid-Associated Family Protein (PLAFP) in lipid-mediated stress response and signaling. I characterized the phosphatidic acid (PA) binding activity of PLAFP and identified a receptor candidate for the PLAFP-PA signal. PLAFP comprises a single PLAT/LH2 domain, which can act to bind lipids and facilitate protein-protein interaction. Using homology modelling, mutagenesis, and lipid overlay studies, I show that the conserved basic residues Lysine-42 and Arginine-82 and an adjacent tryptophan-enriched hydrophobic groove within PLAFP contribute to PA binding and possible solubilization. Consistent with a predicted function in protein-protein interaction, PLAFP co-localizes with receptor-like kinase Vascular Highway 1 Kinase (VH1K) *in vivo*. RNA-Sequencing discovered several dozen differentially expressed genes when *PLAFP* expression levels are altered, which suggests PLAFP elicits downstream transcriptional changes. **Finally**, I developed a novel optogenetics-based method for the investigation of long-distance translocation in plants, which revealed PLAFP is systematically transported. Taken together, PLAFP participates as a phloem-mobile signal in a tightly regulated and specific mechanism for PA-mediated systemic stress response. This represents an emerging field of research to understand the role of lipids in long-distance signaling both as components of the membrane and as signals themselves.

## ACKNOWLEDGEMENTS

I would first like to thank my research advisor, Dr. Susanne Hoffmann-Benning, for her support and for creating opportunities for me to learn and grow as a scientist, as a professional, and as a leader. I had the privilege of working and collaborating with many excellent researchers during my PhD work. Thank you to all the members of the Groth and Zurbruggen Laboratories at Heinrich Heine University in Düsseldorf for sharing their expertise and collegiality, in particular Dr. Alexander Hofmann and Dr. Kun Tang who dedicated their time and talents to tackle challenging research questions with me. I'd like to thank my committee members—Dr. Hideki Takahashi, Dr. Beronda Montgomery, and Dr. Rebecca Grumet—for their encouragement and guidance, and Dr. Cathy Ernst and Alaina Burghardt, without whom I would have never had the resources and footing to succeed. I am endlessly grateful to my Genetics and Genome Sciences student cohort for their advice and, above all, their companionship in celebrating successes and lamenting struggles together. Most especially, I want to thank Dr. Katerina Lay-Pruitt, Dr. Ryan Corbett, Dr. Scott Funkhouser, Rebecca Shay, Dr. Reid Blanchett, and Dr. Anastasiya Lavell for their unyielding friendship. It is an absolute honor to be surrounded by such compassion and brilliance. I want to thank my family—my parents and my sister—for getting me here today and sticking with me every step of the way. I want to thank my partner, Max, for loving me through some of my most stressful moments. Lastly, I'd like to remember my sweet kitty Juniper, who was my little cuddly comfort until his last day.

This research was generously funded by NSF-EAGER 1841251, USDA NIMSS MICL 04147 and 04237, and USDA NIFA National Needs Training grant 2015-38420-23697.

## TABLE OF CONTENTS

LIST OF ABBREVIATIONS .....	vii
CHAPTER 1. Introduction: Unraveling the intersection of lipids and systemic signaling in plant development and stress response .....	1
Abstract.....	2
Introduction .....	3
Fundamentals of the Plant Vascular System .....	4
The Vascular System as a Conduit for Systemic Signaling.....	6
Overview of Plant Lipids as Intracellular Signals.....	9
Phosphatidic Acid as a Key Component of Intracellular Signaling .....	10
Hormones, Lipids, and Lipid-Binding Proteins in Systemic Signaling .....	16
Project Goals and Significance .....	19
CHAPTER 2. Assessment of Phloem-Localized Lipid Binding Proteins as Mobile Signals for Stress Response .....	21
Abstract.....	22
Introduction .....	23
Methods .....	26
Results .....	31
Discussion.....	38
CHAPTER 3. PLAFP comprises a PLAT/LH2 domain, which acts both in lipid binding and protein-protein interaction, to affect overall gene expression .....	42
Abstract.....	43
Introduction .....	44
Methods .....	47
Results .....	51
Discussion.....	62
CHAPTER 4. A novel optogenetics approach reveals systemic transport of PLAFP ....	66
Abstract.....	67
Introduction .....	68
Methods .....	71
Results .....	76
Discussion.....	87
CHAPTER 5. Conclusions and Future Directions .....	90
Summary.....	91
Future Work .....	94
Conclusion .....	97
REFERENCES.....	98

Appendix A. Supplemental Data for Chapter 2.....	125
Appendix B. Supplemental Data for Chapter 3.....	130
Appendix C. Supplemental Data for Chapter 4 .....	155

## LIST OF ABBREVIATIONS

AAPs Amino Acid Permeases

ABA abscisic acid

ABF ABRE Binding Factors

ABI1 ABA Insensitive 1

ABRE ABA-Response Element

ACBP Acyl-CoA Binding Protein

AHL4 AT Hook Motif Nuclear Localized Protein 4

ANN1 Annexin 1

ATC Centroradialis

AZA azelaic acid

AZI1 AZA Induced 1

BEL BEL1-Related Homeotic Protein

BRI1 Brassinosteroid Insensitive 1

BSA Bovine Serum Albumin

CC companion cells

CCA1 Circadian Clock Associated 1

CEPD C-Terminally Encoded Peptide Downstream

CEPDL2 CEPD-like 2

CK cytokinin

CLE25 Clavata3/Embryo-Surrounding Region-Related 25

CTR1 Constitutive Triple Response 1

CYP1 Cyclophilin 1

DAG diacylglycerol  
DEG differentially expressed genes  
DGK Diacylglycerol Kinase  
DHA dehydroabietinal  
DIR1 Defective in Induced Resistance 1  
DOPA dioleoyl phosphatidic acid  
DOPS dioleoyl phosphatidylserine  
DPPA dipalmitoyl phosphatidic acid  
DPPG dipalmitoyl phosphatidylglycerol  
DPPS dipalmitoyl phosphatidylserine  
EARLI1 Early Arabidopsis Aluminum Induced 1  
ELIP1 Early Light Inducible Protein 1  
ETR1 Ethylene Response 1  
FAC Florigen Activation Complex  
FC fold-change  
FT Flowering Locus T  
G3P glycerol-3-phosphate  
GFP Green Fluorescent Protein  
GOI Gene of Interest  
HRP Horseradish Peroxidase  
HY5 Elongated Hypocotyl 5  
IPTG isopropyl  $\beta$ -D-1-thiogalactopyranoside  
JA jasmonic acid

LBP Lipid Binding Proteins

LHY Late Elongated Hypocotyl

LRR leucine-rich repeat

MAP3K MAP kinase kinase kinase

MES 2-morpholinoethanesulfonic acid

miRNA microRNA

MLP Major Latex Protein-like Protein

MPK6 Mitogen Activated Protein (MAP) Kinase 6

NCED3 Nine-Cis-Epoxycarotenoid Dioxygenase 3

ncRNA non-coding RNA

NPR1 Nonexpressor of Pathogenesis Related 1

OPDA 12-oxo-phytodienoic acid

PA phosphatidic acid

PBS Phosphate-buffered saline

PC phosphatidylcholine

PD plasmodesmata

PDI10 Protein Disulfide Isomerase 10

PE phosphatidylethanolamine

PEG polyethylene glycol

PhyB Phytochrome B

PI phosphatidyl inositol

PID Pinoid

PIF6 Phytochrome-Interacting Factor 6

PIN Pin-Formed

PIP phosphatidylinositol phosphate

PLAFP Phloem Lipid Associated Family Protein

PLAT/LH2 polycystin-1, lipoxygenase, alpha toxin/lipoxygenase homology

PLC Phospholipase C

PLD $\alpha$ 1. Phospholipase D $\alpha$ 1

PLD $\delta$  Phospholipase D $\delta$

PMSF phenylmethylsulfonyl fluoride

POTH1 Potato Homeobox 1

PP2A Protein Phosphatase 2A

PULSE Plant Usable Light-Switch Elements

PYR/PYL/RCAR Pyrabactin Resistance/PYR-Like/Regulatory Components of ABA Receptor

RT-qPCR Reverse Transcription-quantitative Polymerase Chain Reaction

SAM shoot apical meristem

SAR systemic acquired resistance

SE sieve elements

SFT Single Flower Truss

siRNA small interfering RNA

SnRK2 SNF1-Related Kinase 2

SOS1 Salt Overly Sensitive 1

SP6A Self-Pruning 6A

START StAR-related lipid transfer

SUTs Sucrose Transporters

SWEETs Sugar Will Eventually be Exported Transporters

TAG triacylglycerol

TBST Tris-buffered saline Tween-20

TF transcription factor

TGD4 Trigalactosyldiacylglycerol 4

TIN1 Tunicamycin Induced 1

TMT1 Tonoplast Monosaccharide Transporter 1

TOC1 Timing of CAB Expression 1

TZF5 Tandem CCCH Zinc Finger Protein 5

UMAMITs Usually Multiple Acids Move In and Out Transporters

VH1K Vascular Highway 1 Kinase

VIK VH1K-Interacting Kinase,

## **CHAPTER 1.**

### **Introduction: Unraveling the intersection of lipids and systemic signaling in plant development and stress response.**

This chapter has been adapted from the following published review articles:

Koenig, A.M. and S. Hoffmann-Benning, (2020) “The interplay of phloem-mobile signals in plant development and stress response.” *Biosci Rep.* **40**(10).

<https://doi.org/10.1042/BSR20193329>

A.M. Koenig, C. Benning, S. Hoffmann-Benning (2020) Chapter 2: “Lipid trafficking and signaling in plants” In: *Lipid Signaling and Metabolism* (ISBN: 978-0-12-819404-1); Ntambi ed.; Elsevier <https://doi.org/10.1016/B978-0-12-819404-1.00002-6>

## **Abstract**

Plants integrate a variety of biotic and abiotic factors for optimal growth in their given environment. While some of these responses are local, others occur distally. Hence, communication of signals perceived in one organ to a second, distal part of the plant requires an intricate signaling system. The coordination of plant development and stress response involves the long-distance transport of signaling molecules. The vascular system acts as an information highway to transmit not only water, energy, and nutrients but also macromolecules as signals throughout the entire organism. The phloem facilitates the integration of environmental cues and the subsequent response by translocating nucleic acids, proteins, hormones, and lipids. The roles of lipids in intracellular signaling include the maintenance of membrane integrity, recruitment and sequestration of proteins, facilitation of protein-protein and protein-DNA interactions, as well as the direct activation and repression of transcription and enzyme activity. More specifically, phosphatidic acid, in particular, has emerged as a key regulator of biological processes like cold, salt, and drought tolerance; ethylene signaling; and pathogen response. Furthermore, lipid binding proteins and lipophilic compounds, including phosphatidic acid, have been identified in phloem sap, suggestive of a function in systemic signaling. The interplay of lipids and lipid-protein complexes during long-distance signaling can precisely communicate the environmental cue and further confer specificity and efficiency for a targeted and coordinated response.

## **Introduction**

Plant resilience and stress tolerance are critical to global food security. The climate is becoming increasingly severe, resulting in strains on resources and harsher growing conditions for plants. Because plants are quite literally rooted in place, their survival hinges on their ability to efficiently adjust physiological and developmental processes to endure the surrounding environmental challenges. At any given moment, plants are experiencing a variety of external stimuli that communicate the status of nutrient and water availability, temperature, light intensity, pathogen attack and more. Often, these stimuli occur simultaneously, exacerbating stresses further and compounding in an interwoven onslaught of stimuli that the plant must perceive, process, and integrate into a rapid, appropriate, and coordinated response.

Environmental cues are sensed locally in different tissues and organs throughout the plant. Broadly, for example, roots surveil water and nutrients in the soil; mature leaves detect light status and photoperiod; various tissues are attacked by insect herbivory, fungal invasion, and bacterial infection; stomata monitor gas exchange. Further, each stimulus is processed and transformed into signals to initiate biological responses. While responses to stresses and developmental cues often manifest locally as intracellular mechanisms, the systemic integration and coordination across the whole plant is critical for effective and streamlined responses. Many macromolecules, such as nucleic acids, proteins, hormones, and lipids, have been implicated in long-distance translocation as mobile signals. In this chapter, I will discuss the roles of lipids, with an emphasis on phosphatidic acid, in stress signaling and the implications of long-distance signaling, including lipid-mediated systemic signaling, on plant development and stress response.

## **Fundamentals of the Plant Vascular System**

The vascular system is essential for systemic transport of energy-rich molecules, building blocks, and nutrients in the plant. It comprises the xylem for unidirectional translocation of water and minerals from roots to shoots and the phloem, whose predominant role is the transport of photoassimilates from source to sink tissues. The xylem pulls water and minerals up through xylem vessels, driven by the water potential gradient between the soil and the atmosphere surrounding the plant. The phloem consists of three main components: the companion cells, the sieve elements, and parenchyma cells. The channel for phloem transport, the sieve elements (SE), are enucleated cells separated by porous sieve plates, through which long distance transport occurs by bulk flow according to Munch's Pressure-Flow Hypothesis [1]. The Pressure-Flow Hypothesis attributes phloem transport to the difference in osmotic pressure between source tissues with high sugar concentration and sink tissues with low concentration of sugars. Source tissues are photosynthetically active, while sink tissues are developing tissues or photosynthetically inactive, and therefore require photoassimilates to be delivered for energy. Importantly, because the phloem stream is driven by this concentration differential, the phloem transports macromolecules to both above and below ground tissue, which makes it an ideal conduit for systemic signaling.

While the sieve elements have few organelles and are not thought to perform transcription or translation, the neighboring companion cells (CC) are fully functional cells that load and unload photoassimilates and other macromolecules into and out of the SE. The loading of photoassimilates can follow several paths, namely, active apoplastic loading facilitated by SWEETs (Sugar Will Eventually be Exported Transporters) and

SUTs (Sucrose Transporters); passive symplastic loading through plasmodesmata between mesophyll, companion cells, and the sieve element; or polymer trapping dependent on the generation of a concentration gradient via the synthesis of raffinose and stachyose from sucrose [2-5]. Unloading occurs either symplastically through specific plasmodesmata [6, 7] or apoplastically mediated by SWEETs [8]. Beyond sugars, the phloem remobilizes carbon and nitrogen from source tissues to sink tissues, often in the form of amino acids [9, 10]. These processes occur, for example, during leaf senescence but also as a consequence of *de novo* amino acid synthesis [10]. Amino acids are thought to be loaded into the phloem via the apoplastic mechanism, regulated by transporters like Usually Multiple Acids Move In and Out Transporters (UMAMITs) for export out of leaf mesophyll cells and Amino Acid Permeases (AAPs) for import into the phloem. Symplastic mechanisms seem to predominate during unloading, with amino acids passing through plasmodesmata from SE into sink tissues [9]. As a result, the phloem is critical for the reallocation of carbon and nitrogen assimilates for the systemic distribution of energy and nutrients in the plant.

Another critical function of the phloem is long-distance signaling, which is necessary for the systemic coordination of plant development under normal conditions as well as during abiotic stress. It is also essential for the response to biotic factors, such as viruses, mutualistic and pathogenic microbiota, fungi, herbivores, and other pathogens such as nematodes and sucking/piercing insects. Our knowledge of phloem anatomy, development, and function was thoroughly reviewed in 2013 [11]. Here I will focus specifically on the review and update of various phloem mobile macromolecules and their roles as systemic signals.

## **The Vascular System as a Conduit for Systemic Signaling**

In addition to photoassimilates, other macromolecules, including nucleic acids, peptides, proteins, hormones, and lipids have been identified in the phloem [12, 13]. Their presence elevates the function of the phloem from simple energy transport to an integral signaling conduit.

Nucleic acids, more specifically RNA species, are among some of the most well-studied phloem-mobile signaling molecules [14-16]. Representatives of many types of RNA, such as mRNA, microRNA (miRNA), small interfering RNA (siRNA), and other non-coding RNA (ncRNA) have been identified in the phloem of many plant species [17-25]. While the existence of mRNA and ncRNA in the vasculature hints at their mobility and possible role in plant development, identification alone does not conclusively prove movement or physiological function. Using predominantly grafting approaches, numerous studies provide evidence for phloem-mobile mRNA [26, 27] and ncRNA [28-31]. Furthermore, data suggest environmental conditions affect transcript mobility independent of changes in gene expression, implicating mobile transcripts as stress response signals [27, 32]. While some studies suggest mRNA mobility can be ascribed to transcript abundance and stability [33], others have identified selective mechanisms including specific sequence motifs, secondary structures, and RNA-binding proteins, that facilitate systemic transport of nucleic acids [34-39]. Regulated loading, translocation, and unloading affirm that phloem-mobile RNA species show directionality, target specificity, and stress-responsiveness indicative of systemic signals. Numerous biological processes are directly regulated by phloem-mobile mRNA and miRNA including potato tuber formation [40-47], phosphate starvation [48-53], and nodulation [54-56].

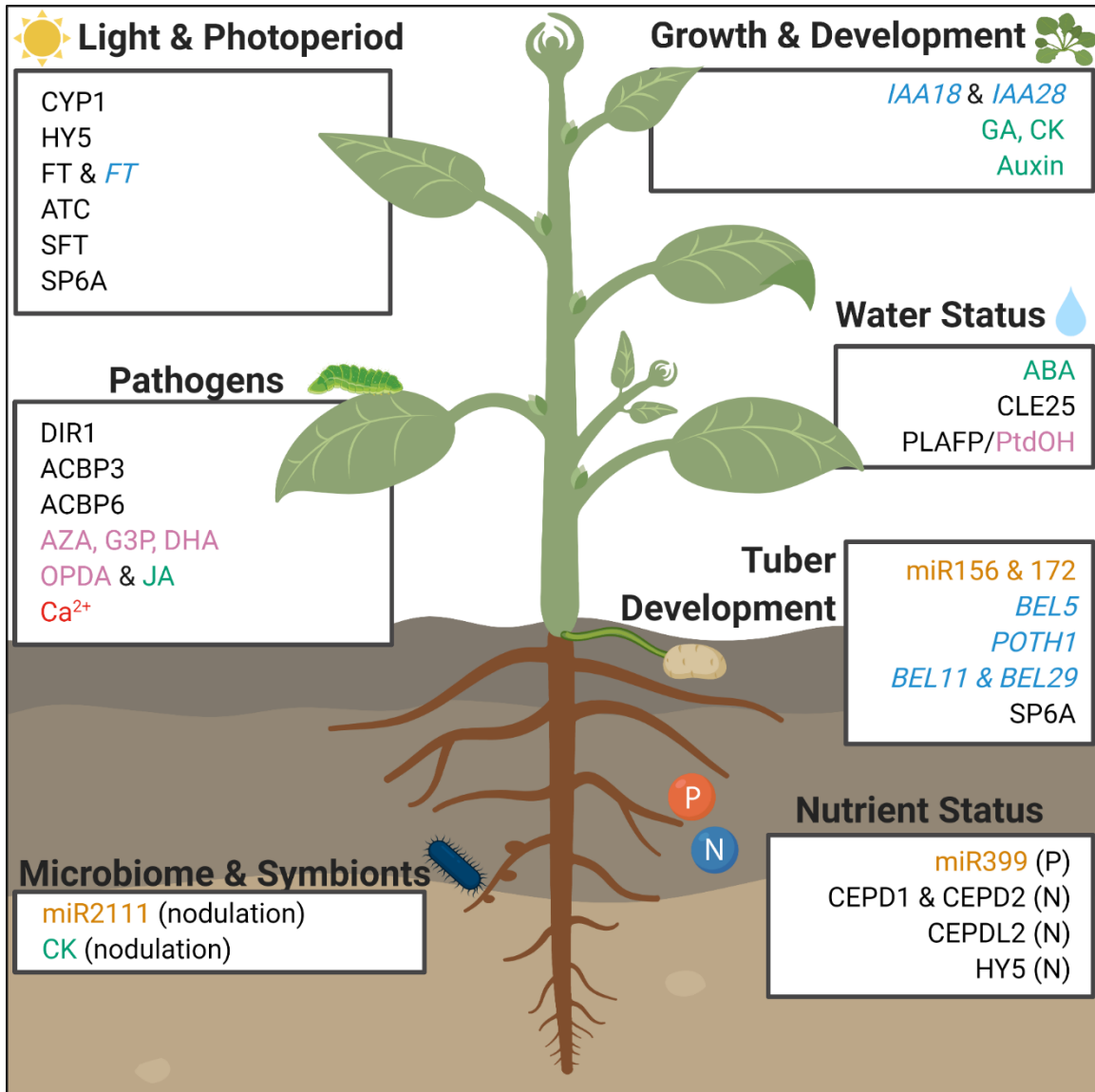


**Figure 1.1 Overview of Long-Distance Signaling in the Phloem.** Mobile signals involved in plant development and stress response are listed: proteins (all-caps; black), lipophilic compounds (pink), ions (red), microRNA (miR, orange), mRNA (italicized; light blue), hormones (green). Figure from Koenig and Hoffmann-Benning, *BioScience Reports* (2020).

Cyclophilin 1, CYP1; Elongated Hypocotyl 5, HY5; Flowering Locus T, FT; Centroradialis, ATC; Single Flower Truss, SFT; Self-Pruning 6A, SP6A; Defective in Induced Resistance 1, DIR1; Acyl-CoA Binding Protein, ACBP; azelaic acid, AZA, glycerol-3-Phosphate, G3P; dehydroabietinal, DHA; 12-oxo-phytodienoic acid, OPDA; Jasmonic acid, JA; cytokinin, CK; abscisic acid, ABA; Clavata3/Embryo-Surrounding Region-Related 25, CLE25; Phloem Lipid Associated Family Protein, PLAFP; BEL1-Related Homeotic Protein, BEL; Potato Homeobox 1, POTH1; C-Terminally Encoded Peptide Downstream 1/2, CEPD1/2; CEPD-like 2, CEPDL2 Created with [BioRender.com](https://www.biorender.com).

Proteins, hundreds up to thousands, have been identified in the phloem, despite little evidence for translation in the sieve tube, which suggests that peptides and proteins are loaded for transport as possible systemic signals [24, 57-61]. It has been debated whether these non-sugar macromolecules diffuse into the phloem by accident [62-64] or enter through targeted transport [65, 66]. At least in some cases these macromolecules have been shown to be carefully regulated, intentionally transported, and essential for successful plant development. Phloem-localized peptides and proteins have been implicated as signals in many processes, including nitrogen acquisition [67-69], systemic acquired resistance (SAR) and biotic stress [70, 71], water stress [72, 73], and flowering [74-87]. An overview of macromolecules involved in systemic signaling is shown in Figure 1.1 and was published in Koenig and Hoffmann-Benning (2020) [88].

The quintessential phloem-mobile signal is the florigen FLOWERING LOCUS T (FT). The transition from vegetative to generative growth in plants is controlled by photoperiod, which is sensed in the leaves. In Arabidopsis, long day conditions and circadian clock components promote the transcription of *CONSTANS* in the leaf vasculature, which then interacts with the *FT* promoter to initiate its expression in the leaf [89]. Several studies have conclusively shown that FT protein or its homologue in other plants is mobile and central to the transition to reproductive growth [74-87]. Upon arrival at the shoot apical meristem (SAM), it interacts with the bZIP transcription factor FD to initiate expression of genes necessary for floral development [90]. Interestingly, specific Phosphatidylcholine (PC) molecular species exhibit diurnal oscillations in the SAM; FT preferentially binds the species that predominates during the day. [91]. A recent structural characterization of Arabidopsis FT suggests PC as a mediating ligand to facilitate

FT/FD/14-3-3 protein interaction to form the Florigen Activation Complex (FAC) and its binding to DNA to promote flowering [92]. Furthermore, Phosphatidylglycerol (PG) sequesters FT to the membrane at low temperatures, conferring temperature-dependent regulation of FT phloem loading and mobility [93] As highlighted by this example, not only genes and proteins but also lipids play an integral role in intracellular signaling as part of local and systemic mechanisms. We propose lipids may mediate systemic signaling as mobile signals themselves.

### **Overview of Plant Lipids as Intracellular Signals**

Stress and developmental signals, like systemic acquired resistance, abscisic acid (ABA)-regulated drought response, and flowering, involve not only changes to gene expression and protein activation or the translocation of transcripts and peptides, but also the modulation of lipids in membranes and as anchors, ligands, and signals. Modifications to membrane composition and architecture are often involved in responses to environmental challenges, such as during phosphate deprivation or freezing [94-97]. Moreover, lipids and lipophilic compounds like phosphoinositides, oxylipins, and phosphatidic acid are implicated in a variety of signaling pathways for stress response and development.

To cope with environmental factors, plants employ a variety of lipophilic signaling molecules. Some of these can be complex lipids such as phospholipids, predominantly phosphatidylinositols (PIs) and phosphatidic acid (PA), ceramides and sphingolipids, and diacylglycerol (DAG); others include small lipophilic molecules such as many plant hormones or pathogen-response molecules like the dicarboxylic acid azelaic acid (for an in-depth review see [98]). Several of these lipids including PA, lyso-PA, DAG, and PIs

can function as second messengers within plant cells. Ceramides and sphingolipids are an integral structural component of plant membranes, particularly for the formation of lipid raft microdomains. Moreover, they participate in developmental and stress signaling such as programmed cell death, temperature stress, and salicylic acid signaling for biotic stress defense. Sphingolipids contribute to these mechanisms by influencing membrane fluidity and forming microdomains for signal recruitment. They are involved in stress perception and serve as signaling compounds [99]. DAG has proven to be an important signaling lipid in animals through its interaction with protein kinases. Although fluctuations in DAG levels have been observed in correlation with developmental and environmental responses in plants, protein targets for DAG in plants have yet to be uncovered or characterized. Rather, these fluctuations in DAG levels could be indicative of PA production and turnover, as PA serves as a pivotal lipid signal in plants [100].

### **Phosphatidic Acid as a Key Component of Intracellular Signaling**

Although understudied compared to similar mechanisms in animals, plant lipids are necessary for the function of transcription factors (TFs), activation of receptors, and interaction with other signaling components [101-106]. Several examples of lipid interaction with TFs have recently been published in plants: phospholipid-TF complexes play roles in flowering [91, 92], the circadian clock [107], nuclear localization [108], and lipid metabolism [109].

PA is emerging as a central regulatory lipid in plant signaling. It acts directly by mediating plant responses to both biotic and abiotic stressors but also indirectly by being the central precursor for other signaling lipids such as PIs and DAG. In this role, it influences plant development and local and systemic stress responses. It executes this

function directly through imposing changes in membrane curvature, or indirectly by binding of receptor proteins in signaling cascades, and through interaction with transcription factors. PA is generated rapidly and transiently in response to environmental cues. Further, the expression and activity of PA-generating enzymes is often promoted by hormones and stress cues.

Various stresses activate different phospholipases which results in the production of distinct PA pools from different origins, thereby supplying PA as a lipid mediator in stress-specific mechanisms [110-117]. For example, Phospholipase D $\alpha$ 1 (PLD $\alpha$ 1) and Phospholipase D $\delta$  (PLD $\delta$ ) are two isoforms of PLD that mediate the production of PA in response to drought/ABA-mediated pathways while the Phospholipase C/DAG Kinase (PLC/DGK) pathway is used in cold response [118-120]. An overview of phospholipase-derived PA mechanisms is shown in Figure 1.2 [113, 121, 122]. Often the PA species generated has an acyl composition specific for a certain stress and, thereby conveys binding specificity with interacting proteins. Phosphatidic acid plays a regulatory role by modifying membrane structure and curvature, sequestering and/or tethering proteins to the membrane, and as a secondary messenger, as well as protein-lipid interactions that impact signaling directly.

X= choline, ethanolamine, serine, glycerol, inositol, inositol phosphates

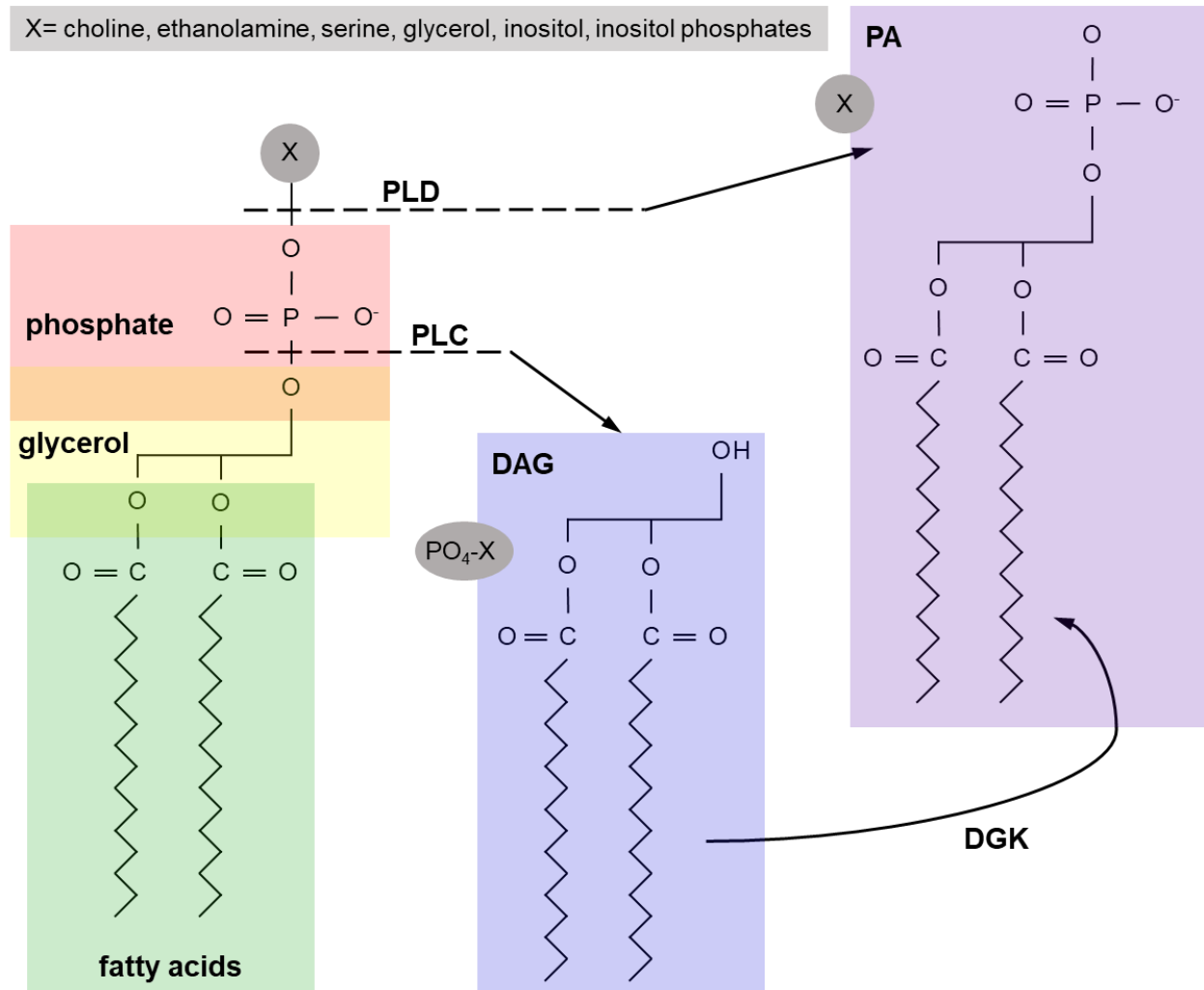


**Figure 1.2 Schematic of Phospholipase-derived Phosphatidic Acid.** Phospholipases cleave phospholipids to generate phosphatidic acid (PA, purple). Members of the Phospholipase D (PLD) family produce PA directly by removing various head groups (gray). Phospholipase Cs (PLCs) cut off the phosphate (red) to make diacylglycerol (DAG, blue). Diacylglycerol kinases (DGKs) can then phosphorylate DAG to yield PA. The length and saturation of fatty acid acyl chains (green) can influence phospholipase specificity and downstream protein-lipid interactions. Mechanisms involving Phospholipase As, Lyso-PA Acyl Transferases (LPAATs) and Lyso-PA intermediates can also generate PA (not shown). This figure was adapted from [113, 121-122].

Cold stress encompasses both chilling and freezing conditions, two distinct stresses that elicit different plant responses. Cold stress can severely impede plant growth by disrupting normal cell structure and function. For example, chilling stress disrupts normal water uptake, and freezing stress causes cell dehydration and ruptures the plasma membrane as a result of ice accumulation in the intercellular space [123]. PA participates in both chilling and freezing tolerance, though it is generated through distinct pathways depending on the temperature stress [118]. Contrary to its role in other environmental signaling, where it serves as a signal or membrane tether, in cold responses it functions by modifying the physical properties of membranes [124, 125]. The molecular shape of PA can influence lipid phases and membrane curvature in response to changes in physiological conditions [126]. Moreover, shifts in the membrane's biophysical properties affect protein binding and PA's accessibility to its protein targets [127]. Overall, PA may adjust the stability of the membrane in response to the cell's physiological status during cold stress, rather than or, perhaps in addition to, participating as a signal molecule.

Drought is a complex stress that causes a myriad of connected but distinct physiological pressures throughout the plant that require not only local but also systemic responses. Briefly, on the local scale, under water deprivation, the phytohormone ABA accumulates resultant of increased expression of the rate-limiting ABA synthesis enzyme Nine-Cis-Epoxycarotenoid Dioxygenase 3 (NCED3) [128, 129]. ABA is sensed by its receptor Pyrabactin Resistance (PYR)/PYR-Like (PYL)/Regulatory Components of ABA Receptor (RCAR), and the protein phosphatase 2C enzyme ABA Insensitive 1 (ABI1) is sequestered, in part, by interacting with Phospholipase D $\alpha$ 1-derived PA [130]. With ABI1

no longer available to dephosphorylate and repress SNF1-Related Kinase 2 (SnRK2) activity, SnRK2s can then phosphorylate ABA-Response Element (ABRE) Binding/ABRE Binding Factors (AREB/ABF) transcription factors, which initiate the expression of drought-responsive genes by interacting with ABA response elements in promoter regions. This production of an array of drought-responsive genes and proteins ultimately causes shifts in plant anatomy, like stomatal closure and modulated root morphology, for heightened drought tolerance [131]. Here, PA contributes to signaling by interacting with proteins in a sequestration-type mechanism. However, PA also actively participates in signaling through protein-lipid interactions that influence protein activation, localization, and DNA-binding. During seed germination, AT Hook Motif Nuclear Localized Protein 4 (AHL4) binds PA, which causes inhibition of DNA-binding and promotes triacylglycerol (TAG) degradation [109]. Phospholipids mediate transcriptional regulation by direct interaction with proteins and transcription factors, whether it be activation of expression, as is the case with PC during flowering discussed here previously, or repression, exhibited by AHL4-PA during seedling establishment [91, 92, 109].

During salt stress, PLD $\alpha$ 1-derived PA is a proposed activator of MAP kinase MPK6, which phosphorylates Salt Overly Sensitive 1 (SOS1), a Na<sup>+</sup>/H<sup>+</sup> antiporter localized in the plasma membrane [132]. SOS1, when activated, maintains ionic homeostasis by exporting Na<sup>+</sup> out of the cytoplasm and into the apoplast [133]. In another salt stress mechanism, PA facilitates Pin-Formed (PIN) and Pinoid (PID) localization and activation as well as regulates Protein Phosphatase 2A (PP2A) activity, resulting in modulation of salt-responsive auxin transport and auxin-dependent gravitropism [134, 135]. Deactivation of the negative regulator Constitutive Triple Response 1 (CTR1) during

ethylene signaling involves the interaction between ethylene-bound receptors and CTR1. Testerink *et al.* (2007) showed that CTR1 binds PA, which inhibits CTR1 kinase activity, thereby promoting ethylene signaling [136, 137]. Moreover, PA seems to interfere with CTR1-Ethylene Response 1 (ETR1) interaction. PA also binds circadian clock proteins Late Elongated Hypocotyl (LHY) and Circadian Clock Associated 1 (CCA1) to inhibit their DNA-binding activity and prevent the suppression of *Timing of CAB Expression 1 (TOC1)* expression, a key circadian rhythm regulator in plants [107].

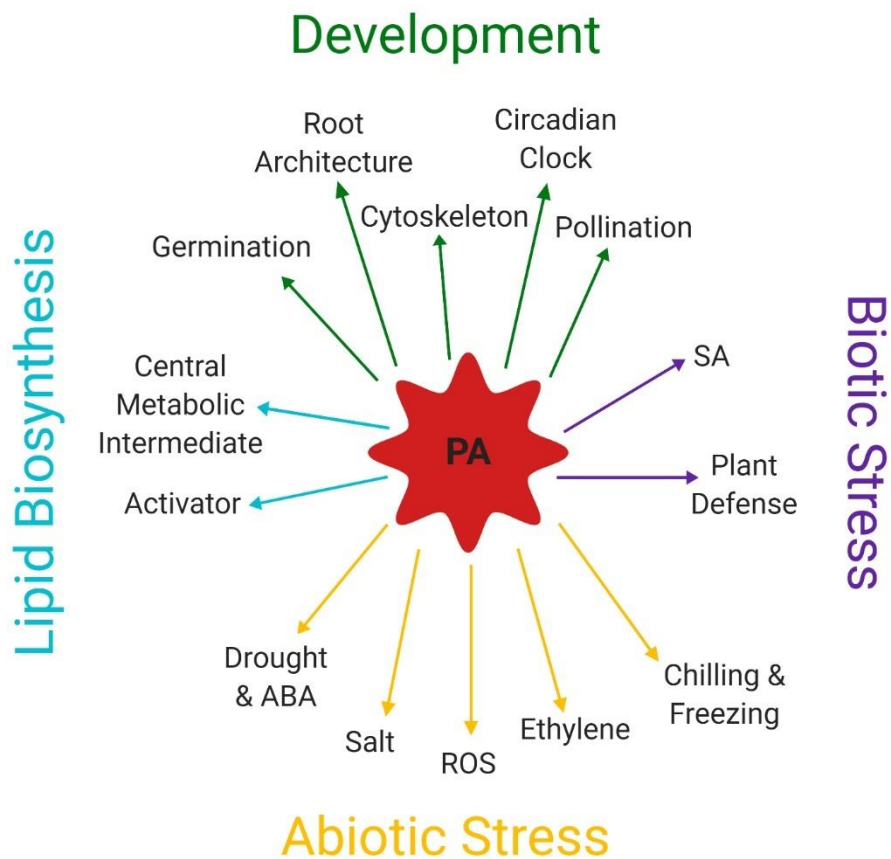


**Figure 1.3 Summary of Phosphatidic Acid Signals in Plants.** Phosphatidic acid (PA) is generated by several, often stress-dependent pathways, and it functions in various capacities in many developmental, environmental, and metabolic processes in plants. Figure from Koenig *et al.* (2020) *Lipid Signaling and Metabolism*. Created with [Biorender.com](https://biorender.com). SA, salicylic acid signaling; ROS, reactive oxygen species; ABA, abscisic acid

In pathogen defense mechanisms, PLD activity and PA accumulation impact the translocation of Nonexpressor of Pathogenesis Related 1 (NPR1) from the cytosol to the nucleus during salicylic acid signaling for biotic stress response [138, 139]. Therefore, PA acts as a central regulator with roles not only within the membrane as a structural component and anchor but also in direct interaction with signaling proteins to influence activation, localization, inhibition, and DNA-binding (Figure 1.3). Beyond intracellular action, PA may also participate in systemic signaling in conjunction with a phloem-mobile lipid transport protein, which is the focus of this dissertation.

### **Hormones, Lipids, and Lipid-Binding Proteins in Systemic Signaling**

In addition to nucleic acids and proteins, the phloem has been implicated in the systemic translocation of phytohormones, including auxins, gibberellins, cytokinins (CKs), jasmonic acid (JA), and abscisic acid (ABA) [140-143]. As a conduit for photoassimilates, the phloem is an aqueous, hydrophilic environment, and yet hydrophobic compounds including fatty acids, hormones, and lipids, such as phospholipids like phosphatidic acid, have been identified in the phloem [13, 144, 145]. One group of important systemic signaling lipids are oxylipins, oxygenated polyunsaturated fatty acids that are derived from acyl groups of the galactolipids in the chloroplast membrane. They are important for regulating aspects of plant growth and development as well as the response to pathogens and abiotic stresses [146, 147]. As such, they affect the balance between growth and defense [148].

While some of these hormones and other molecules may act as independent mobile signals or translocate as water-soluble conjugates, lipophilic compounds may need to interact with proteins to facilitate their transport and signaling activity [144, 149,

150]. Protein-associated long-distance lipid transport is a widely accepted mechanism for signaling in animal systems [151-154]. While less studied in plant systems, some roles for plant protein-lipid complexes in systemic signaling echo those in animal systems.

Among the proteins involved in SAR long distance signaling, there are several predicted lipid-interacting proteins, including Defective in Induced Resistance 1 (DIR1), Acyl-CoA Binding Proteins (ACBPs), and a major latex protein-like protein (MLP). In addition, several lipophilic compounds such as dehydroabietinal (DHA), azelaic acid (AZA), and glycerol-3-phosphate (G3P) derivatives have been found to play a role in SAR [13, 155-158]. The accumulation of these proteins in the phloem during SAR suggests a role for lipid-binding proteins in conveying a lipophilic compound as part of the SAR signal. DIR1 is a lipid transfer protein that has been shown to be phloem mobile during SAR and is required for systemic resistance [70, 71]. While DIR1 alone does not induce resistance in distant tissues, it may be required for the transport of other SAR signals like DHA [159]. Additionally, AZA Induced 1 (AZI1) and Early Arabidopsis Aluminum Induced 1 (EARL1) may play a role in the loading and transport of AZA as a mobile SAR signal [160].

Other wound-response genes include acyl-CoA binding proteins *ACBP3* and *ACBP6*. *ACBP6* is expressed in companion cells in response to wounding, and the protein is found in phloem exudates [161]. The same is true for *ACBP3*. Grafting studies indicate that *ACBP3* is phloem mobile and moves from shoots to roots. Furthermore, the absence of *ACBP3* impairs defense response in both locally wounded and distal tissue [162]. ACBPs play a role in maintaining acyl-CoA pools and lipid metabolism. Along these same lines, both *ACBP3* and *ACBP6* affect the fatty acid composition of the phloem, more specifically a group of defense-related fatty acids, the oxylipins such as 12-oxo-

phytodienoic acid (OPDA) and methyl jasmonate [162]. These oxylipins have long been suggested as mobile signals for wounding, pathogenesis, and SAR [163-166]. Jasmonate is involved both locally and distally for the transmission and perception of systemic wounding signals [167]. The jasmonic acid precursor OPDA and its derivatives have been shown to translocate via the phloem from wounded shoots to undamaged root tissue, where these precursors are converted to bioactive JA-Ile for systemic defense response [13, 168].

Systemic signaling for abiotic stress is understudied compared to biotic stress responses like SAR. Nonetheless, hormones, proteins, and peptides in the phloem seem to play an important role in the coordination of systemic abiotic stress response as well. One crucial environmental factor/stress is the availability of water. We can distinguish between different water stresses: too much, too little, or inaccessibility due to high salt/osmotic properties of the soil or freezing temperatures. Whether water stress perception predominates in the roots or the leaves is an active area of research [169]. The drought hormone ABA itself is proposed as a mobile signal and its long-distance transport has been attributed to both the xylem [170-173] and the phloem [174-177], with reports of both root- and shoot-derived ABA pools during water stress [178-180]. Protein-lipid complexes may be involved in drought signaling as well.

The Hoffmann-Benning Lab identified several small putative lipid binding proteins (LBPs) in the phloem and proposed they play a role in long-distance signaling [13, 98, 181]. Phloem Lipid Associated Family Protein (PLAFP) may be involved in drought response and ABA signaling. We found that *PLAFP* is expressed in the vasculature and its expression increases in response to treatment with ABA and drought stress [181].

PLAFP interacts specifically with PA, known to be involved in ABA signaling and detected in phloem exudate [13, 130, 181-184]. Based on these data, we propose the PLAFP-PA complex as a possible phloem-mobile signal for the systemic coordination of drought response [98, 185]. My dissertation focuses on furthering this work by investigating LBPs in the phloem, with an emphasis on PLAFP-PA as a systemic signal.

### **Project Goals and Significance**

Lipid-protein complexes in the phloem represent an emerging field of highly specific and targeted signals for the systemic coordination of development and stress response. In this dissertation, I investigate lipid-mediated long distance signaling mechanisms, with a specific focus on Phloem Lipid-Associated Family Protein (PLAFP) and phosphatidic acid as a novel mobile signal (Figure 1.4). I assessed several putative lipid binding proteins identified in the phloem to determine their expression profiles during abiotic stress, their lipid ligands, and their subcellular localization (Chapter 2). In Chapter 3, I identified a phosphatidic acid binding region in PLAFP comprised of basic amino acid residues, Lysine-42 and Arginine-82, in a predicted flexible loop adjacent to multiple hydrophobic Tryptophan residues. Further, I evaluated Vascular Highway 1 Kinase as a PLAFP receptor candidate and assessed the impact of *PLAFP* expression on downstream gene expression and processes (Chapter 3). Finally, I established a novel optogenetics approach to study long-distance transport and determined that PLAFP moves systemically (Chapter 4). Taken together, PLAFP acts as a phloem-mobile signal in a likely PA-mediated mechanism for systemic coordination of abiotic stress response.

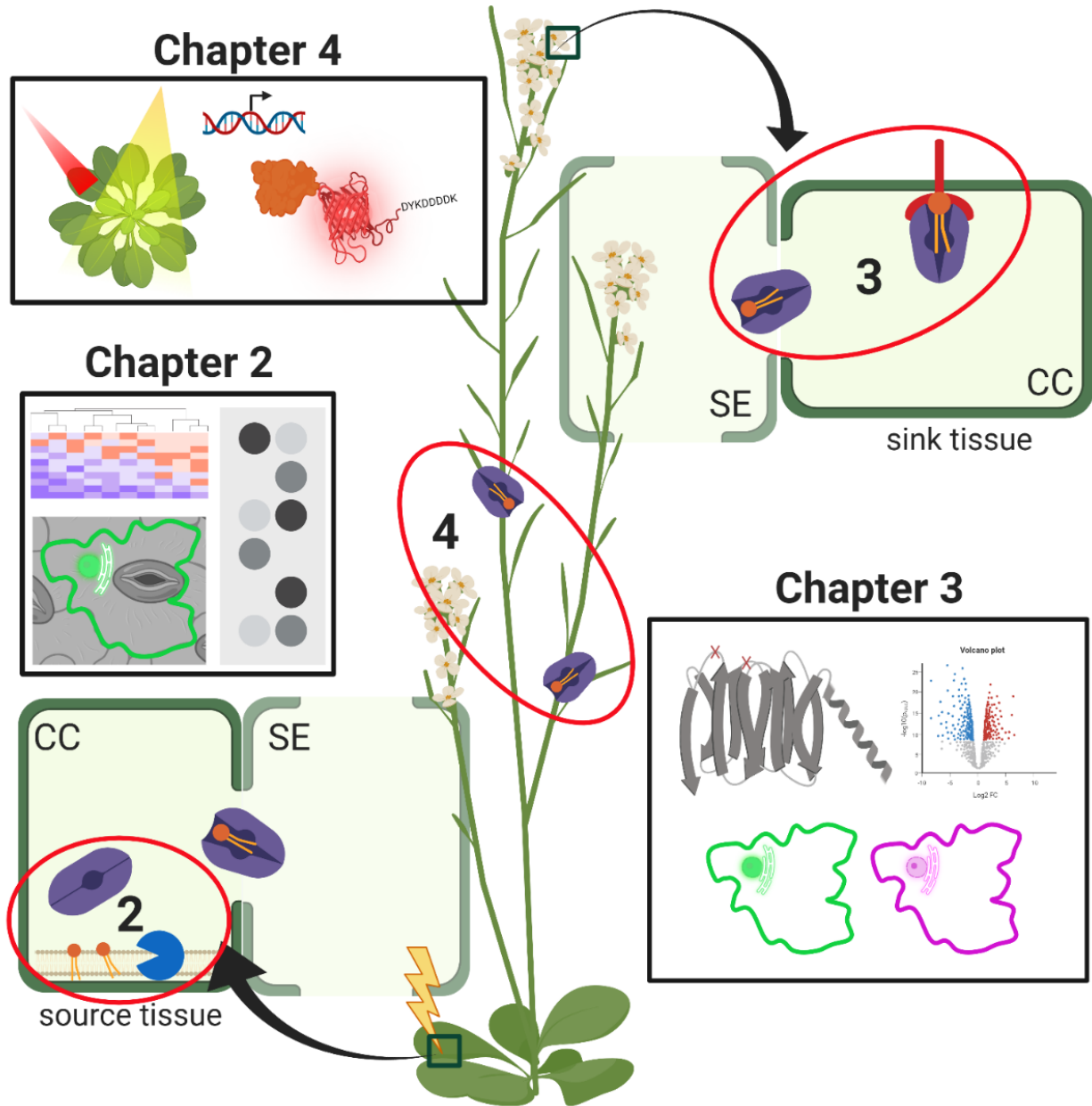


**Figure 1.4 Summary of Dissertation.** Chapter 2 investigates the gene expression, subcellular localization, and lipid-binding of small phloem-localized proteins. Chapter 3 focuses on the PLAT/LH2 protein Phloem Lipid-Associated Family Protein (PLAFFP) and its lipid binding mechanism, protein-protein interaction, and effect on gene expression. In Chapter 4, I develop an optogenetic-based approach to study PLAFFP-RFP-Flag systemic movement.

Created with [BioRender.com](https://www.biorender.com). Adapted from Koenig *et al.* (2020).

## **CHAPTER 2.**

### **Assessment of Phloem-Localized Lipid Binding Proteins as Mobile Signals for Stress Response.**

## Abstract

While the phloem is predominantly responsible for the transport of photosynthates from source to sink tissues, the consistent presence of nucleic acids, proteins, and lipophilic compounds, in addition to the classically transported metabolites, suggests a dynamic role for the phloem as a conduit for systemic signaling. Our lab identified several putative lipid-binding proteins (LBPs) in phloem sap that may facilitate the transport of lipids in the aqueous environment of the phloem. Annexin 1 (ANN1), Major Latex-Like Proteins 43 and 423 (MLP43 and MLP423), Bet v1 Allergen, and Phloem Lipid-Associated Family Protein (PLAFP) were characterized further as lipid-mediated systemic signaling candidates. The lipid-binding activity of these phloem-localized LBPs was confirmed with lipid overlay assays that show binding to neutral and negatively charged phospholipid species. *ANN1* and *PLAFP* expression increase in response to drought-associated stimuli, whereas *MLP43* and *MLP423* expression decreases when treated with the drought hormone abscisic acid and NaCl, respectively. These data suggest the protein candidates respond to related but distinct stresses. These expression profiles were correlated with various stress responsive phospholipases that act to generate the signaling lipid phosphatidic acid (PA). To further assess the function of these putative LBPs, the cellular localization was determined by confocal microscopy: predominantly in the cell periphery, likely cytoplasmic, and occasionally nuclear localization. Overall, this chapter further elucidated the functions of lipid-associated proteins found in the phloem and highlighted promising candidates for lipid-mediated long-distance signaling mechanisms.

## Introduction

Plant resiliency and survival hinges on rapid, efficient, and targeted responses to a myriad of stresses and environmental challenges, while simultaneously maintaining development, growth, and reproduction. These processes involve the perception of external cues and stimuli, and subsequent integration and transmission of distinct signals for stress and developmental responses. To communicate these signals quickly and systemically, plants transport macromolecules long distance via their vascular system. The xylem and the phloem are major components of the plant vascular system. While the xylem transports water and minerals from roots to shoots, the phloem is predominantly responsible for the bidirectional transport of photosynthates from energy-source tissues to energy sinks like roots, flowers, and developing leaves. Moreover, the phloem is a highly dynamic tissue that acts as an information highway, delivering nucleic acids, proteins, hormones, and lipids from local to distal tissues.

Researchers have identified thousands of nucleic acids, proteins, and other compounds in phloem exudates in many plant species [12, 13, 66]. Furthermore, studies have demonstrated that these molecules are purposely translocated to distal tissues to initiate signaling for development and stress response [14, 66, 88]. Several systemic signaling mechanisms for development, nutrient status, and stress response are well-characterized [88]. Tuber formation, for example, uses systemic signals by circadian-related proteins and nucleic acids to coordinate above-ground cues with below ground tuber development [186]. The transition from vegetative to reproductive growth largely depends on the florigen FLOWERING LOCUS T (FT), which is translocated in the phloem from photoperiod-sensing leaf tissue to the shoot apical meristem and triggers flowering

[75]. Systemic acquired resistance involves multiple hormones, proteins, and lipophilic compounds as the proposed phloem-mobile signals for the response to pathogen infection [187]. The interplay among these mobile compounds and other signaling actors both up- and downstream of their transport is essential for effective development and stress response. The roles of these phloem-mobile players are summarized in a review Koenig and Hoffmann-Benning (2020) [88].

Protein-lipid interactions are critical for the direct regulation of stress and developmental signaling mechanisms, both locally and distally. Often, the role of lipids in signaling involves shifts in membrane composition, accumulation of stress responsive species, and recruitment of proteins to the membrane that trigger physiological responses [110, 117, 130, 188-191]. For example, during drought stress, phosphatidic acid is required to sequester phosphatase ABA Insensitive 1 (ABI1), inhibiting its activity and promoting ABA signaling [130]. However, the discovery of several lipid-mediated pathways indicate that lipid-protein complexes can play a more direct role in transcriptional regulation, enzyme activation, and perception by receptors [91, 92, 109, 192, 193]. For example, the interaction between FT and a diurnally modulated species of phosphatidylcholine (PC) tunes the transition from vegetative to reproductive growth by facilitating DNA-binding [91, 92]. Phosphatidic acid disrupts AT-hook motif-containing nuclear localized 4 (AHL4) interaction with the promoters of TAG degradation genes as part of a feedback mechanism for the regulation of lipid catabolism during seedling development [109]. In animals, the perception of Wnt by Frizzled and other receptors requires palmitoylation [106, 194].

These emerging roles of lipids outside the context of the membrane may also include long-distance transport and systemic signaling. Lipids and lipophilic compounds have been identified in the aqueous environment of the phloem, along with several dozen predicted lipid-binding proteins (LBPs) [88, 144]. GDSL lipase, PIG-P and PLAFP, for example, each bind lipids, including phosphatidylinositol phosphates (PIPs) and phosphatidic acid [181]. Moreover, *GDSL lipase* and *PLAFP* gene expression changes in response to abiotic stress [181]. Here, I investigated several more of these phloem-localized putative LBPs to uncover their involvement in long-distance lipid-mediated signaling for abiotic stress response: *Annexin 1 (ANN1)* encodes a  $\text{Ca}^{2+}$ -binding protein associated with a wide variety of biotic and abiotic stress responses and development [195]; the major latex protein-like proteins (MLP43 and MLP423) and Bet v1 Allergen are members of the Bet v1 family of StAR-related lipid transfer (START) domain proteins with similar tertiary structures capable of binding hydrophobic ligands [196-198]. MLP43 has been linked to drought tolerance and ABA signaling [196], while little is known about the physiological roles of MLP423 and Bet v1 Allergen. First, lipid overlays were used to confirm lipid-binding activity and to determine which lipids the phloem LBPs bind. Second, the gene expression profiles of phloem LBPs—*ANN1*, *PLAFP*, *GDSL lipase*, *PIG-P*, *MLP43*, *MLP423*, *Bet v1 Allergen*, *14-3-3*, *Sec14*—were examined during twelve hours of various abiotic stress conditions. Gene expression patterns were compared to the expression of phospholipases, lipid ligand generating enzymes, under the same stress conditions. Finally, I assessed the subcellular localization of these LBPs using confocal microscopy. My findings confirm lipid-binding activity of the LBPs and indicate that the

LBP's show distinct responses to various abiotic stress factors. Their possible roles are discussed below.

## **Methods**

### ***Plant growth and culture***

*Arabidopsis thaliana* Col-0 seeds were sterilized with 0.05% Triton X-100, 20% bleach solution for 15 minutes, followed by washing with water for 5 minutes, 5 times, while shaking. The sterilized seeds were plated on ½ strength Murashige-Skoog agar plates and were left in the dark at 4°C for 2 days. The seed plates were moved to the growth chamber to germinate and grow for 2-3 weeks under a 12-hour photoperiod.

### ***Hydroponic stress treatment***

Five pipette tip boxes were filled with sterile Millipore water and 2-3 weeks old Col-0 seedlings were transplanted from the agar plates into pipette tip racks, with the roots submerged in the water. Seedlings acclimated in the water for 24 hours before stress treatments were applied. Concentrated solutions of D-mannitol, abscisic acid (ABA), NaCl, or polyethylene glycol 6000 (PEG) were added to the water in the pipette tip boxes to final concentrations 200 mM D-mannitol, 150 µM ABA, 150 mM NaCl, or 30% (m/v) PEG. Whole seedlings were collected in triplicate at 0, 2, 5, 8, 10, and 12 hours after stress induction. Samples were briefly dried on Kimwipes, immediately frozen in liquid nitrogen, and stored at -80°C. The 0-hour time point consists of a triplicate set of seedlings that had acclimated for 24 hours and were harvested prior to the application of stress.

### ***Reverse transcription quantitative polymerase chain reaction (RT-qPCR)***

Frozen seedling samples were ground to a powder using mortar and pestle, then RNA was extracted using RNEasy Plant Mini Kit (Qiagen) according to the manufacturer's

instructions. RNase-Free DNase Set (Qiagen) was used for on-column DNA digestion. RNA concentrations were determined using Qubit RNA Broad Range Assay Kit (Invitrogen). The volume of RNA from each sample necessary for a final concentration of 25 ng/μL cDNA was calculated, and the High-Capacity cDNA Reverse Transcription Kit (Applied Biosystems) with RNase Inhibitor (Applied Biosystems) was used according to the manufacturer's instructions, adjusted for 50 μl reactions.

The qPCR reactions were performed in 384-well plates with Power SYBR Green PCR Master Mix (Applied Biosystems) and run on the QuantStudio 7 Flex PCR System (Applied Biosystems). *ACTIN 8* (AT1G49240) was used as the housekeeping gene and the primer sequences are described in Table A.1.

### ***RT-qPCR Analysis***

The  $\Delta\Delta\text{Ct}$  Method was used to analyze the qPCR data. First, the  $\Delta\text{Ct}$  value for each technical replicate within three biological replicates was determined.

$$\Delta\text{Ct}_{T_n} = Ct_{ACT8} - Ct_{GOI}$$

Then the  $\Delta\text{Ct}$  values across technical replicates were averaged within a biological replicate for each timepoint and stress condition.

$$\Delta\text{Ct}_{Avg} = (\Delta\text{Ct}_{T_1} + \Delta\text{Ct}_{T_2} + \dots + \Delta\text{Ct}_{T_n})/n$$

The  $\Delta\Delta\text{Ct}$  values were then calculated by subtracting the 0-hour timepoint in the untreated control group from the experimental sample value for each timepoint within each stress treatment. These values were used for the box plot figures (Figure A.2).

$$\Delta\Delta\text{Ct}(\text{timepoint } n)_{StressA} = \Delta\text{Ct}(\text{timepoint } n)_{StressA} - \Delta\text{Ct}(\text{timepoint } 0)_{Control}$$

$$\Delta\Delta\text{Ct}(\text{timepoint } n)_{StressB} = \Delta\text{Ct}(\text{timepoint } n)_{StressB} - \Delta\text{Ct}(\text{timepoint } 0)_{Control}$$

A second  $\Delta\Delta\text{Ct}$  value, calculated by subtracting the control timepoint from corresponding stress timepoint, was used for the heatmap (Figure 2.2) to show the expression level relative to the control level at the same time.

$$\Delta\Delta\text{Ct}(\text{timepoint } n)_{\text{StressA}} = \Delta\text{Ct}(\text{timepoint } n)_{\text{StressA}} - \Delta\text{Ct}(\text{timepoint } n)_{\text{Control}}$$

$$\Delta\Delta\text{Ct}(\text{timepoint } n)_{\text{StressB}} = \Delta\text{Ct}(\text{timepoint } n)_{\text{StressB}} - \Delta\text{Ct}(\text{timepoint } n)_{\text{Control}}$$

The respective  $\Delta\Delta\text{Ct}$  values were then transformed into fold-change (FC) values:  $2^{-\Delta\Delta\text{Ct}}$ . At this point, the fold-changes for biological replicates were averaged and the standard error was calculated. Finally, the  $\log_2\text{FC}$  was used to create the heatmap with the R package [pheatmap](#).

### **Cloning**

*ANN1*, *MLP43*, *MLP423*, and *Bet v1 Allergen* were amplified from cDNA using primers with attB sites (Table A.2), and amplicons were inserted into pDONR221 (Invitrogen) using Gateway BP Clonase II Enzyme Mix (Invitrogen) according to manufacturer's instructions. The Entry vector constructs were recombined with the Gateway pEarleyGate 103 (pEG103) expression vector (Arabidopsis Biological Resource Center) [199] using Gateway LR Clonase II Enzyme Mix (Invitrogen) according to manufacturer's instructions. One Shot TOP10 Chemically Competent Cells (ThermoFisher) were used for colony selection. Vectors were transformed into *Agrobacterium tumefaciens* GV3101 Electrocompetent Cells (GoldBio) using electroporation.

Genes were amplified from cDNA using In-Fusion primers (Table A.2) and then cloned into pET15b (Novagen) expression vector using In-Fusion HD Cloning Kit (Clontech) according to the manufacturer's instructions. The constructs were transformed

into TOP10 cells for selection. Finally, constructs were transformed into BL21(DE3) Competent Cells (Thermo Scientific) for protein expression.

### ***Transient expression in tobacco and microscopy***

35S::ANN1-GFP, 35S::MLP423-GFP, 35S::MLP43-GFP, and 35S::Bet v1 Allergen-GFP in pEG103 Agrobacteria were grown in Luria Broth (100  $\mu$ M acetosyringone, 50  $\mu$ M kanamycin, 10  $\mu$ M gentamicin, and 10  $\mu$ M rifamycin) at 28°C to an OD600 of approximately 0.6, then centrifuged at 3000 xg for 10 minutes, and the cell pellet was resuspended in infiltration buffer (10 mM MES pH 5.7, 10 mM MgCl<sub>2</sub>, 100  $\mu$ M acetosyringone) to an OD600 of 0.6. Resuspended cells were incubated at room temperature for 1-3 hours before infiltrating into *Nicotiana tabacum* with a 1 mL needleless syringe. The infiltrated plants were left in the Percival growth chamber at 22°C on a 12-12 day/night cycle for 2 days.

The spectral-based Olympus FluoView 1000 confocal laser-scanning microscope was used to image GFP and chlorophyll autofluorescence in tobacco leaves. GFP and chlorophyll were visualized by exciting with the 488 nm and 559 nm lasers, respectively. GFP emission was captured between wavelengths 500 nm and 560 nm and chlorophyll was captured in the wavelength range 655-755 nm.

### ***Protein expression and purification***

The LBPs were N-terminally tagged with 6xHis affinity tag in the pET15b vector. The transformed BL21(DE3) cells were grown in Luria Broth (100  $\mu$ M ampicillin) at 37°C to an OD600 between 0.6 and 0.8. Protein expression was induced with 0.5 mM isopropyl  $\beta$ -D-1-thiogalactopyranoside (IPTG) and shaken in the incubator at 16°C overnight. The cell pellets were harvested by centrifuging the cultures at 3000 xg for 15 minutes. Cell

pellets were resuspended in lysis buffer (1X phosphate-buffered saline (PBS-137 mM NaCl, 2.7 mM KCl, 10 mM Na<sub>2</sub>HPO<sub>4</sub>, 1.8 mM KH<sub>2</sub>PO<sub>4</sub>, pH 7.4), 0.002% phenylmethylsulfonyl fluoride (PMSF), cOmplete Mini EDTA-free Protease Inhibitor Cocktail tablet (Roche), DNase I) and then lysed by sonication. The lysed cells were centrifuged at 40,000xg for 30 minutes and supernatant was transferred to a new tube. Equilibrated Ni-NTA agarose resin (Qiagen) was added to the lysate and the mixture was gently shaken at 4°C for 2 hours. The lysate-resin mixture was then loaded into a gravity column. The column was washed with 100 mM imidazole in 1X PBS three times, and the bound proteins were eluted with 500 mM imidazole in 1X PBS. The elution fraction was concentrated to 2.5 ml using Amicon Ultra-15 3K (Millipore) by centrifugation and de-salted and exchanged back into 1X PBS with PD-10 columns (Cytiva) according to the manufacturer's instructions. Proteins were validated with SDS-PAGE and Western blot (Figure A.1), and concentrations were determined by Bradford assay using the Bovine Gamma Globulin Standard Set (BioRad).

### ***Lipid binding assays***

The lipid overlay assays were carried out according to the following protocol, modified from [200]. 5 µg of each phospholipid (Avanti) in 50% chloroform 50% methanol was spotted on Amersham Protran Supported 0.2 µm nitrocellulose blotting membrane (GE Healthcare). The membrane was briefly left to dry, blocked with 3% fatty acid free bovine serum albumin (BSA, Roche) in 1X Tris-buffered saline Tween-20 (TBST-20 mM Tris, 150mM NaCl, 0.1% Tween-20) for 2 hours and incubated in 5 µg/ml protein in 3% BSA in 1X TBST at 4°C overnight. The membrane was washed with 1X TBST 5 times for 10 minutes each. The membrane was then incubated in 1:10,000 6X His tag HRP-

conjugated mouse monoclonal antibody (Rockland) in 3% BSA in 1X TBST at 4°C for 2.5 hours. The membrane was washed with 1X TBST 3 times for 10 minutes and then imaged using ECL Prime Western Blotting Detection Reagents (Amersham).

## Results

### ***Proteins identified in aqueous phloem exudates bind phospholipids.***

The phloem is a hydrophilic, aqueous environment, and yet lipophilic compounds have been identified in phloem exudates [13]. As it is not energetically favorable for hydrophobic compounds to be loaded into and transported through the phloem, transport requires proteins to facilitate solubilization and translocation. Several predicted lipid-binding proteins were identified in phloem sap using proteomics [13, 144], and their lipid binding activity was investigated. We have previously reported on Phloem Lipid-Associated Family Protein (PLAFP) which specifically binds phosphatidic acid (PA) species [144, 181]. Here, I observed that full native PLAFP binds PA as well as 16:0/16:0 phosphatidylserine (DPPS) and phosphatidylglycerol (DPPG) species *in vitro* (Fig. 2.1 A). My investigation of additional phloem-localized proteins, Annexin 1 (ANN1), Bet v1 Allergen, Major Latex-like Protein 43 (MLP43), and Major Latex-like Protein 423 (MLP423) reveals that they also bind PA, PG, and PS, with no affinity for the positively charged phospholipids, PC and phosphatidylethanolamine (PE) (Fig 2.1 B-E). Overlays shown here are representatives of triplicate experiments.

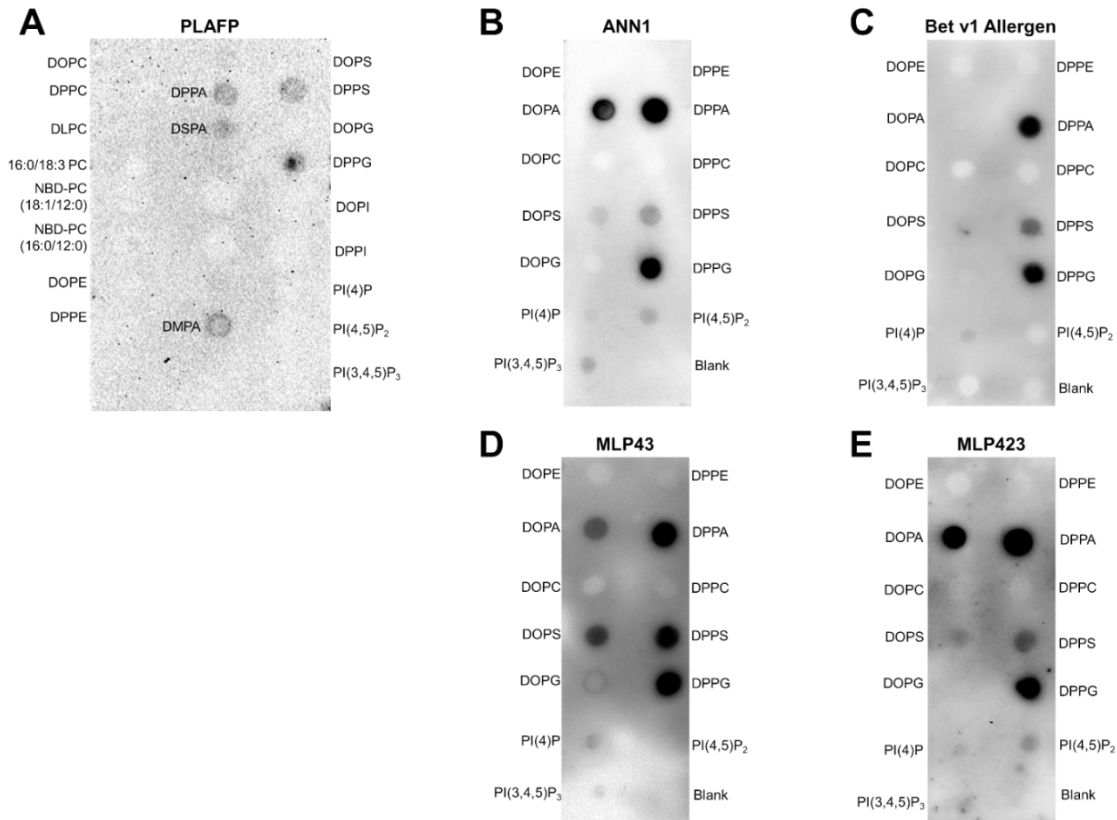


**Figure 2.1 Phloem Localized Proteins Bind Lipids.** Protein Lipid Overlays were performed to determine which lipids were bound by proteins identified in the phloem. Lipid blots were incubated with native PLAFP (A), ANN1 (B), Bet v1 Allergen (C), MLP43 (D), and MLP423 (E) and proteins were detected using anti-His antibody. The immunoblots were imaged with chemiluminescence. All proteins tested bind phospholipids, with some variation in affinity. The lipids spotted in the middle column of blot (A) are various molecular species of phosphatidic acid as follows (top to bottom): DOPA, DPPA, DSPA, 16:0/18:3 PA, NBD-PA (18:1/12:0), NBD-PA(16:0/12:0), POPA, DMPA. Overlays shown are representative of N=3 replicates.

PLAFP, Phloem Lipid-Associated Family Protein; ANN1, Annexin 1; MLP43, Major Latex Protein-Like Protein 43; MLP423, Major Latex Protein-Like Protein 423; DOPC, dioleoyl (18:1/18:1) phosphatidylcholine; DPPC, dipalmitoyl (16:0/16:0) phosphatidylcholine; DLPC, dilauroyl (12:0/12:0) phosphatidylcholine; NBD, nitrobenzoxadiazol; DOPE, dioleoyl phosphatidylethanolamine; DPPE, dipalmitoyl phosphatidylethanolamine; DOPA, dioleoyl phosphatidic acid; DPPA, dipalmitoyl phosphatidic acid; DSPA, distearoyl (18:0/18:0) phosphatidic acid; POPA, palmitoyl oleoyl (16:0/18:1) phosphatidic acid; DMPA, dimyristol (14:0/14:0) phosphatidic acid; DOPS, dioleoyl phosphatidylserine; DPPS, dipalmitoyl phosphatidylserine; DOPG, dioleoyl phosphatidylglycerol; DPPG, dipalmitoyl phosphatidylglycerol; DOPI, dioleoyl phosphatidylinositol; DPPI, dipalmitoyl phosphatidylinositol; PI(4)P, phosphatidylinositol phosphate; PI(4,5)P<sub>2</sub>, dioleoyl phosphatidylinositol 4,5 bisphosphate; PI(3,4,5)P<sub>3</sub>, dioleoyl phosphatidylinositol 3,4,5 trisphosphate

ANN1 appears to display the least specificity for specific lipid classes and lipid species. It shows strong affinity for DPPA, DOPA, and DPPG and weak binding to DPPS, DOPS and all three PIPs (Figure 2.1 B). Bet v1 Allergen binds DPPA, DPPS, and DPPG, as well as PI(4)P, exhibiting a preference for the saturated phospholipids (Figure 2.1 C). MLP43 binds DOPA, DPPA, DOPS, DPPS, and DPPG, as well as PI(4)P and PI(3,4,5)P<sub>3</sub> (Figure 2.1 D). Comparable to MLP43, MLP423 also binds DOPA, DPPA, DOPS, DPPS, and DPPG. However, MLP423 appears to bind to all PIP species (Figure 2.1 E). Overall, the phloem LBPs surveyed bind neutral or negatively charged phospholipids, with a slight preference for saturated lipid species.

***The expression profiles of phloem-localized LBPs vary across abiotic stresses and correlate with the expression patterns of stress-induced phospholipases.***

The function of predicted LBPs in phloem sap is unknown. While some of these proteins have been characterized for local stress response at specific timepoints or developmental stages [195, 196, 201-205], a more comprehensive survey of gene expression during several abiotic stresses across the span of a day can illuminate patterns and thereby be informative of possible involvement in signaling pathways. Because several of the phloem LBPs interact with PA, we correlated these findings with the expression pattern of several phospholipase Ds and C as these are known to generate PA from PC under specific stress conditions. Arabidopsis seedlings were subjected to drought stress (PEG), a drought-responsive phytohormone (ABA), osmotic stress (mannitol), and salt stress (NaCl), then seedlings were collected and analyzed using RT-qPCR to examine gene expression for several lipid-binding and phloem associated proteins.

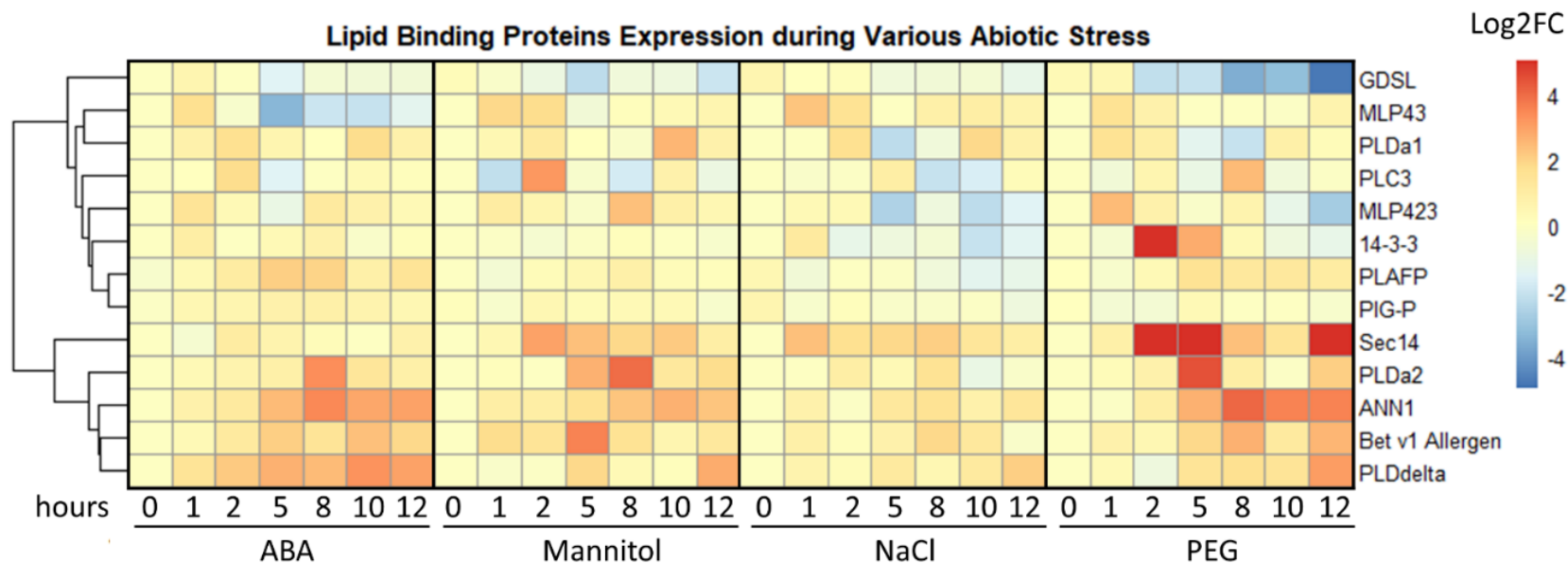


**Figure 2.2 Heatmap Summarizing the Gene Expression Profiles of Lipid Binding Proteins during Abiotic Stress Treatment.** Arabidopsis seedlings were treated with 150  $\mu$ M ABA, 200 mM D-mannitol, 150 mM NaCl, or 30% (w/v) PEG for 12 hours. Seedlings were sampled at 0, 1, 2, 5, 8, 10, and 12 hours and RT-qPCR was used to assess gene expression of several lipid binding proteins. The data is summarized in a heatmap, displaying the Log<sub>2</sub>Fold-Change (Log<sub>2</sub>FC) relative to the corresponding timepoint under control treatment in water. The timepoint and stress include N=2-6 replicates.

ABA, abscisic acid; NaCl, sodium chloride; PEG, polyethylene glycol; MLP43, Major Latex Protein-like Protein 43; PLDa1; Phospholipase D $\alpha$ 1; PLC3, Phospholipase C3; MLP423, major latex protein-like protein 423; PLAFP, Phloem Lipid-Associated Family Protein; PLDa2; Phospholipase D $\alpha$ 2; ANN1, Annexin 1; PLD $\delta$ ; Phospholipase D $\delta$

The gene expression patterns of phloem-localized proteins vary across stresses and are distinct from one another, indicating unique roles for proteins found in the phloem (Figure 2.2). *Major Latex Protein-like 43 (MLP43)* decreases in response to ABA, but remains mostly constant during osmotic, salt, and drought stress. *Major Latex Protein-like 423 (MLP423)* decreases in response to salt stress and eventually drought stress. *Annexin 1 (ANN1)* increases across all stress factors, most dramatically during PEG treatment and more mildly during salt stress. *Bet v1 Allergen* shows minor increases across all stress conditions tested. The expression of these genes also clusters with some phospholipase genes, which may indicate co-expression. For example, the expression patterns of *PLAFP* and *ANN1* correlate with the patterns observed for genes like *Phospholipase D $\alpha$ 2 (PLD $\alpha$ 2)* and *Phospholipase D $\delta$  (PLD $\delta$ )*. These PLDs are known to generate PA in response to abiotic stress, which is one of the lipids that strongly binds to the proteins. These data suggest roles for phloem LBPs and their lipid ligands in stress response, and these pathways correlate with the expression of phospholipases.

***ANN1, Bet v1 Allergen, MLP43, and MLP423 predominantly localize to the cell periphery and cytoplasm, with some indications of ER and/or nuclear subcellular localization.***

ANN1, Bet v1 Allergen, MLP43, and MLP423 have all been identified in phloem exudates [13]. To further assess localization prior to phloem loading, the genes were transiently expressed under a 35S promoter in tobacco and fused eGFP tag was detected using confocal fluorescence microscopy. ANN1 localizes in a pattern indicative of endoplasmic reticulum (ER), surrounding the nucleus and ER strands throughout the cell

(Figure 2.3 A). Bet v1 Allergen is observed in the periphery of the cell, as well as exhibits nuclear localization and cytoplasmic stranding, indicated by the white arrows (Figure 2.3 B). The major latex-like proteins, MLP43 and MLP423, also display localization around the periphery of the cell, cytoplasmic or ER strands, and some nuclear localization (Figure 2.3 C-D). Taken together, these results suggest overall localization to the ER and the cytoplasm, consistent with soluble proteins capable of loading into and transport throughout the phloem.

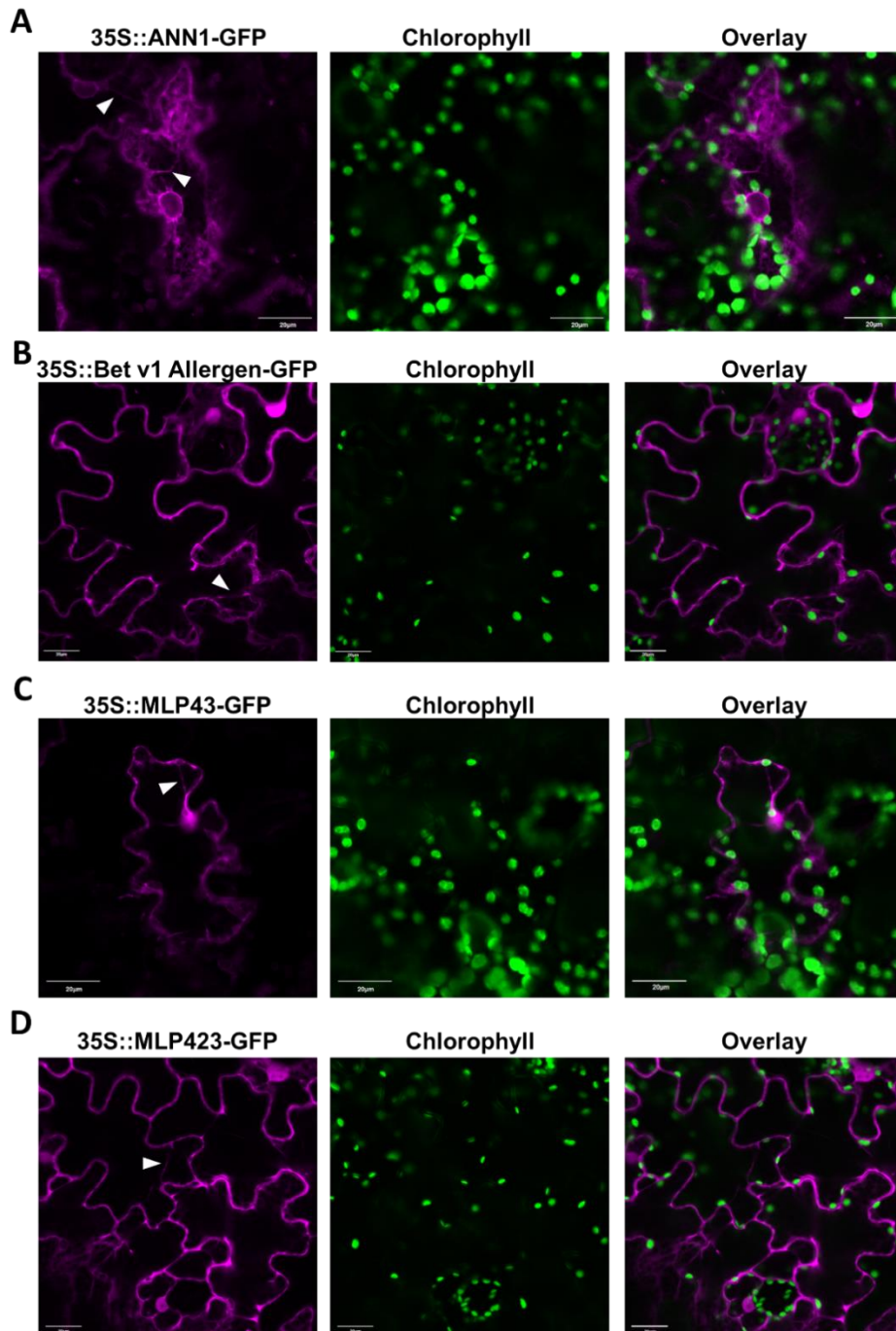


**Figure 2.3 Subcellular Localization of Phloem Lipid Binding Proteins.** ANN1 (A), Bet v1 Allergen (B), MLP43 (C), and MLP423 (D) were tagged with eGFP and transiently expressed under the CaMV 35S promoter in *N. tabacum*. The proteins (magenta, left panel) and chlorophyll (green, middle panel) were detected with confocal laser-scanning microscopy. White arrows highlight localization to cytoplasmic strands. Overlays of the proteins and chlorophyll show no co-localization with chloroplasts (right panel), but rather the proteins predominantly localize to cell periphery, likely cytoplasmic, and possibly endoplasmic reticulum.

## Discussion

In addition to its primary role in energy transport, the complex and dynamic phloem tissue transmits systemic signals throughout the plant. Critical to this process is tightly regulated and highly specific signals that can convey the stress and initiate the appropriate response efficiently. Lipid-binding proteins in the phloem have the potential to act in concert with stress-induced lipid ligands to deliver signals to distal tissue and coordinate stress and development across the entire organism. By binding phospholipids, known intracellular stress signals [88, 191, 206], proteins gain an additional layer of specificity to generate a clear, controlled message for stress response.

In this chapter, I investigated several potential phloem-mobile proteins as candidates for lipid-mediated systemic signaling. Several predicted lipid-interacting proteins were previously identified in phloem exudates, pointing to a role for lipid transport as long-distance signals [98, 181]. Here, I surveyed four of these candidates and further assessed their lipid binding activity, gene expression profiles, and subcellular localization.

ANN1, Bet v1 Allergen, MLP43, and MLP423 all bind phospholipids, with no clear specificity for any single lipid species. However, overall, the LBPs did not bind the positively charged structural lipids PC or PE but rather displayed an affinity for neutral or negatively charged lipids. Furthermore, there may be a preference for saturated shorter chain fatty acids. Bet v1 Allergen, MLP43, and MLP423 are all Bet v1 family START domain proteins, therefore we expect their lipid binding activity to be similar. An array of candidate metabolites has been identified as plant START domain ligands, however ligand specificity varies across proteins [207]. Bet v1 Allergen homolog in birch is proposed to have two non-competitive binding sites, but displays a higher binding affinity

for fatty acids over cytokinins, for example [208]. Further, birch Bet v1 Allergen preferentially binds shorter chain fatty acids, consistent with the lipid overlay results here (Figure 2.1) [208].

The gene expression profiles of phloem LBPs vary across stresses indicating functions in different biological processes and signaling mechanisms. *ANN1* is known to be involved in a variety of stress responses, including dehydration, salinity, temperature, and herbivory [209-211]. The increases in *ANN1* expression observed here over 12 hours of all abiotic stress factors is consistent with and further elaborates on limited timepoints in previously reported results [211]. The decrease in *MLP43* expression during ABA treatment (Figure 2.2) is consistent with previously reported expression levels, in which ABA was determined as an inhibitor of *MLP43* expression in a negative feedback loop [196]. While *MLP43* enhances drought tolerance, the specific role of *MLP43* in ABA signaling remains ambiguous and may involve a function as a long-distance signal to expedite ABA signaling in distal tissues. While some transcriptomic studies have identified *MLP423* among the differentially expressed genes during arsenic treatment [212] as well as in mutants for flowering [213], trichome development [214], and glyoxylate cycle [215], very little is known about its function. The significant decrease in *MLP423* expression during salt stress points to a possible role in salt stress as well, perhaps as a negative regulator of the stress response (Figure 2.2). Bet v1 Allergen has been reported to be involved in cytokinin signaling, hormone crosstalk, and shoot formation [201, 216-218] as well as exhibiting decreased expression during prolonged salt stress [202]. Here, we observe a small but significant increase of *Bet v1 Allergen* expression compared to untreated samples at the 8 hour timepoint for ABA and PEG treatments (Figure 2.2;

Figure A.2 B). Bet v1 Allergen may play a role in both developmental and abiotic stress response.

Critically, there is some correlation between expression patterns of phospholipase enzymes that generate lipid ligands and these LBPs. Phospholipases have been shown to be stress responsive and generate signaling lipids from structural lipids in the membrane [219]. As phospholipases are activated by stress stimuli, they produce signaling lipids like diacylglycerol (DAG) and PA. We can hypothesize that the stress-specific molecular species accumulate as the LBPs are simultaneously produced. The LBPs can bind the now readily abundant ligands, and the protein-lipid may function as a complex in downstream signaling pathways. In this way, the plant ensures multiple levels of regulation—the phospholipase activity, the LBP levels, and the protein-lipid complex formation—to respond to a stress with precision.

Disperse localization around the periphery of the cell, as is observed here, can be indicative of plasma membrane localization or, alternatively, it may be a result of the enlarged epidermal vacuole pushing the cytoplasm against the cell wall. Furthermore, cytoplasmic strands are evident in all images (Figure 2.3). The localization in the cytoplasm observed in this study confirms previous reports of ANN1, MLP43, and MLP423 in the cytoplasm [196, 220, 221]. Although MLP43 and MLP423 nuclear localization is corroborated in the literature [196, 220], sequestration to the nucleus can be a consequence of excessive overexpression. Tichá *et al.* (2020) reported on ANN1 localization, with an emphasis on root tissue; the results in this chapter elaborate further on the above ground tissue localization to the ER and cytoplasm [221]. ANN1 has also been shown to re-localize from the cytosol to membranes during stress [222], is predicted

to be secreted [195], and is proposed to also localize in the apoplast [223]. Given ANN1 readily re-localizes in response to stress and its overall promiscuous localization including in extracellular space, the ER, plasma membrane, and cytosol, ANN1 may be involved in long-distance transport as well. PLAFP subcellular localization has previously been described in the periphery of the cell [181]. Overall, localization in the cytoplasm as soluble proteins and in the ER, which passes through plasmodesmata, allow for loading into the phloem for systemic translocation.

This chapter confirmed and expanded upon our knowledge of lipid-binding proteins in intracellular signaling. Nevertheless, the reason for their presence in phloem exudates and their possible functions in long-distance lipid transport and systemic signaling are unclear. Both Bet v1 Allergen protein and mRNA have been identified in phloem sap [13, 27], which makes it an interesting candidate for further investigation. However, its transcriptional response to abiotic stress is minor (Figure 2.2), making it a less likely to be involved in systemic abiotic stress response. While *MLP43* and *MLP423* exhibit decreases in expression during abiotic stress, ANN1 and PLAFP are of the most interest based on their significant increase in gene expression during drought-related stress (Figure 2.2). Further, ANN1's subcellular localization in the ER and PLAFP's punctate patterning in the periphery of the cell may be congruous with loading into the phloem through the plasmodesmata (Figure 2.3) [181]. Both *ANN1* and *PLAFP* are expressed in the vasculature, specifically the phloem [181, 224], and both proteins have been detected in the sieve tube of the phloem [13, 225]. Because ANN1 is already heavily researched, the rest of this dissertation will focus on PLAFP as a model protein for lipid-mediated long-distance signaling for abiotic stress response.

## CHAPTER 3.

**PLAFP comprises a PLAT/LH2 domain, which acts both in lipid binding and protein-protein interaction, to affect overall gene expression.**

Results from this chapter are part of a manuscript for submission to *Plant Physiology*:

Hurlock, A.M.\* , Koenig, A.M.\* , Benning, U.F.\* , Jie, L., and Hoffmann-Benning, S.

Role of PLAFP in the translocation of phosphatidic acid and response to abiotic stress.

## Abstract

Phloem Lipid-Associated Family Protein (PLAFP) comprises a single domain, specifically a PLAT/LH2 domain, predicted to be important both for lipid binding and protein-protein interactions. PLAFP is known to interact with phosphatidic acid (PA). Although there is no explicit and conserved PA-binding motif, PA-binding proteins consistently contain regions enriched in basic amino acid residues proximate to hydrophobic regions. The negatively charged phosphate headgroup of PA necessitates basic amino acid residues for binding, while the binding and consequential solubilization of the acyl chains requires a hydrophobic pocket. Primary sequence alignments and homology modeling, coupled with *in vitro* lipid overlays, indicate a possible role for conserved residues Lysine-42, Arginine-82, and several tryptophan residues in PLAFP binding and solubilization of phosphatidic acid. The PLAT/LH2 domain likely also facilitates protein-protein interactions. To this effect, I have identified a receptor candidate for the perception of the PLAFP or PLAFP-PA signal: PLAFP interacts with receptor-like kinase Vascular Highway 1 Kinase (VH1K) and these proteins co-localize *in vivo*. Further, genes involved in abiotic stress response, ABA-regulated processes, as well as ER stress are differentially expressed when *PLAFP* expression levels are altered. These DEGs encode proteins involved in transcriptional regulation and signaling. Overall, data suggests the PLAT-containing protein PLAFP may be involved in a PA-mediated signaling mechanism that affects downstream gene expression.

## Introduction

Phloem Lipid-Associated Family Protein (PLAFP) is a lipid-binding protein that has been identified in aqueous phloem exudate, suggesting a possible role in long-distance lipid transport [13, 144, 181]. The structure of PLAFP is integral in uncovering the function of the protein and the protein-lipid complex. PLAFP comprises a single polycystin-1, lipoxygenase, alpha toxin/lipoxygenase homology (PLAT/LH2) domain. Two 4-stranded beta sheets form a beta sandwich that makes up the PLAT/LH2 domain, which is an highly conserved non-catalytic domain primarily found in lipoxygenases [226, 227]. Several functions of PLAT/LH2 domains have been proposed, however the function has yet to be definitively determined [226]. The PLAT/LH2 domain has been implicated in membrane association or binding, often in a calcium-dependent manner [226, 228-230], binding to lipid ligands such as phosphatidic acid [144, 181], phosphatidylserine, and phosphatidylinositol phosphates (PIPs) [230], as well as protein stabilization and allosteric regulation of the catalytic activity in lipoxygenases [231, 232]. Furthermore, the PLAT/LH2 exhibits structural similarity to C2 domains, known to mediate protein-protein interactions.

The function of PLAT/LH2 domains is studied in more detail in human and mammalian systems and is understood predominantly within the context of lipoxygenases in which the PLAT domain is only one of several domains. However, PLAFP is entirely composed of this single non-catalytic PLAT/LH2 domain. Single PLAT domain proteins are involved in plant stress and development, including nitrogen-fixation and nodulation [233-235], insect resistance [236], and drought stress, as is the case for PLAFP [181, 237, 238]. Moreover, PLAFP specifically binds phosphatidic acid (PA), which is involved in abiotic and biotic stress response as well as plant development signaling mechanisms

[110, 113, 184, 185, 239]. Not only is PA involved in intracellular signaling, but it has also been identified in phloem exudates, indicating a possible role in systemic signaling as well [13, 144].

Given that PLAFP binds PA and both have been identified in the phloem, PLAFP may act as a transport protein that solubilizes PA to be loaded as a protein-lipid complex into the hydrophilic environment of the phloem. The structure and binding mechanism of the PLAFP-PA complex informs whether PLAFP acts as a mobile lipid transport protein or rather anchors to the membrane. While there is not a defined PA binding motif, PA-binding typically requires positively charged, basic residues and hydrophobic tryptophan residues [240]. For example, in the case of Trigalactosyldiacylglycerol 4 (TGD4), a lipid transfer protein located in the chloroplast membrane, a 35-amino acid soluble loop motif containing several basic residues is sufficient to bind phosphatidic acid [241]. Furthermore, a short stretch of basic amino acids in human Raf1-kinase binds PA [242, 243]. However, these conserved residues in the Raf1 homolog Constitutive Triple Response 1 (CTR1), involved in ethylene response in plants, were not responsible for PA-binding; instead, a separate motif on the C-terminus conferred PA-binding in CTR1 [136]. Although PA-binding motifs vary across proteins, PA binding consistently involves positively charged amino acids, and often adjacent hydrophobic residues also contribute to lipid binding [136, 241-245].

In addition to lipid-binding activity, the PLAT domain and PLAFP are predicted to exhibit protein-protein interaction, which indicates a role in signal transduction via interaction with a receptor-like protein. The Hoffmann-Benning lab has identified several dozen putative PLAFP interactors using a whole leaf protein pull-down. Among these are

Vascular Highway 1 Kinase (VH1K), a receptor-like kinase, and VH1K-Interacting Kinase (VIK), a MAP kinase kinase kinase (MAP3K), both of which interact with PLAFP *in vitro*, as shown in the yeast two-hybrid assay (Figure 3.1).

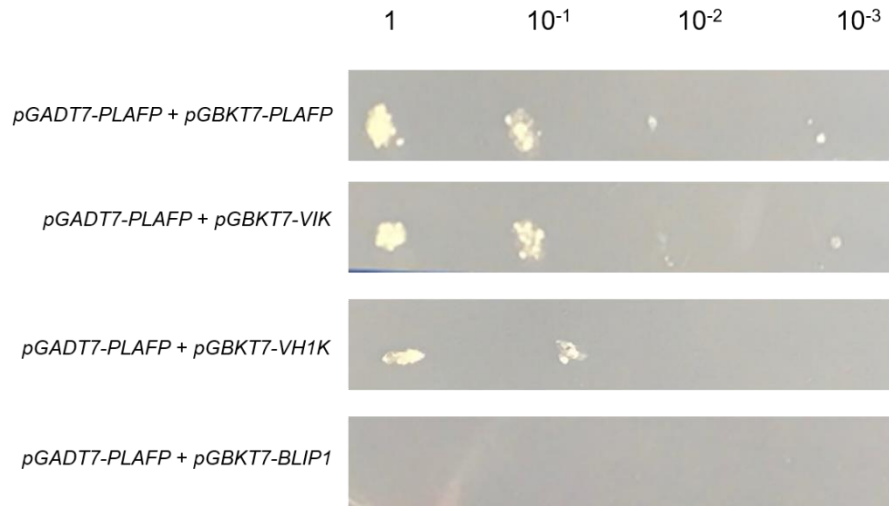


**Figure 3.1 PLAFP binds VH1K and VIK *in vitro*.** A yeast two-hybrid assay, performed by Jie Li, shows that PLAFP interacts with Vascular Highway Kinase 1 (VH1K) and VH1K Interacting Kinase (VIK), as well as interaction with itself. BLIP1 was used as the negative control.

VH1K was first described as a leucine-rich repeat (LRR) receptor kinase involved in early vascular development and phloem transport [246]. Although VH1K was identified as a homolog of Brassinosteroid Insensitive 1 (BRI1) among a family of brassinosteroid receptors, VH1K (also called BRL2, BRI-Like 2) was determined not to be a brassinosteroid receptor, as it does not bind brassinosteroids nor does it complement *bri1* Arabidopsis mutants [247]. The signal ligand for VH1K has yet to be determined. VH1K interacts with VIK, which was also identified in our PLAFP pull-down, and VH1K's interactors suggest involvement in signal transduction and protein degradation [248]. The MAP3K VIK participates in vacuolar glucose import via phosphorylation of Tonoplast Monosaccharide Transporter 1 (TMT1) [249]. Overall, the ligand for VH1K remains

unknown and the targets of VH1K and VIK are largely unexplored, however their relation to the vascular system is consistent with a possible role in systemic signaling.

In this chapter, I investigate PLAFP's lipid binding activity and protein-protein interactions. I identified critical amino acids for PA binding and a putative receptor for the PLAFP-PA complex. Finally, I used RNA-Seq to hone in on the downstream processes affected by PLAFP signaling.

## **Methods**

### ***Homology modeling***

PLAFP protein structure was predicted using Robetta [250-255] with the human Stable-5-Lipoxygenase (PDB 3O8Y) as a template [256]. The homology model was visualized with Chimera [257].

### ***Cloning***

PLAFP without its signaling peptide was cloned into pETEV16b for protein expression. PLAFP was cut out of the pET15b vector [181] with NdeI, the pETEV16b vector (Figure B.1) was linearized with NdeI, and ligated. With this PLAFP pETEV16b construct as a template, the Q5 Site-Directed Mutagenesis Kit (NEB) was used to mutate amino acid residues of interest to alanine residues as indicated later in the chapter. The primers used are outlined in Table B.1. The mutagenesis was carried out according to the manufacturer's instructions and transformed into One Shot TOP10 Chemically Competent Cells (ThermoFisher). Candidate colonies were minipreped and sequenced. Positive plasmids were transformed into BL21(DE3) Competent Cells (Thermo Scientific) for protein expression. The W41A/R82A double mutant was constructed in the same way

but with the R82A construct as the template and using the W41A primers described in Table B.1.

PLAFP-RFP was amplified from Level 1 *PLAFP* in pDGB1 $\alpha$ 1 (Chapter 4) using Gateway cloning primers (Table B.1) and cloned into pDONR221. PLAFP-RFP was amplified from the pENTR221 vector using In-Fusion (Takara) primers (Table B.1) and inserted into the pEarleyGate 103 (pEG103) vector linearized with XhoI. The RFP stop codon was retained, so eGFP in the pEG103 vector backbone was not translated in the PLAFP-RFP construct (Figure B.2). VH1K and VIK were amplified from Arabidopsis cDNA with primers described in Table B.1. VIK and VH1K were cloned into pENTR/D-TOPO vector using the pENTR/D-TOPO Cloning Kit (Invitrogen) according to manufacturer's instructions. VIK was subsequently cloned into pEG103 with the Gateway LR Clonase II Enzyme Mix (Invitrogen). VH1K was amplified from the entry vector using In-Fusion primers (Table B.1) and inserted into pEG103 using XhoI and the In-Fusion HD Cloning Kit (Takara Bio) according to manufacturer's instructions. One Shot TOP10 Chemically Competent Cells (ThermoFisher) were used for colony selection. All vectors were transformed into *Agrobacterium tumefaciens* GV3101 Electrocompetent Cells (GoldBio) using electroporation.

### ***Protein expression and purification***

Native PLAFP and the PLAFP mutants are N-terminally tagged with 10xHis affinity tag in the pETEV16b vector. The transformed BL21(DE3) cells were grown in Luria Broth (100  $\mu$ M ampicillin) at 37°C to an OD600 between 0.6 and 0.8. Protein expression was induced with 0.5 mM isopropyl  $\beta$ -D-1-thiogalactopyranoside (IPTG) and shaken in the incubator at 16°C for 1-2 hours. The cell pellets were harvested by centrifuging the

cultures at 7000 xg for 10 minutes. Cell pellets were resuspended in lysis buffer (10mM imidazole in 100mM HEPES pH7.5, cOmplete Mini EDTA-free Protease Inhibitor Cocktail tablet (Roche)) and then lysed by sonication. The lysed cells were centrifuged at 8000 xg for 20 minutes and the supernatant was transferred to a new tube. Equilibrated Ni-NTA agarose resin (Qiagen) was added to the lysate along with 50 mM  $\beta$ -mercaptoethanol (Sigma). The mixture was gently shaken at 4°C for 1-2 hours. The lysate-resin mixture was loaded into a gravity column. The column was washed first with 100 mM imidazole in 100 mM HEPES then with 250 mM imidazole in 100 mM HEPES. The bound proteins were eluted with 500 mM imidazole in 100 mM HEPES. The elution fraction was de-salted, and buffer exchanged into 10 mM  $\text{KH}_2\text{PO}_4$  pH 7.4 with PD-10 columns (Cytiva) according to the manufacturer's instructions. The protein samples were concentrated to 2.5 ml using Amicon Ultra-15 3K (Millipore) by centrifugation and concentrations were determined by Bradford assay with the Bovine Gamma Globulin Standard Set (BioRad). Proteins were validated with SDS-PAGE and Western blot (Figure B.3).

### ***Lipid binding assays***

Lipid overlays were performed as described in Chapter 2 Methods. The lipids were spotted in a dilution series: 5 ug, 1 ug, 0.5 ug, 0.1 ug, 0.05 ug, and 0.01 ug.

### ***Microscopy***

GV3101 *Agrobacterium tumefaciens* transformed with 35S::PLAFP-RFP, 35S::VH1K-GFP, or 35S::VIK-GFP in pEG103 vectors were grown in Luria Broth (100  $\mu\text{M}$  acetosyringone, 50  $\mu\text{M}$  kanamycin, 10  $\mu\text{M}$  gentamicin, and 10  $\mu\text{M}$  rifamycin) at 28°C to an OD600 of approximately 0.6 then centrifuged at 3000 xg for 10 minutes. The cell pellet was resuspended in infiltration buffer (10 mM MES 10 mM MgCl 100  $\mu\text{M}$  acetosyringone)

to an OD600 of 0.6. Resuspended cells were incubated at room temperature for 1-3 hours before infiltrating into *Nicotiana tabacum* with a 1 mL needleless syringe. Tobacco plants were infiltrated with either the constructs individually or co-infiltrated with PLAFP and VH1K or VIK. The infiltrated plants were left in the Percival growth chamber at 22°C on a 12-12 day/night cycle for 2 days.

The spectral-based Olympus FluoView 1000 confocal laser-scanning microscope was used to image GFP, RFP, and chlorophyll autofluorescence in tobacco leaves. GFP was visualized by exciting with the 488 nm laser, and RFP and chlorophyll autofluorescence were excited with the 559 nm laser. GFP emission was captured between wavelengths 500 nm and 560 nm, RFP between 570 nm and 620 nm, and chlorophyll in the wavelength range 655-755 nm.

### ***RNA-Sequencing and bioinformatics pipeline***

Arabidopsis rosettes from 6 week old Col-0, knockdown, and two overexpression lines (AOX3 and AOX5) were harvested in triplicate and frozen in liquid nitrogen. RNA was extracted with the RNEasy Plant Mini Kit (Qiagen) according to the manufacturer's instructions. The Genomics Core at the Research Technology Support Facility prepared indexed samples with the TruSeq Stranded mRNA Library Preparation Kit (Illumina) and sequenced the RNA samples on the Illumina NovaSeq 6000 platform. Sequences trimmed with Trimmomatic [258] were aligned to the Araport11 transcriptome [259] and quantified using Salmon [260]. DESeq2 was used to determine differential gene expression.

## Results

### ***Conserved basic and hydrophobic residues in predicted loop regions of PLAFP contribute to phosphatidic acid binding.***

The PLAT/LH2 domain that comprises PLAFP is conserved in lipoxygenases and other proteins throughout many species, including plant and mammalian species. Moreover, orthologs of PLAFP itself are found across monocots and dicots. A sequence alignment was performed using tools available through the Bio-Analytical Resource for Plant Biology (BAR, <http://bar.utoronto.ca/>) to determine conserved residues with potential relevance for lipid-binding (Figure 3.2). Unlike for proteins that bind lipids like PC or PIPs, there is no defined conserved domain for PA binding but rather several requirements [136, 200, 241, 242, 244]: multiple basic amino acids to interact with the negatively charged phosphate head group and a hydrophobic area nearby. The PLAFP orthologs exhibit strong primary sequence similarity, and several basic and hydrophobic residues are conserved across species, highlighted in red in Figure 3.2. As they are good candidates for the protein-PA interaction, the residues highlighted with red boxes were chosen as candidates for further investigation as PA-binding sites.

Because there is no experimentally resolved structure of PLAFP, Robetta homology modelling software (<https://rosetta.bakerlab.org/>) was used to build a homology model of PLAFP (Figure 3.3) based on the PLAT domain of a human lipoxygenase (PDB: 3O8Y). This structure was used as a predictive tool to better hypothesize critical amino acid residues and PA binding regions. In the model, residues Trp-41 and Lys-42 are located on a surface loop adjacent to a second loop containing residue Arg-82 (Figure 3.3 A). Arg-82 and Lys-42 constitute a positively charged region, shown in blue in the

model with surface rendering colored by predicted electrostatic charge (Figure 3.3 B). This positively charged region is adjacent to a neutral, hydrophobic region (Figure 3.3 C, green) containing Trp-115 and Trp-141. The importance of tryptophan residues in PLA<sub>2</sub> for PA-binding was previously confirmed by assessment of binding affinity with tryptophan fluorescence quenching assays, in which interaction with a ligand is determined by measuring changes in tryptophan autofluorescence (Hurlock *et al.*, in preparation). The cluster of conserved basic residues Arg-82 and Lys-42 may interact with the negatively charged phosphate headgroup of PA, while the adjacent tryptophans can stabilize and solubilize the fatty acyl chains.

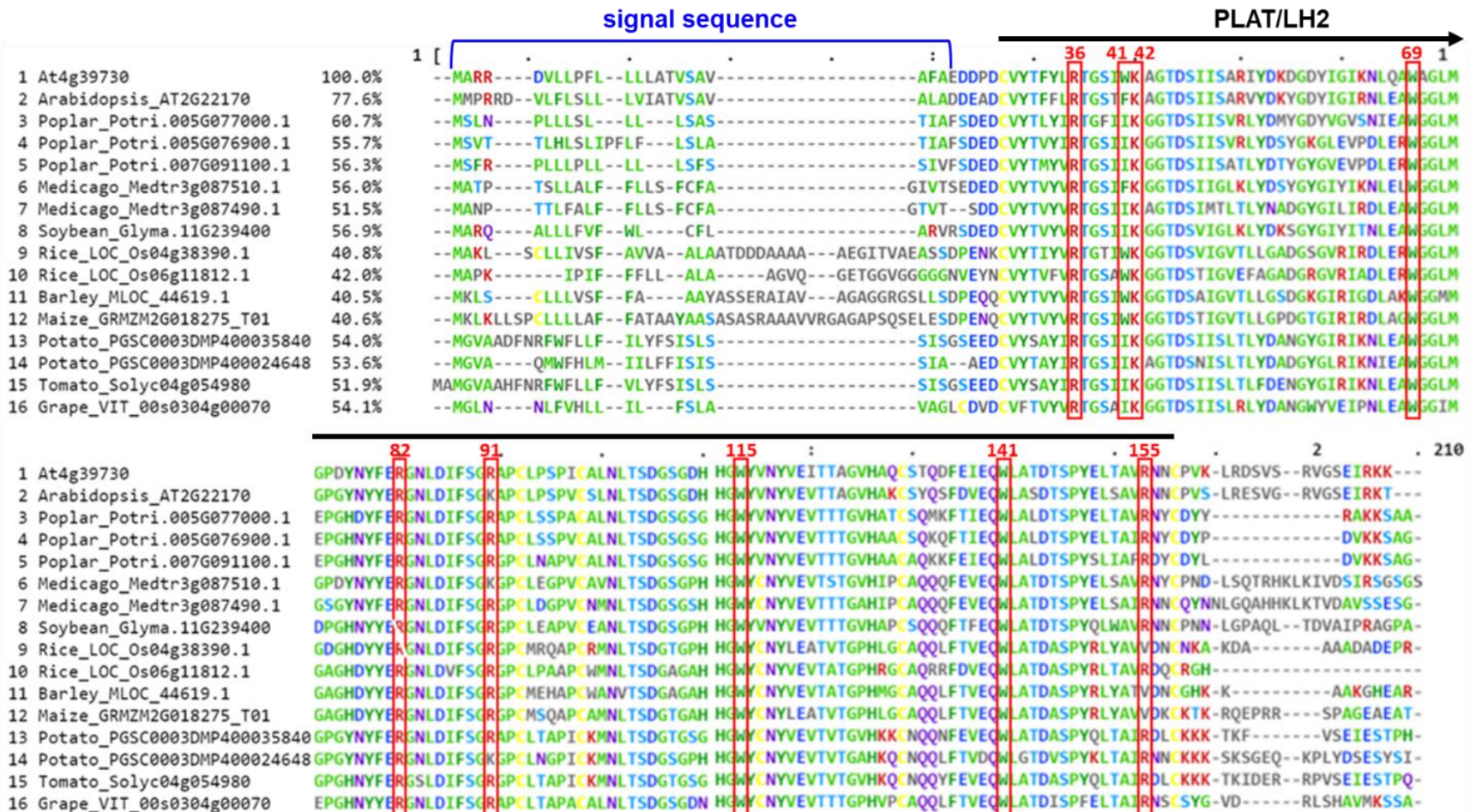


**Figure 3.2 Primary Sequence Alignments of PLAFP Orthologs** across monocots and dicots, generated using [bar.utoronto.ca](http://bar.utoronto.ca). Conserved basic and hydrophobic residues as candidates for phosphatidic acid binding are highlighted in red boxes and the residue number for AtPLAFP is indicated in red. AtPLAFP contains a predicted secretory signal peptide (blue bracket) on the N-terminus, which targets it to the endoplasmic reticulum ([SignalP](http://signalp.uconn.edu)). The PLAT/LH2 domain is denoted by the bold black line. As expected, this region contains the highest sequence similarity.

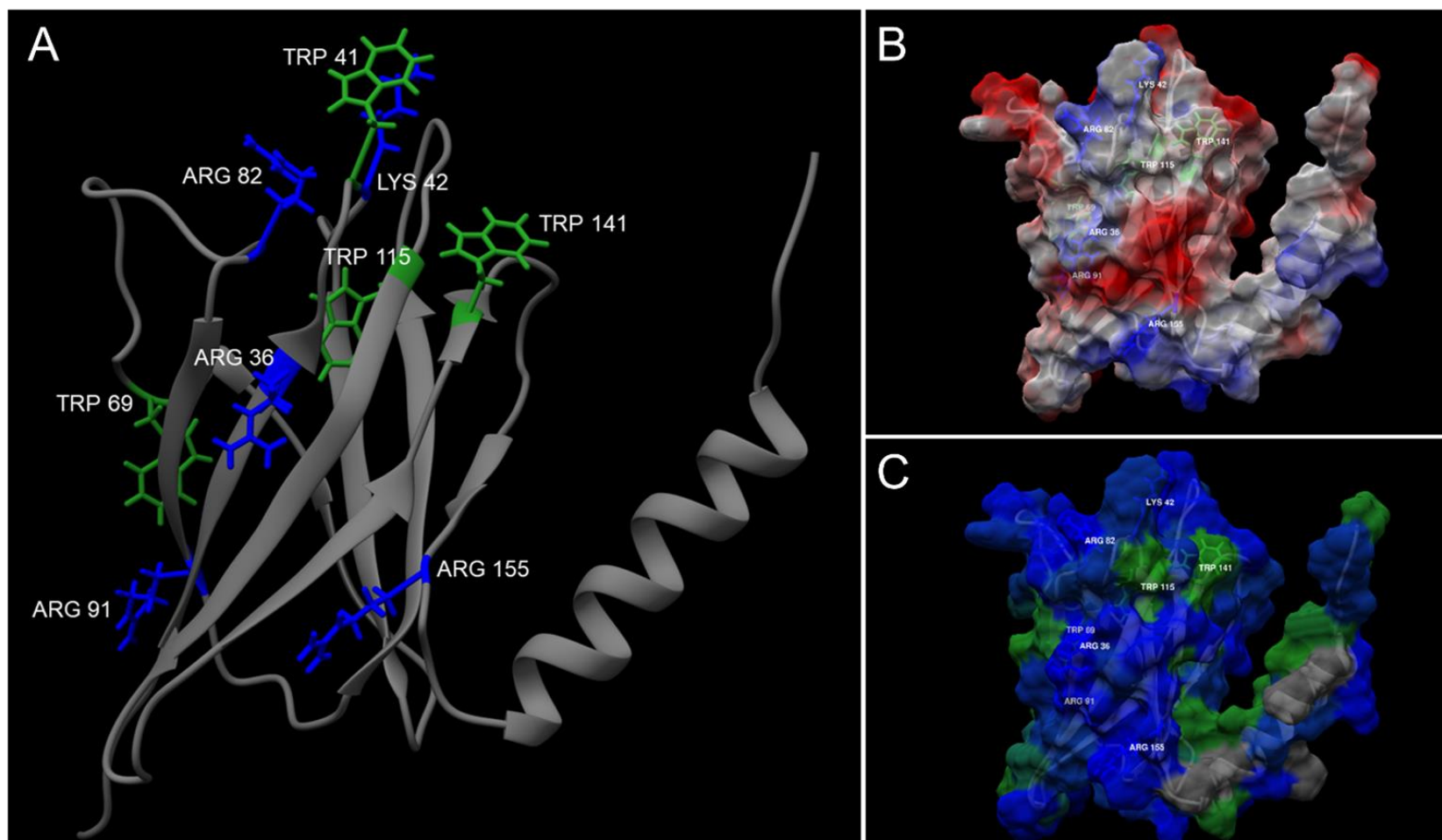


**Figure 3.3 Homology Model of Arabidopsis PLAFP.** PLAFP comprises a PLAT/LH2 domain made up of two 4-strand beta sheets and a flexible C-terminal alpha helix, shown as a ribbon structure in (A). Basic (blue) and hydrophobic (green) residues of interest—arginines, lysines, and tryptophans—are highlighted with stick molecular structures and labeled with residue number. The surface rendering in the top right panel (B) is colored according to predicted electrostatic charge, with positively charged regions in blue, negatively charged regions in red, and neutral regions in white. The surface rendering in the bottom right panel (C) is colored according to hydrophobicity, with hydrophilic regions in blue and hydrophobic regions in green.

To test the role of the candidate residues, His-tagged PLAFP R82A single mutant and W41A/R82A double mutant were generated using site-directed mutagenesis. The proteins were recombinantly expressed in *E. coli* and purified with a Ni affinity column. Lipid overlays were used to probe phospholipid binding and changes in affinity. Native PLAFP binds DOPA, DPPA, DOPS, DPPS, DOPG, and DPPG (Figure 3.4 A). Native PLAFP exhibits the highest affinity for DPPG, with protein detected as low as 0.05  $\mu\text{g}$  DPPG and DPPA with binding between 0.1 and 0.5  $\mu\text{g}$ , DPPS, DOPS, DOPG, and DOPA (Figure 3.4 A). Surprisingly, DPPA binding increases in the R82A single mutant and W41A/R82A double mutant compared to native PLAFP (Figure 3.4 B). Loss of affinity for DPPS is observed when Arg-82 is knocked out (Figure 3.4 C). Similarly, the W41A/R82A double mutant no longer binds DPPS (Figure 3.4 C). Binding affinities for DPPG are comparable across PLAFP and the mutants (Figure 3.4 D). Overall, the single- and double-point mutations tested do not abolish phospholipid binding nor do they dramatically affect affinity, as detected by this qualitative assay (Figure B.4). However, the effects observed in the overlays coupled with the orientation of conserved basic residues adjacent to hydrophobic regions (Figure 3.3), recognized in the literature as a pattern for PA-binding regions, indicate that Arg-82 and Trp-41 may work in concert with other conserved residues (Lys-42, Trp-115, Trp-141) to bind phosphatidic acid.

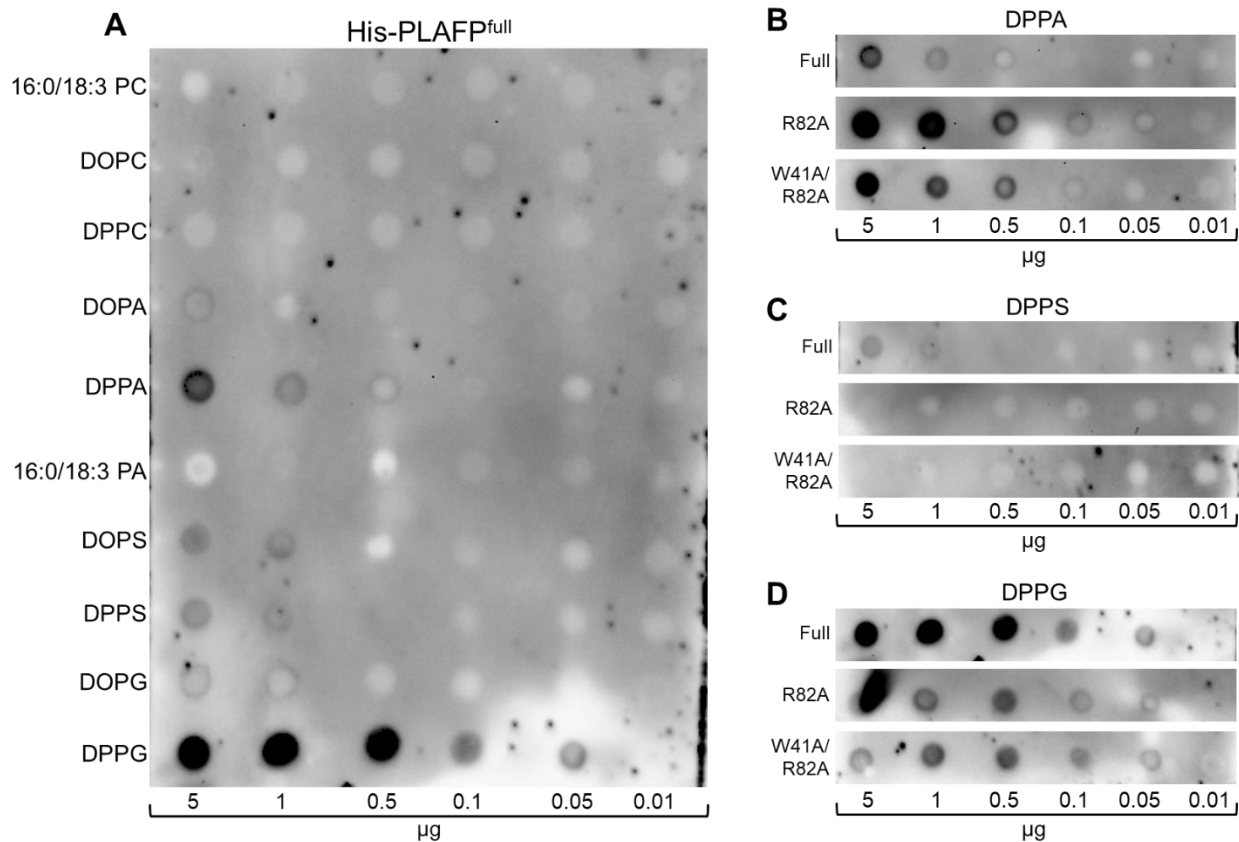


**Figure 3.4 Protein-Lipid Overlays of PLAFP Point Mutants.** Membranes spotted with dilution series of several phospholipid species were incubated in His-tagged PLAFP and PLAFP point mutants. Anti-His-HRP antibody was used to detect spots where the protein is bound, indicating lipid-protein interaction. (A) Native PLAFP protein binds to DOPA, DPPA, DOPS, DPPS, DOPG, and DPPG, and does not bind any positively charged phosphatidylcholine species. The binding affinities of native PLAFP, R82A single mutant, and R82A/W41A double mutants are compared for (B) DPPA, (C) DPPS, and (D) DPPG. Overlays are representative images of N=3 replicates.

PC, phosphatidylcholine; DOPC, dioleoyl (18:1/18:1) phosphatidylcholine; DPPC, dipalmitoyl (16:0/16:0) phosphatidylcholine; DOPA, dioleoyl phosphatidic acid; DPPA, dipalmitoyl phosphatidic acid; PA, phosphatidic acid; DOPS, dioleoyl phosphatidylserine; DPPS, dipalmitoyl phosphatidylserine; DOPG, dioleoyl phosphatidylglycerol; DPPG, dipalmitoyl phosphatidylglycerol; PLAFP, Phloem Lipid-Associated Family Protein; R82A, Arginine-82 mutated to Alanine; W41A, Tryptophan-41 mutated to Alanine

***PLAFP co-localizes with VH1K in vivo.***

PLAFP comprises a PLAT/LH2 domain, which facilitates protein-protein interactions. A whole leaf pull-down assay was performed to identify PLAFP interactors (Hurlock *et al.*, in preparation). Sixty putative interacting proteins were identified, a quarter of which are annotated with functions in signaling. Two kinases were among these signaling interaction candidates: a receptor-like kinase, Vascular Highway 1 Kinase (VH1K) and a MAP3K, VH1K Interacting Kinase (VIK). Yeast two-hybrid results indicate that PLAFP interacts with both kinases *in vitro* (Figure 3.1, Hurlock *et al.*, in preparation). Furthermore, PLAFP interacts with itself in this assay, consistent with PLAT/LH2 domains as protein-protein interaction domains. While these data suggest that PLAFP interacts with signaling kinases VH1K and VIK, the interaction needs to be confirmed *in vivo* to be biologically relevant. To do this, constitutively expressed VH1K-GFP or VIK-GFP were co-infiltrated with PLAFP-RFP in tobacco and confocal microscopy was used to assess co-localization *in vivo*.

Both PLAFP-RFP (magenta) and VH1K-GFP (green) localize in the periphery of the cell in a punctate pattern. The representative images (Figure 3.5 A, B “Overlay”) show co-localization of VH1K with PLAFP fluorescence (white). However, PLAFP does not co-localize with VIK (Figure 3.5 C, D), which, rather, shows nuclear localization and appears in a diffuse pattern near the periphery of the cell. This suggests that *in vivo* PLAFP interacts with receptor-like kinase VH1K only and hence binds to the receptor rather than act directly in the MAP3K intracellular signaling path.

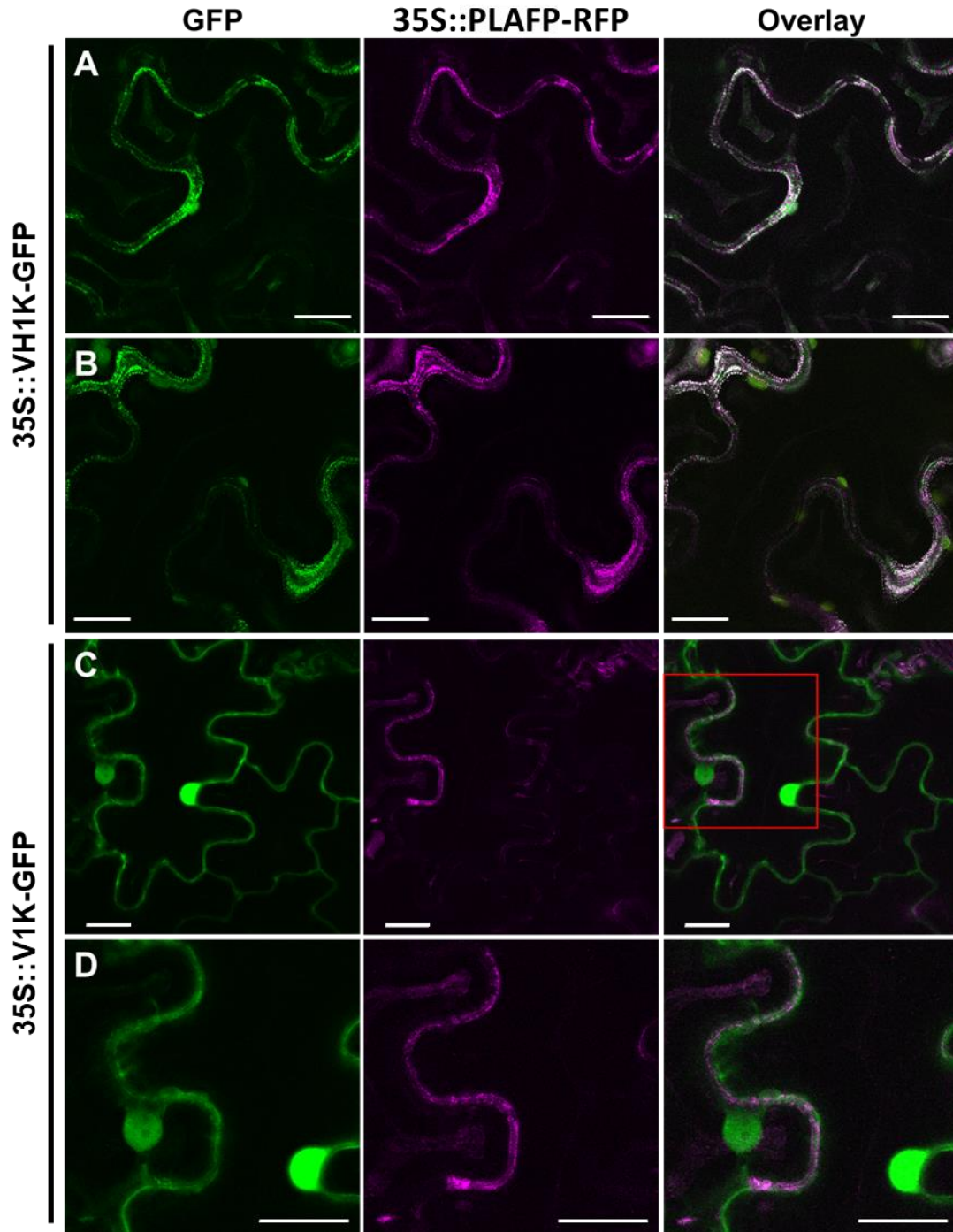


**Figure 3.5 PLAFP Co-localization with Putative Interacting Kinases.** PLAFP (magenta) co-localizes with receptor-like kinase VH1K (green) (A, B), but does not co-localize with MAP3K VIK (green) (C). (D) shows the region highlighted with the red box zoomed in, where distinct RFP and GFP signals can be observed in contrast to the white signal indicating co-localization in panels (A) and (B). PLAFP, Phloem Lipid-Associated Family Protein; VH1K, Vascular Highway 1 Kinase; VIK, VH1K Interacting Kinase

**PLAFP expression levels are associated with differentially expressed genes.**

RNA-Sequencing was performed to determine the impact of *PLAFP* expression on the Arabidopsis transcriptome and identify processes regulated by PLAFP activity. The transcriptomes of two *PLAFP* overexpression lines (AOX3 and AOX5) and one *PLAFP* knock-down (KD) line were compared to Col-0. Genes are considered significantly differentially expressed if the FDR  $\leq$  0.05. Genes are considered down- or up-regulated if expression is at least halved or doubled ( $-1 \geq \text{Log}_2\text{Fold-Change} \geq 1$ ), respectively.

In overexpression line AOX3, 16 genes are significantly up-regulated, and 9 genes are significantly down-regulated (Figure 3.6 A). In independent overexpression line AOX5, 34 genes are significantly up-regulated, and 14 genes are significantly downregulated (Figure 3.6 B). 10 genes are up-regulated in both overexpression lines, and 3 genes are down-regulated in both overexpression lines at the more stringent statistical significance threshold (Table 3.1). Gene Ontology Enrichment (GOE) analysis using [g:Profiler](#) [261] highlighted unfolded protein response and endoplasmic reticulum (ER) stress as significantly enriched molecular functions and biological processes in genes upregulated in overexpression line AOX5. Further, several differentially expressed genes (DEGs) identified in both overexpression lines are annotated to be involved in ER stress and the unfolded protein response: *UDP-Galactose Transporter 3*, *Tunicamycin Induced 1 (TIN1)*, *Protein Disulfide Isomerase 10 (PDI10)* (Table 3.1). These genes are significantly up-regulated when *PLAFP* is overexpressed, suggesting activation in a PLAFP-mediated mechanism.

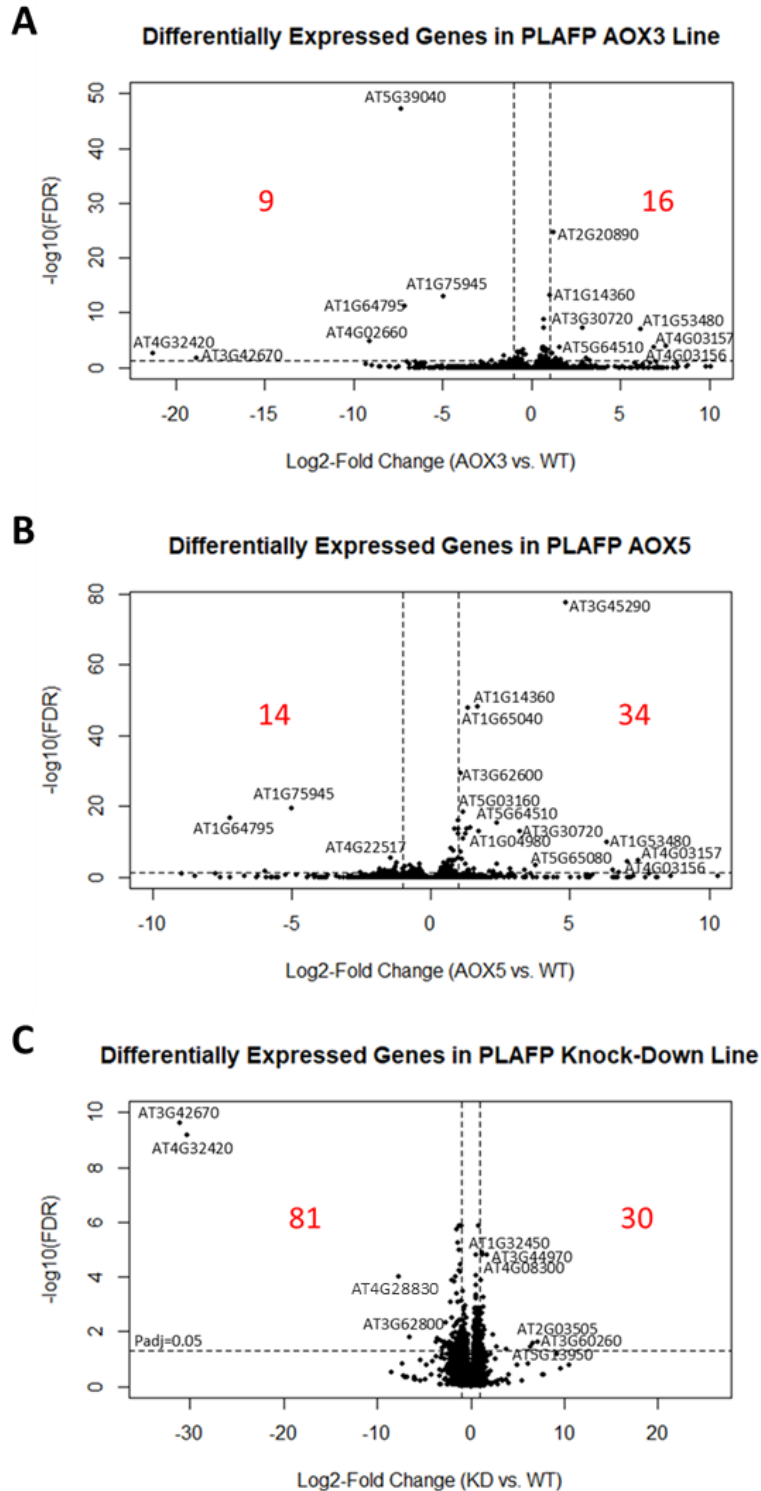


**Figure 3.6 Volcano Plots Showing Differentially Expressed Genes (DEGs) in *PLAFP* AOX3, AOX5, and Knock-Down Lines.** The horizontal dashed line represents  $P_{adj}=0.5$  and the vertical dashed lines denote Log2 Fold-Change -1 and 1, indicating expression reduced by half and doubled expression, respectively. The number of significant DEGs is shown in red.

When *PLAFP* expression is knocked down (approximately 7% that of wild-type levels, Figure B.5), 30 genes are significantly up-regulated and 81 genes are significantly down-regulated (Figure 3.6 C). These genes are significantly enriched for general responses to stimuli and stress (g:Profiler). More specifically, genes that are up-regulated when *PLAFP* is knocked down (genes potentially repressed by *PLAFP* activity) are enriched for sulfur stress response and biotic stress response, whereas genes down-regulated when *PLAFP* is knocked down (activated by *PLAFP* activity) are enriched for transcription regulation and response to abiotic stress.

Several genes were identified in both the 2018 and 2022 KD samples (highlighted genes in Table B.2). The up-regulated genes include a cytochrome P450 (AT3G44970) and Early Light Inducible Protein 1 (ELIP1, AT3G22840). Genes down-regulated in both KD sample sets are candidates that may be activated by a *PLAFP*-mediated mechanism. These include genes involved in stomatal opening during abiotic stress (AT2G21660) [262] and ABA-mediated dormancy (AT1G28330). Additionally, a drought- and ABA-inducible linker histone (HIS1-3, AT2G18050), involved in dehydration and salt stress response [263, 264], is among down-regulated genes in the KD lines. Furthermore, an RNA-regulator protein Tandem CCCH Zinc Finger Protein 5 (TZF5, AT5G44260) is significantly down-regulated in *PLAFP* KD lines and is associated with seed germination and drought response [265, 266]. Another transcriptional regulator, bHLH transcription factor P1R3 (AT3G29370) is also among the DEGs in *PLAFP* KD samples.

**Table 3.1 Summary of Differentially Expression Genes in *PLAFP* Expression Lines.** The bolded accession numbers are significantly up-regulated (red) or down-regulated (blue) in both overexpression lines at a significance level of  $p_{adj} \leq 0.05$ . The accession numbers in normal font are significantly differentially expressed in the overexpression lines at  $p_{adj} \leq 0.1$ . The significance in the knockdown line for each gene is denoted by \* for  $p_{adj} \leq 0.1$  and \*\* for  $p_{adj} \leq 0.05$ .

GENE	Log <sub>2</sub> Fold-Change			ANNOTATION (TAIR)
	AOX3	AOX5	KD	
<b>AT4G39730</b>	4.564	5.032	-3.853**	PLAFP
<b>AT1G14360</b>	1.056	1.671	0.1297	UDP-Galactose Transporter 3; ER UPR
<b>AT3G30720</b>	2.839	3.208	-0.6956	DEG6; C/N allocation, starch regulation
<b>AT1G53480</b>	6.122	6.331	-0.0238	MRD1; methionine accumulation
<b>AT4G03157</b>	7.564	7.452	0	hypothetical protein
<b>AT4G03156</b>	6.883	7.040	-0.3083	small GTPase-like protein
<b>AT5G64510</b>	1.559	2.388	0.2477	TIN1, Tunicamycin Induced 1; ER stress
<b>AT1G04980</b>	1.082	1.722	-0.1897	PDI10, Protein Disulfide Isomerase 10; ER stress
<b>AT1G26390</b>	3.0897	2.845	1.330	BBE4, FAD-binding Berberine family protein
<b>AT5G18937</b>	1.612	1.567	-0.7904	transmembrane protein
<b>AT5G65080</b>	3.250	3.766	2.712	MAF5, MADS Affecting Flowering 5; vernalization
<b>AT1G75945</b>	-4.938	-5.002	0.2165	hypothetical protein
<b>AT1G64795</b>	-7.104	-7.218	-0.8853*	hypothetical protein
<b>AT4G22513</b>	-1.019	-1.210	-1.269**	protease inhibitor/seed storage/LTP family prot.
<b>AT4G21680</b>	-2.865	-2.535	-1.543	NRT1.8, Nitrate Transporter 1.8; nitrate removal from xylem, cadmium tolerance
<b>AT1G18710</b>	-1.712	-1.827	-1.810**	MYB47; seed longevity, seed coat development

## Discussion

The results presented in this chapter confirm and further elucidate the phosphatidic acid binding activity of PLAFP and elaborate on PLAFP's function in protein-protein interaction and downstream signaling. When Arg-82 is mutated to Alanine, we observe some minor loss of binding to phosphatidylserine species and a possible increase in binding phosphatidic acid (Figure 3.4 B, C). This *in vitro* experiment does not directly mimic the membrane environment, so PLAFP mutants may maintain binding affinity to

phospholipids because the acyl chains are more readily accessible compared to a typical lipid bilayer. The loss of basic residue function, in R82A for example, may reduce lipid headgroup specificity without preventing binding to the fatty acid component. This may explain the unexpected increase in mutant-PA binding compared to native protein. Moreover, we initiated a collaboration with the Vermaas laboratory to simulate this mechanism using computation modelling and molecular dynamics. Preliminary findings confirm the amino acid residues we identified as critical for PA binding and corroborate preferential binding to PA and interaction with PG and PS. Based on our experimental data and the computational modelling, we suggest a mechanism in which Arg-82, Lys-42, and Trp-41 detect the negatively charged phosphatidic acid headgroup and facilitate the acyl chains flipping out of the membrane and into a hydrophobic pocket within PLAFP, enriched with conserved tryptophan residues, for solubilization and translocation. Liposome binding assays, where the acyl chain is oriented inside the micelle, could further clarify this.

Phosphatidic acid binding domains, while largely undefined, typically require multiple residues to affect binding [241, 267]. Therefore, shifts in PA-binding strength and specificity are likely minimal for single point mutations. If residue Arginine-82 works in conjunction with Lysine-42 in the adjacent flexible loop to confer binding specificity, for example, Lysine-42 may partially compensate for loss-of-function in the R82A mutant. Furthermore, Tryptophan-41 contributes to membrane association and PA ligand solubilization, but other nearby conserved residues like Tryptophan-115 and Tryptophan-141 in the  $\beta$ -sheet likely also contribute to solubilizing the hydrophobic fatty acid chains. Multi-residue deletions or mutations may be necessary to abolish PLAFP lipid binding

activity. Alternatively, quantitative methods that more accurately simulate the membrane environment, like liposome binding assays or tryptophan fluorescence quenching, may be sensitive enough to delineate the influence of single residues on lipid binding.

Regardless, Trp-41 and Arg-82 appear important for PLAFP association with the membrane. Molecular dynamics modeling (collaboration with Vermaas Lab, Martin Kulke) suggests that they may insert into the membrane and extract PA in a tweezer-like motion for movement sequestration in complex with PLAFP and translocation to a target tissue, where the protein and/or lipid interact with a receptor. One such candidate would be VH1K, which interacts with PLAFP *in vitro* and *in vivo*. Despite its similarity to brassinosteroid receptors BRL1 and BRL3, VH1K does not bind brassinolide [247]. While VH1K is responsive to hormones auxin and cytokinin, it contains an LRR domain that is known to bind small peptides [246, 268]. Given its ligand remains unknown and VH1K interacts and co-localizes with PLAFP (Figure 3.5 A, B), it is possible that PLAFP may activate VH1K. Furthermore, VH1K interacts with the MAP3K VIK [248]. VIK is associated with glucose uptake into the vacuole in Arabidopsis [249], however tonoplast transporters are likely not its only target. For example, the VIK ortholog in potato was implicated in infection and disease [269] and, in date palm, VIK is involved in abiotic stress response, including salt and drought tolerance [270]. Taken together, VH1K is a promising candidate for perception of the PLAFP-PA signal, which then triggers a signaling cascade promoted by VIK to alter overall gene expression.

Given that we postulate PLAFP-PA to be involved in a targeted, highly specific signaling mechanism rather than act as a master regulator or transcription factor, we would not expect altered *PLAFP* expression to yield many differentially expressed genes.

If, for example, PLAFP signaling requires the activation of VH1K in a PA-mediated mechanism, *PLAFP* overexpression would be insufficient to trigger a robust transcriptional response without a concurrent increase in PA production. Rather, a select few candidates from the RNA-Seq results can be informative about the possible processes PLAFP regulates. Several interesting candidates were identified among the differentially expressed genes. Broadly, PLAFP likely functions as an activator, given that more genes are up-regulated compared to down-regulated when *PLAFP* is overexpressed and vice versa in the knockdown lines. Among the DEGs are transcription factors, histone variants, and enzymes involved in signaling like a GTPase, some of which are ABA- and dehydration-responsive, consistent with previously observed and reported PLAFP function in drought response [181, 237, 238]. Assessment of the transcriptome differences among *PLAFP* expression lines during drought stress or when treated with ABA may be informative. In conclusion, I propose that PLAFP may participate in ABA-mediated drought stress response in a PA- and VH1K-dependent mechanism.

## **CHAPTER 4.**

**A novel optogenetics approach reveals systemic transport of PLAFP.**

## Abstract

The systemic mobility of macromolecules is crucial for the communication of stress and developmental cues in the plant. Many compounds have been identified in phloem sap and are interesting candidates for phloem-mobile signaling. However, the existing tools to study long distance translocation are limited and challenging. The traditional approach to investigate systemic transport is grafting, which is a delicate and complicated method requiring expertise and resources. Additionally, chemical induction can be imprecise and toxic, among other constraints; whereas an optogenetics-based approach confers high spatio-temporal resolution, greatly reduces off-target effects, and permits flexibility of environmental conditions. The Plant Usable Light-Switch Elements (PULSE) tool utilizes a blue-light repressor and red-light activator to control gene expression. Here, I applied this technology to pioneer a new method for the study of systemic transport in plants. The approach was optimized using confocal fluorescence microscopy, immunoblots, and PCR in protoplasts, tobacco, and stable Arabidopsis lines. Phloem Lipid-Associated Family Protein (PLAFP) was previously identified in phloem exudates and proposed as a mobile signal for abiotic stress response. The PULSE system was used in combination with the MultispeQ instrument to activate expression of *PLAFP* in source tissue, and the presence of PLAFP was detected in untreated distal tissue, left in transcriptionally repressive white light conditions. Therefore, this novel light-inducible method successfully revealed PLAFP as a likely phloem-mobile protein.

## Introduction

Systemic signaling mechanisms are critical for the coordination of sustained responses to environmental and developmental cues. Although the vascular system in plants is primarily employed for the transport of water, minerals, nutrients, and photoassimilates, the xylem and phloem are well suited to facilitate long-distance transport of mobile signals. While several systemic signals, from roots to shoots, have been attributed to the xylem [73, 164, 271-275], the phloem is particularly adept at the translocation of signaling molecules, as its flow is bi-directional and can thereby move signals from source tissues to both above and below ground sink tissues. Nucleic acids, proteins, hormones, and lipophilic compounds have all been identified in phloem exudates [88]. Some studies assert that these compounds end up in the phloem by accidental diffusion [62-64]. However, the transport of macromolecules through the phloem has been shown to be highly regulated. For example, specific sequences and secondary structures facilitate loading [37, 38, 276]. The indiscriminate loss of nucleic acids, proteins, and other compounds to the phloem stream is wasteful and energy inefficient for the plant. Plasmodesmata, the gateway between cells and into the phloem, are morphologically dynamic and tightly regulated in response to development and stress. Callose deposition, membrane lipids, like sphingolipids, and plasmodesmata (PD) associated proteins all contribute to meticulous control of the macromolecules that are loaded into and unloaded out of the phloem [277-283]. Further, phloem-mobile molecules often also depend on other proteins to facilitate their loading [284]. Phloem-localized macromolecules are purposefully loaded, targeted to specific tissues, and play roles in stress response and development [14, 88].

A prominent example of systemic signaling is the flowering hormone florigen, which triggers the transition from vegetative to reproductive growth. It is now known that the protein Flowering Locus T (FT) is the predominant mobile signal in flowering. It originates in photosynthetic leaf tissue where its expression is regulated by the circadian clock [89]. FT is loaded into the phloem and translocates to the shoot apical meristem where it interacts with FD to promote the transition to flowering [285]. FT is a well understood long distance signaling mechanism, but there are many more examples of phloem-mobile molecules for systemic signaling involved in disease resistance, abiotic stress response, nutrient acquisition, and development that have only just scratched the surface. I have summarized what is known about these signaling pathways in Koenig and Hoffmann-Benning (2020) [88].

The classic approach to studying long distance transport in the phloem is grafting, in which the rootstock and scion of different species, ecotypes, or genotypes are grafted to one another and mobility of molecules of interest can be determined by various methods, such as comparative transcriptomics or proteomics or detection of specific tagged compounds [286-288]. Grafting and micrografting in seedlings is a delicate procedure that requires expertise and skill. Importantly, it depends on the formation of a functional graft junction with newly connected vascular bundles. Since micrografting approaches were first pioneered for *Arabidopsis* seedlings [289], several modifications to the original protocol made the procedure more successful, including facilitation of grafting using agar or pin-fasteners as well as the development of a micrografting chip apparatus [290-293]. While these advancements have improved the efficiency and approachability of grafting, the method remains technically intricate, and some devices are not widely

available. Moreover, grafting requires multiple well-established genotypes, like overexpression and knockout lines. For example, knockouts of critical genes are often lethal, limiting comprehensive grafting studies. Additionally, constitutive expression of genes of interest can deviate from normal developmental processes or result in off-target effects. In addition, it does induce injury that can lead to secondary effects not at all associated with the molecule of interest.

A tightly regulated method for inducible expression with high spatio-temporal resolution can alleviate many of the barriers to the study of long-distance transport and systemic signaling. Chemically induced promoters can amend some shortcomings of grafting, however the chemical inducers also present problems of their own like: challenges with precise application, off-target effects, toxicity, possible mobility of the inducer, and inability to switch off expression rapidly [294]. Light-inducible systems are minimally invasive, non-toxic and highly specific, making them desirable for genetic manipulation. The plant usable light-switch elements (PULSE) tool was developed to accommodate plant dependence on light for survival while imparting tightly regulated optogenetic control of expression using a blue-light off/red light on switch [295]. Under the PULSE system, plants can be grown in ambient white light conditions without inducing expression, due to the EL222 blue light repressor, and expression can be switched on in specific tissues with the red light wavelengths via a PhyB/PIF6 activator module [295]. This level of spatio-temporal resolution facilitates the study of long-distance transport; a single source leaf, for example, can be treated with red light, inducing expression of a tagged gene of interest while expression remains repressed in distal tissues in white light. Then distal tissue, under repressive light conditions, can be probed for the tagged protein,

suggesting that the protein translocated from induced tissue. In this chapter, I applied the PULSE optogenetic switch to investigate the long-distance transport of PLAFP as a putative phloem mobile signal.

## **Methods**

### ***Cloning***

The GoldenBraid cloning strategy was used to generate the constructs [296-298]. An overview of the cloning strategy is shown in Figure 4.1. The genes of interest were amplified from *Arabidopsis* or soybean (*Glycine max*) cDNA and fluorescent tags were amplified from vectors using primers encoding BbsI cut sites and affinity tags, described in Table C.1. Genes of interest were cloned into pL0-S and the tags were restriction cloned into pL0-C vectors. These Level 0 constructs were combined with separate vectors containing the components of the pOpto promoter and a T35S terminator and cloned into pDGB1 $\alpha$ 1 or pDGB1 $\alpha$ 2 with BsaI. Sanger sequencing revealed errors at the new ligation sites, so Q5 Site-Directed Mutagenesis Kit (New England BioLabs) with primers specified in Table C.1 was used to repair the construct before proceeding. The corrected Level 1 *PLAFP* (pDGB1 $\alpha$ 1) construct was inserted into pDGB3 $\Omega$ 2R using BsmBI restriction cloning to reorient the cassette. Finally, the reversed Level 2 *PLAFP* (pDGB3 $\Omega$ 2R) construct was combined with pROF450 (pDGB3 $\Omega$ 1) containing the genes encoding the EL222 repressor and the PhyB and PIF6 activator modules under pAtUbq10 promoters (Figure C.1) into the pDGB3 $\alpha$ 1 backbone. One Shot TOP10 Chemically Competent Cells (ThermoFisher) were used for colony selection. All constructs were confirmed with

restriction digests and Sanger sequencing. The final PULSE-PLAFP (Figure C.1) construct was transformed into *Agrobacterium tumefaciens* GV3101 by electroporation.

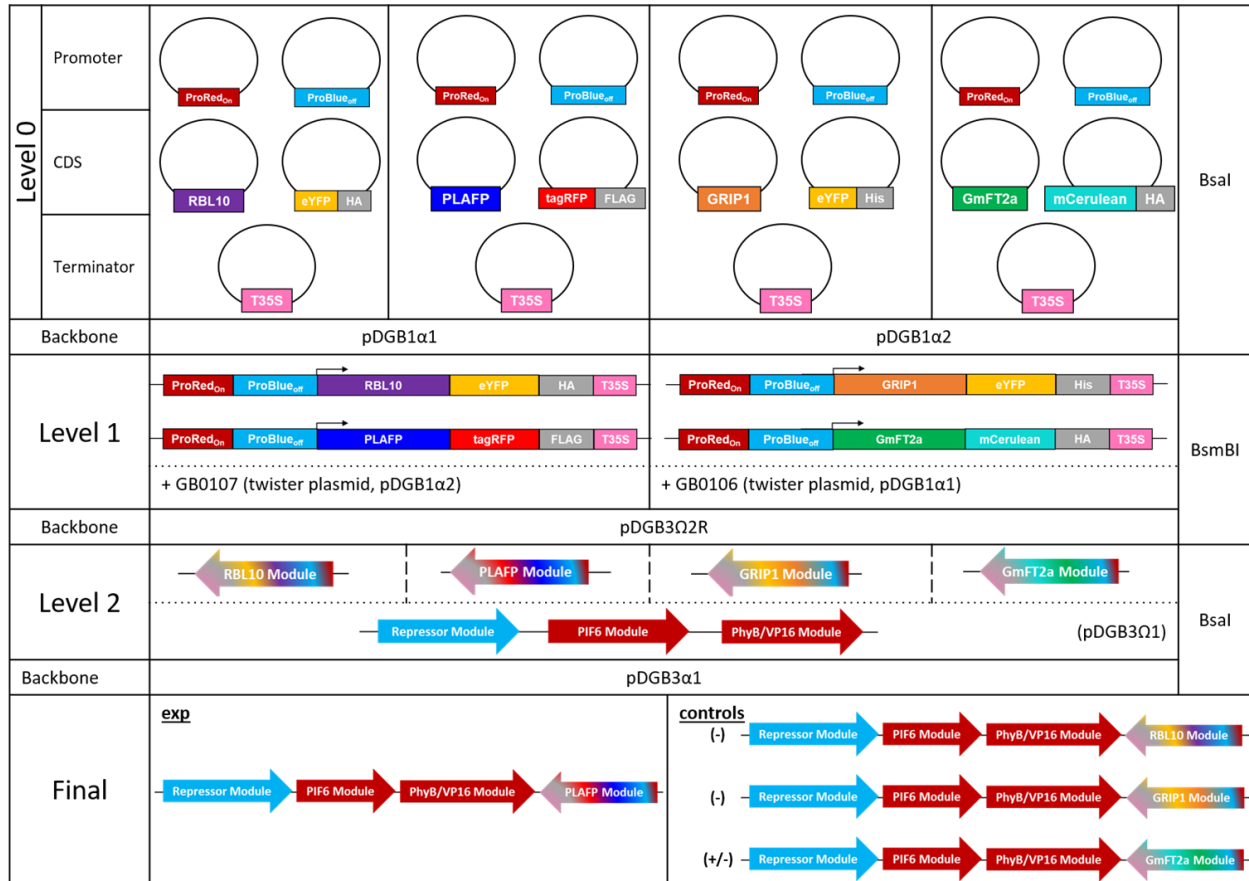


**Figure 4.1 GoldenBraid Cloning Strategy to Generate Optogenetics Constructs.**

### **Protoplast Transfection**

Protoplasts were isolated from 3-4 week old Col-0 Arabidopsis plants and transfected according to Yoo *et al.* (2007) [299]. The Level 1 constructs for pOpto::PLAFP-RFP-Flag and pOpto::GmFT2a-mCerulean-HA (pDGB1α1/2) were each transfected into protoplasts with a light-independent, constitutively expressed activator module, pMZ824 (Figure C.2) [300]. The transfected protoplasts were incubated at room temperature overnight and imaged the following day.

### ***Optogenetics Expression in Tobacco System***

*Nicotiana tabacum* were infiltrated with the PULSE-PLAFP (pDGB3 $\alpha$ 1) construct according to the method described in Chapter 2. 48 hours after infiltration, tobacco plants were moved into white light, 670 nm red light (10  $\mu\text{mol m}^{-2} \text{s}^{-1}$ ), 470 nm blue light (10  $\mu\text{mol m}^{-2} \text{s}^{-1}$ ), or the dark for up to 48 hours. Leaf tissue was collected at 2, 8, 10, 12, 24, and 48 hours for immunoblot analysis, and tobacco plants were imaged with confocal microscopy after 48 hours of light treatment.

### ***Generation of Transgenic Arabidopsis Line***

PULSE-PLAFP construct (Figure C.1) was stably transformed into Arabidopsis Col-0 by floral-dip [301, 302]. Seedlings were sterilized, plated, and germinated as described in Chapter 2 Methods. Kanamycin selection was used to ascertain transformants and T3 homozygous lines. Successful transformation was confirmed by genotyping with PCR (Table C.1). Functionality of the PULSE system was established by exposing transgenic plants to red light (670 nm) and PLAFP-RFP production was assessed by confocal microscopy (Figure C.3).

### ***Systemic Transport Assay***

The light conditions for optogenetic expression of PLAFP in Arabidopsis lines were first optimized in Trichromatic Percival Chambers. PULSE-PLAFP Arabidopsis plants were acclimated in the dark overnight and then moved to the Percival chambers with red light (670 nm) only or white light for 18-24 hours. Several red light intensities (10  $\mu\text{mol m}^{-2} \text{s}^{-1}$ , 20  $\mu\text{mol m}^{-2} \text{s}^{-1}$ , and 40  $\mu\text{mol m}^{-2} \text{s}^{-1}$ ) were tested, and 40  $\mu\text{mol m}^{-2} \text{s}^{-1}$  was determined to be the optimal intensity. The plants were imaged with confocal microscopy

and tissue was collected for further analysis by immunoblot and qPCR prior to and after light treatment.

The MultispeQ V 2.0 [303] was used to expose a single source leaf to red light while the rest of the plant remained in repressive light conditions (i.e. white light or dark). The plants were acclimated in the dark overnight, imaged with confocal microscopy before red light treatment and then placed in white light. The LED panel in the main body of the MultispeQ was set to emit 655 nm light at  $40 \mu\text{mol m}^{-2} \text{s}^{-1}$  for 4 hours and the MultispeQ was clamped to a mature source leaf. After 2 hours, the MultispeQ was opened briefly to allow for gas exchange and then re-clamped for the remaining 2 hours. The red-light treated source leaf and leaves left in white light (“sink”) were imaged, and tissues were collected for further analysis.

### ***Microscopy***

The spectral-based Olympus FluoView 1000 confocal laser-scanning microscope was used to image TagRFP, mCerulean, and chlorophyll autofluorescence. In GmFT2a protoplasts, mCerulean was excited with the 458 nm laser and emission was captured between 480 and 495 nm; chlorophyll autofluorescence was excited by the 515 nm laser and emission was captured above 650 nm. In protoplasts, tobacco, and Arabidopsis, TagRFP and chlorophyll were visualized by exciting with the 559 nm lasers. TagRFP emission was captured between wavelengths 580 nm and 635 nm and chlorophyll was captured in the wavelength range 655-755 nm.

### ***Plant Protein Purification and Immunoblots***

Frozen tobacco leaf samples were ground with a mortar and pestle. 100 mg aliquots were resuspended in 150 mM Tris-HCl (pH 6.8), 7.5%  $\beta$ -mercaptoethanol ( $\beta$ -

me), 3% sodium dodecyl sulfate (SDS), and half a cOmplete mini protease inhibitor tablet (Roche). The samples were centrifuged at 17,000xg at 4°C for 10 minutes. The supernatant was removed and dispensed in a new tube. Protein concentrations were determined by Bradford assay using the Bovine Gamma Globulin Standard Set (BioRad).

Protein samples were combined with 4X Laemmli Buffer (200 mM Tris (pH 6.8), 8% SDS, 40% glycerol, 20%  $\beta$ -me, 0.2% Bromophenol blue) and boiled at 95°C for 5 minutes. 40  $\mu$ l were loaded onto a 10% Mini-PROTEAN TGX pre-cast gel with the Dual Color Protein Ladder (Bio-Rad). The SDS-PAGE ran at 100V for 1.5 hours, then transferred to PVDF at 100V for 2 hours. The blot was stained with Ponceau S staining solution (0.5% (w/v) Ponceau S, 1% acetic acid), rinsed with water, then blocked with 5% milk in TBST for one hour. The blots were incubated in 1:2000 rabbit anti-FLAG antibody (PhytoAB Inc.) in 5% milk in TBST overnight at 4°C. The blots were washed five times with TBST for 10 minutes each. The blots incubated in 1:10,000 goat anti-rabbit IgG HRP secondary antibody (PhytoAB Inc.) in TBST for 1 hour. The blots were washed with TBST 3 times, 10 minutes each, then developed with ECL Prime Western Blotting Detection Reagents (Amersham).

## Results

### ***The PIF6-PhyB module activates expression of genes of interest under the pOpto promoter in Arabidopsis protoplasts.***

The activation mechanism of the PULSE system requires the PhyB-VP16 component binds to PIF6 in a red-light dependent manner. The VP16 transactivator recruits transcription factors to the pOpto promoter, inducing expression in the absence of the blue light repressor complex (Figure 4.2).

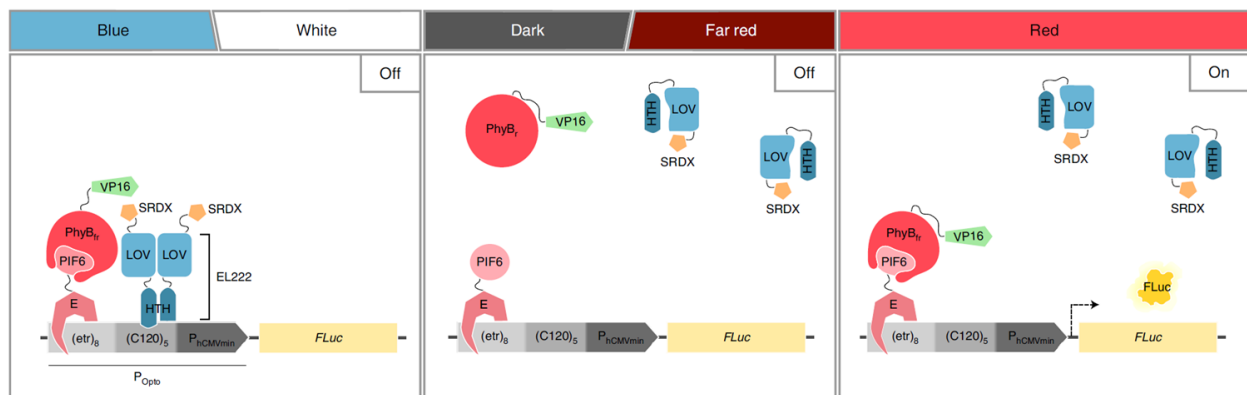


**Figure 4.2 Schematic of the PULSE System.** In blue/white light, the EL222 repressor dimerizes to inhibit expression. The PhyB fragment fused to the VP16 activator only interacts with PIF6 in red light. The PIF6-PhyB-VP16 complex binds the pOpto promoter to initiate transcription. Figure from Ochoa-Fernandez *et al.* (2020).

To confirm that the pOpto promoter properly regulates the expression of downstream genes of interest, *PLAFP* and *GmFT2a* fluorescent protein fusion constructs were co-transfected into protoplasts with a light-independent activator, pMZ824 [300]. The pMZ824 construct contains the VP16 transactivator fused to the DNA-binding E protein and a nuclear localization sequence (Figure C.2). This complex, therefore, does not require red light to interact with the pOpto *etr*<sub>8</sub> region and can activate gene expression in ambient light conditions. The transfected protoplasts were imaged using confocal microscopy. Both *PLAFP*-RFP (Fig 4.3 Top) and *GmFT2a*-mCerulean (Fig 4.3

Bottom) were detected in protoplasts co-transfected with the pMZ824 construct. PLAFP appears in a punctate pattern previously observed in other localization studies. GmFT2a localizes in the cytoplasm of the protoplasts, as expected. These data indicate that the activator module binds the pOpto promoter upstream of *PLAFP* and *GmFT2a* and induces expression in Arabidopsis protoplasts.

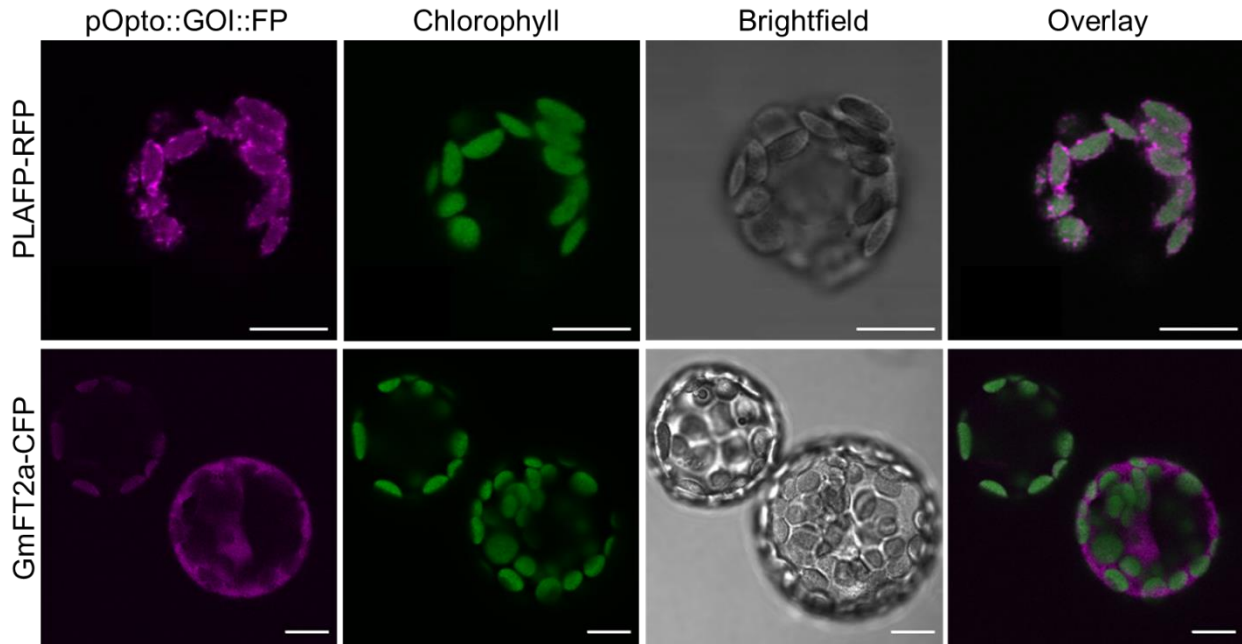


**Figure 4.3 Expression of pOpto Constructs in Protoplasts.** Protoplasts were co-transfected with constitutive activator pMZ824 and pOpto::PLAFP-RFP-Flag (magenta, top panel) or pOpto::GmFT2a-CFP-HA (magenta, bottom panel). Microscopy was used to detect the fluorescently tagged proteins and confirm the functionality of the pOpto promoter. Chlorophyll autofluorescence is shown in green. Scale bar represents 10  $\mu$ m.

***Optimal light conditions for optogenetics control of PLAFP expression were determined with transient expression in tobacco.***

Next, the functionality of the PULSE system was tested in tobacco. *PLAFP* expression and protein detection were optimized using transient expression in tobacco. Tobacco plants infiltrated with the PULSE-PLAFP construct were exposed to red, blue, white light or left in the dark. The plants were imaged with confocal microscopy using the

same acquisition parameters across treatments. PLAFP-RFP was detected only in tobacco plants exposed to red light (Figure 4.4 A, D). Plants left in the dark did not show PLAFP-RFP signal, affirming that expression remains inactive without red light, and *PLAFP* expression is not leaky in this system (Figure 4.4 B). Furthermore, no signal was detected when plants were exposed to white or blue light, indicating that the blue light repressor effectively inhibits expression in these conditions (Figure 4.4 C, E). Therefore, *PLAFP-RFP* expression is inactive or repressed in plants exposed to dark, white, or blue light conditions, and PLAFP-RFP is only produced in red light.

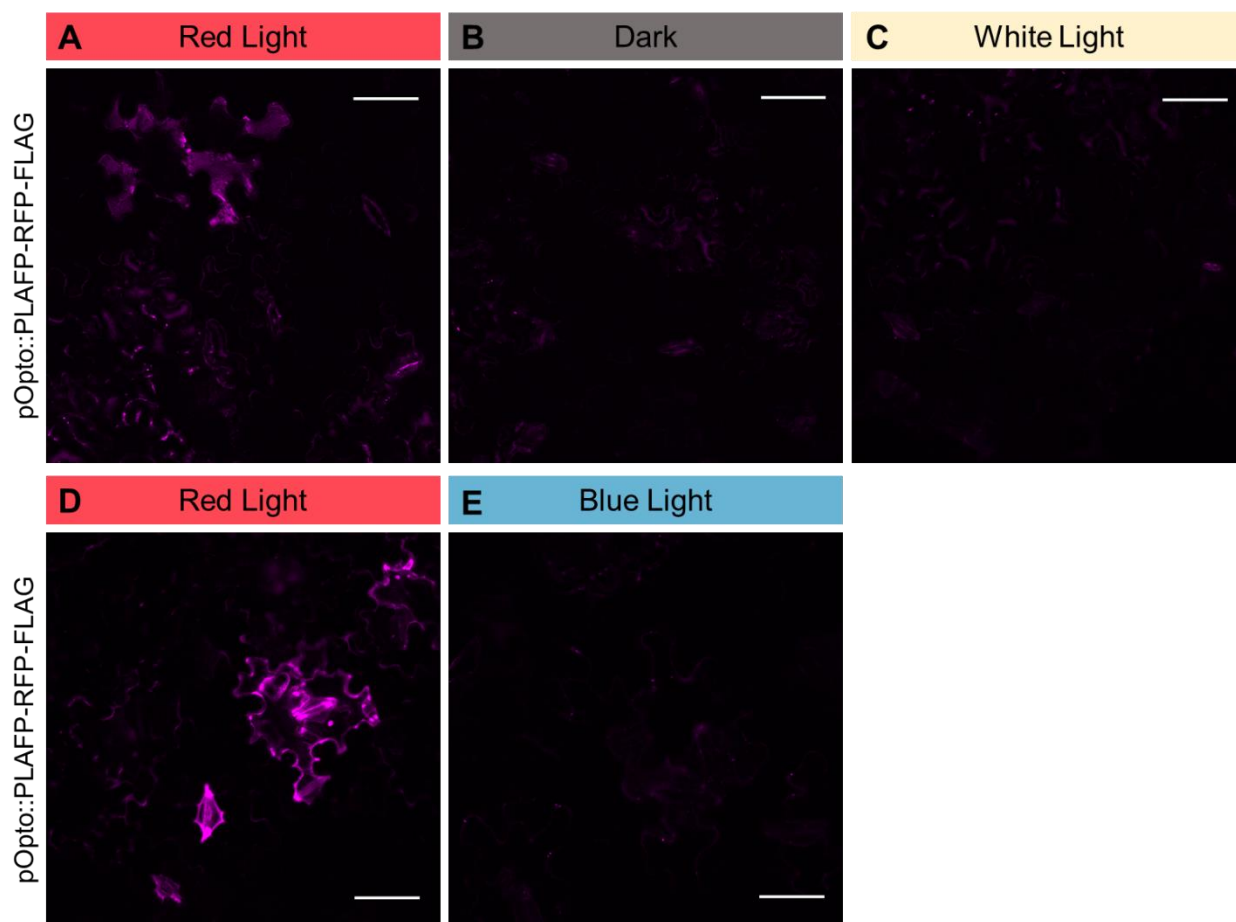


**Figure 4.4 Light Activation and Repression of PULSE-PLAFP in tobacco.** Tobacco infiltrated with PULSE-PLAFP was exposed to red ( $10 \mu\text{mol m}^{-2} \text{s}^{-1}$ ), white, or blue ( $10 \mu\text{mol m}^{-2} \text{s}^{-1}$ ) light or left in the dark for 10 hours (A-C) or 48 hours (D, E) to optimize optogenetically controlled *PLAFP-RFP-Flag* expression. RFP signal is detected after both 10 and 48 hours of red light exposure, indicating activation of *PULSE-PLAFP* expression (A, D). RFP is not detected in dark (B), white (C), or blue (E) light treated plants, which confirms that the PULSE-PLAFP module is inactive in the dark (B) and effectively repressed in the presence of blue light wavelengths (C, E). Scale bar represents 50  $\mu\text{m}$ .

The microscopy images were acquired after 48 hours in each light condition. Tissue samples were harvested for Western blot analysis at 2, 8, 12, 24, and 48 hours of exposure to red or white light. Western blot was used to determine when the PLAFP-RFP-Flag is detectable after activation by red light. When tobacco plants are exposed to red light, a double-band is visible with a smaller band evident at 45 kDa as early as 2

hours and more clearly at 8 hours and later (Figure 4.5 B, C). The ~50 kDa band, representing the large subunit of Rubisco, is present in both the red and white light treated samples, while the smaller 45 kDa PLAFP-RFP-Flag protein band is only observed in red light samples (Figure 4.5). The combination of western blot and confocal microscopy shows that red light induces *PLAFP* expression while blue and white light effectively repress *PLAFP* expression, and exposure to  $10 \mu\text{mol m}^{-2} \text{s}^{-1}$  red light for as little as 2 hours is sufficient to activate detectable PLAFP production in tobacco.

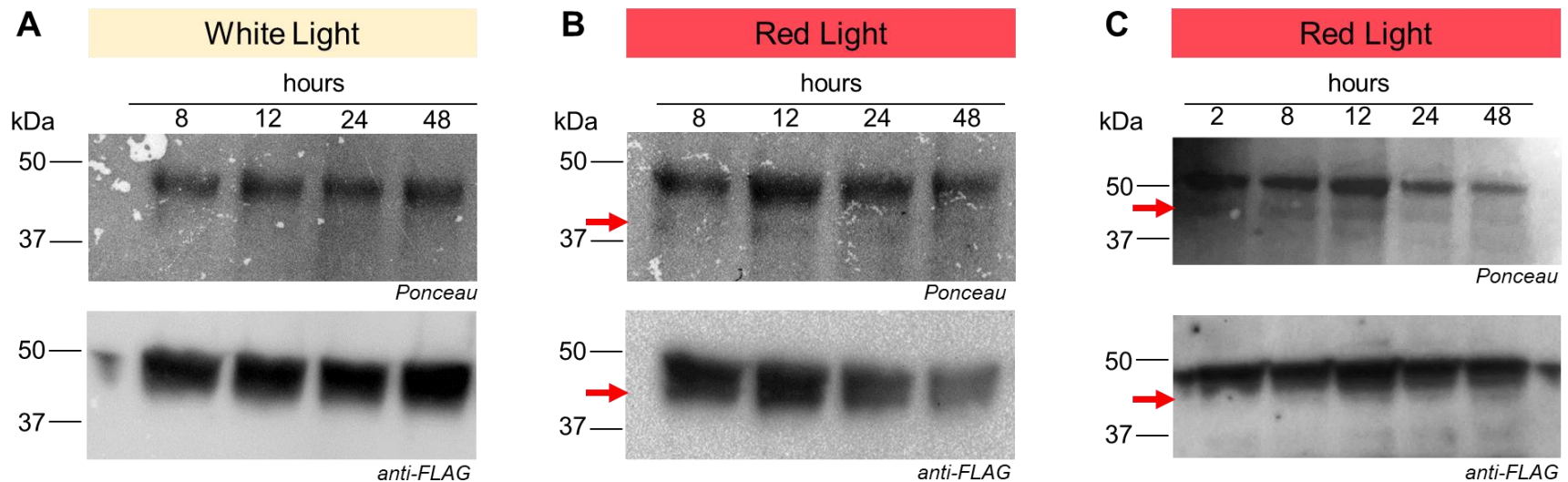


**Figure 4.5 SDS-PAGE and Western Blot Confirmation of PLAFP-RFP-Flag in Tobacco.** *N. tabacum* infiltrated with the PULSE-PLAFP construct was exposed to ambient white light (A) or  $10 \mu\text{mol m}^{-2} \text{s}^{-1}$  red light (B, C) for 48 hours. Blots were first stained with Ponceau, then subsequently an anti-Flag antibody was used to detect PLAFP-RFP-Flag. The large subunit of rubisco is present in both red and white light samples (52.9 kDa), however a smaller band below it, denoted by red arrows, is only observed in red light treated samples (B, C), indicating that PLAFP-RFP-Flag (45.5 kDa) is produced only when plants are exposed to red light.

***PLAFP is detected in untreated sink tissue when a source tissue is activated with red light, indicative of systemic movement.***

First, PLAFP production in stably transformed Arabidopsis lines was confirmed by exposing entire plants to red or white light in Trichromatic Percival chambers and assessing the presence of PLAFP-RFP with confocal microscopy. When a whole PULSE-PLAFP plant was exposed to  $10 \mu\text{mol m}^{-2} \text{s}^{-1}$  red light, RFP signal is detected in a Z-series image (Figure 4.6 A). The RFP signal is absent in wildtype plants treated with the same red light conditions (Figure 4.6 C). Conversely, when the PULSE-PLAFP plant is placed in ambient white light, little to no RFP signal is observed, indicating that expression is repressed by the blue light component (Figure 4.6 B). Several stable PULSE-PLAFP lines were evaluated in red and dark conditions (Figure C.3), and lines 5-5 and 8-4 were selected as the best lines for further study.

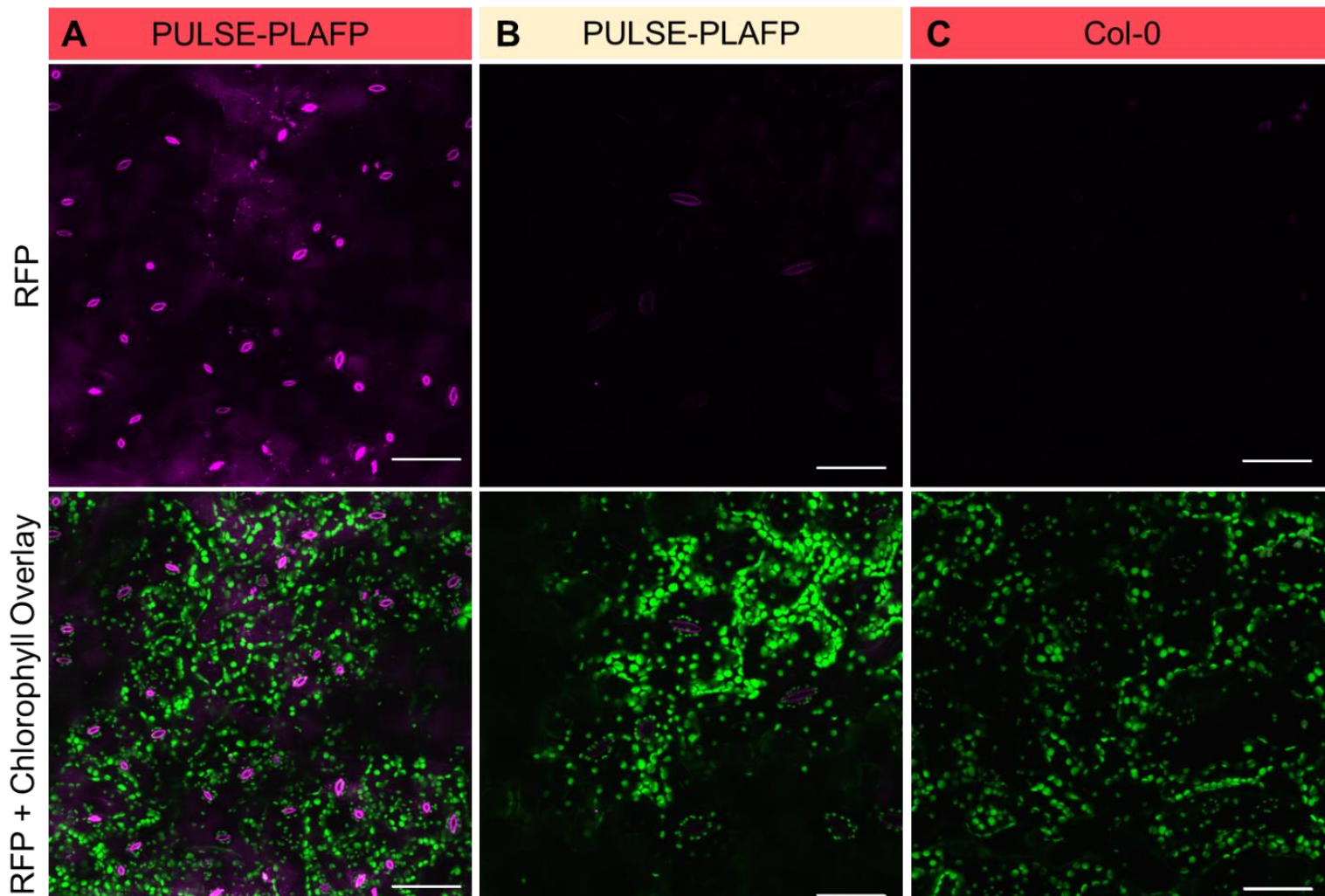


**Figure 4.6 Assessment of PULSE-PLAFP Activation in Transgenic Arabidopsis.** A Z-series of T1 transgenic Arabidopsis plants (confirmed with genotyping) was captured using confocal microscopy to assess PULSE-PLAFP activation in red light. The Z-stacks show RFP signal in the red light ( $10 \mu\text{mol m}^{-2} \text{s}^{-1}$ ) treated transgenic plant (A), whereas little to no RFP is observed in the PULSE-PLAFP plant exposed to ambient white light (B) or the wild-type plant in red light (C). Scale bar represents 50  $\mu\text{m}$ .

To assess systemic movement of PLAFP, a single mature leaf of stable PULSE-PLAFP transgenic Arabidopsis lines was exposed to  $40 \mu\text{mol m}^{-2} \text{s}^{-1}$  red light for 4 hours using the MultispeQ. All other leaves remained in ambient white light to repress *PLAFP* expression in distal tissues (Figure 4.7). The red light intensity was increased in these experiments to ensure adequate expression throughout the leaf during a shorter length of time, which was necessary to minimize limitations to gas exchange in the MultispeQ.

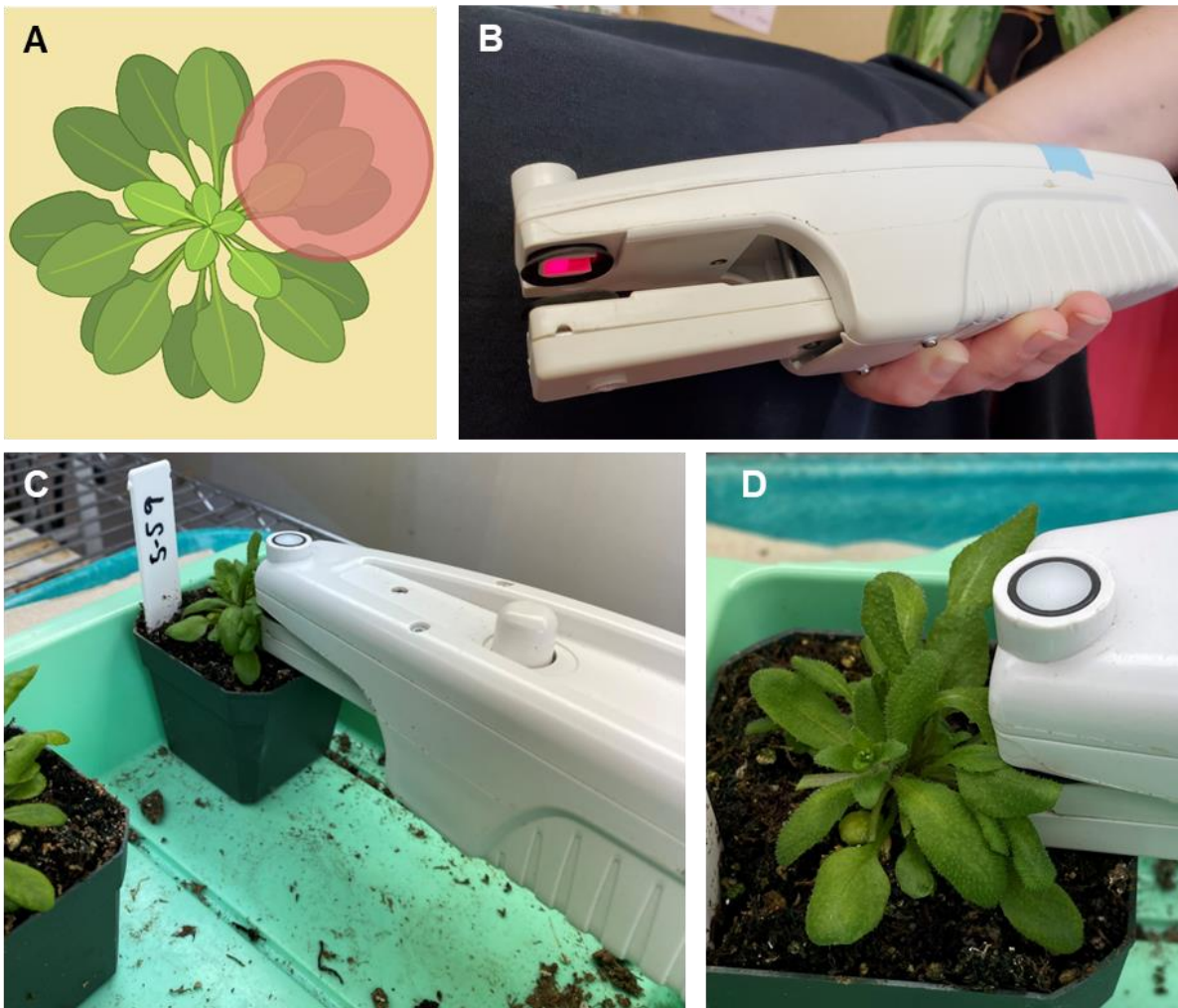


**Figure 4.7 Experimental Setup for Systemic Movement using the MultispeQ.** A cartoon shows Arabidopsis rosette in ambient white light (yellow) and red light exposure targeted to specific leaves (A). The MultispeQ clamp is open to reveal red LEDs in the chamber (B). The MultispeQ is clamped on a single leaf of PULSE-PLAFP transgenic plants to treat a source leaf with red light and optogenetically activate expression. Meanwhile, the rest of the plant remains in white light to repress expression in distal tissue (C,D).

The presence of PLAFP was determined with confocal microscopy, and tissues were collected for further analysis using qPCR and Western blot. This will indicate whether RNA or protein are the mobile compounds. Before exposure to red light, there was no detectable RFP signal in Arabidopsis line PULSE-PLAFP 5-5 (Figure 4.8 A). After a single (source) leaf was treated with red light for 4 hours, PLAFP is observed not only in tissue activated by red light and expressing *PLAFP* (Figure 4.8 B) but also in distal untreated leaves that are transcriptionally repressed in white light conditions (Figure 4.8 C). RFP signal was detected in both treated local tissue and untreated distal tissue in multiple independent PULSE-PLAFP lines. These data suggest PLAFP is produced in a transcriptionally activated source tissue and is then systemically transported to transcriptionally repressed distal tissues.

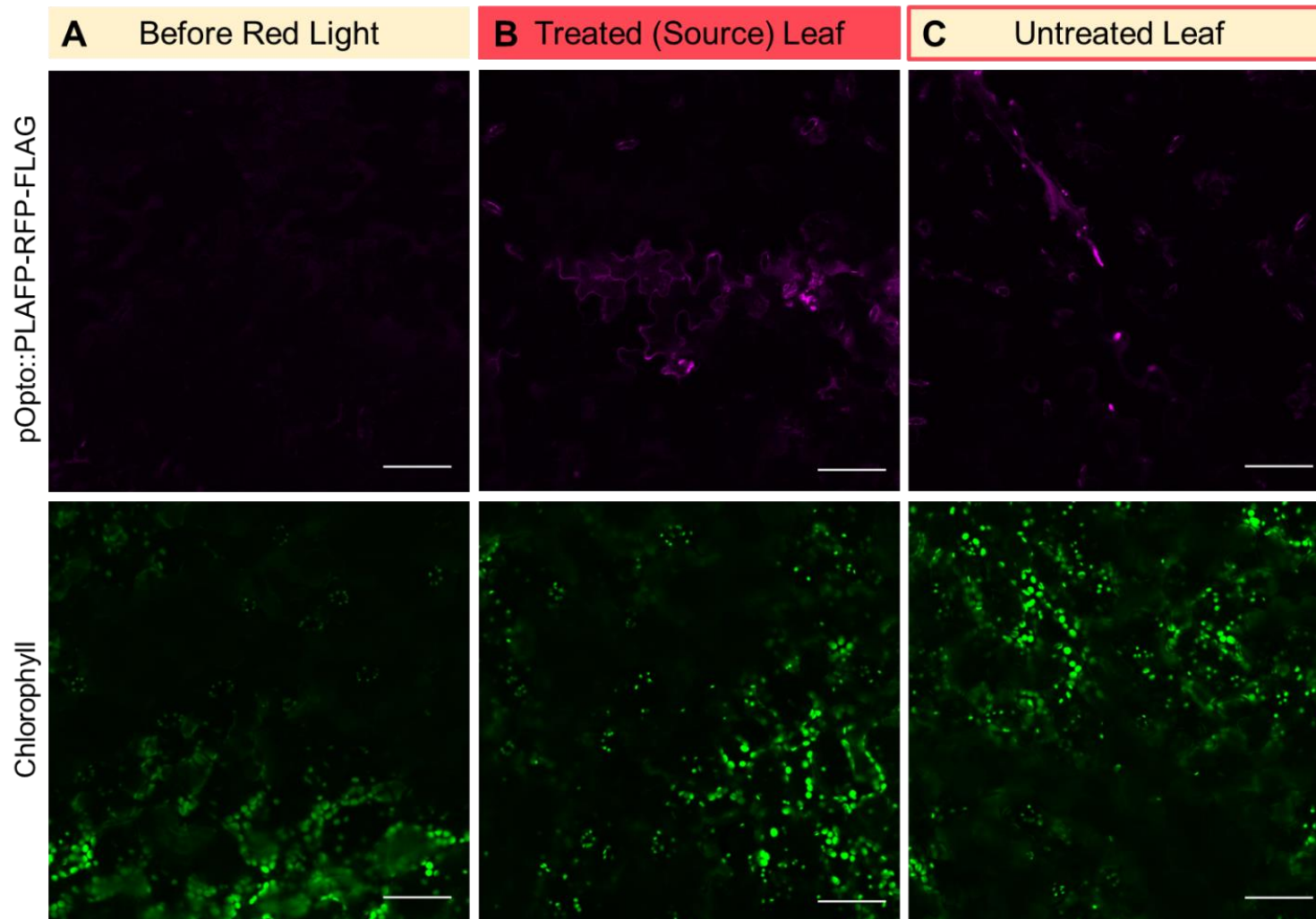


**Figure 4.8 Systemic Movement of PLAFP-RFP in Arabidopsis.** A single source leaf was exposed to red light ( $40 \mu\text{mol m}^{-2} \text{s}^{-1}$ ) with the MultispeQ. After 4 hours of red light treatment, the source leaf (B) and untreated leaves (C) were imaged using confocal microscopy. Before exposure to red light, no PLAFP-RFP was detected (A). PLAFP-RFP is observed not only the source leaf (B), but also the untreated leaf in transcriptionally repressive light conditions (C), which suggests that PLAFP-RFP is generated in the treated leaf and moves systemically from source tissue to untreated “sink” tissue. Scale bar represents 50  $\mu\text{m}$ .

## Discussion

Grafting has been the standard method for the study of long-distance movement and systemic signaling, despite the complexity and intricacy of a technique that requires expertise and multiple transgenic resources. Inducible systems offer a more accessible and widely applicable alternative to grafting. However, chemically inducible systems run the risk of off-target effects, toxicity, or mobility of the chemical itself. Hence, the development of a light-inducible system for the investigation of systemic movement in plants allows for a precisely tunable and dynamic switch that can better pinpoint long-distance translocation. In this chapter, I developed a method to study systemic transport of proteins in plants using optogenetics tools, and consequently showed that PLAFP is translocated from local to distal tissues.

This novel method for understanding mobile signals *in planta* employs an optogenetics tool called PULSE, in which transgenic plants can be grown under normal (white-) light conditions and the transgene(s) is only activated in red light [295]. This tool enables the study of a wide array of processes with direct manipulation of specific signaling components, while maintaining the closest approximation to natural growth conditions. In this application, I activated expression in a single leaf while the rest of the plant remained in normal white light to study systemic transport of proteins from local to distal tissues. The PULSE system reported detectable proteins within 6 hours of exposure to  $10 \mu\text{mol m}^{-2} \text{s}^{-1}$  red light [295]. Using this innovative optogenetics tool, I was able to detect labelled protein in as little as 2 hours after exposure to red light (Figure 4.4), demonstrating the rapidness with which this system can be employed. Although the phloem flow velocity can vary according to developmental stage, the diurnal cycle, plant

species, or in response to stresses like drought and wounding [304-307], average reported phloem flow velocities fall in the 0.1-0.6 mm s<sup>-1</sup> range [304]. Phloem-mobile signals move in accordance with the speed of phloem stream. Even at the lower end of the velocity range, macromolecules could be translocated across an Arabidopsis plant in 30 minutes [6]. Detection of PLAFP-RFP in distal tissue requires sufficient time for activation of the PULSE-PLAFP, production of PLAFP-RFP, and translocation from treated source tissue to untreated “sink.” Given that PLAFP-RFP is observed in red light treated leaves within 2 hours (Figure 4.4), 4 hours of red light treatment was sufficient to detect PLAFP-RFP in untreated distal leaves (Figure 4.8C) Longer exposure to red light or delayed detection after treatment may increase signal in the distal tissue.

During the interrogation of PLAFP systemic movement, PLAFP-RFP signal is observed in distal tissue that was transcriptionally repressed in white light (Figure 4.6C), which purports systemic translocation from treated tissue to other parts of the plant. PLAFP-RFP localizes to the periphery of the epidermal cells in the treated source tissue, however the localization in distal tissue is sometimes different from the source (Figure 4.6 A, C). Here, we may be observing PLAFP in the apoplastic space during phloem unloading. Phloem loading and unloading occurs by multiple different mechanisms, including symplastic and apoplastic pathways [2, 308]. In symplastic mechanisms, photosynthates and other macromolecules are transported from the phloem stream via plasmodesmata, from cytoplasm to cytoplasm. However, some unloading utilizes the apoplastic space between cells to move molecules from the sieve element to cells in the distal tissue [309]. For example, root-derived cytokinin is distributed in shoots via apoplastic unloading [310]. PLAFP most likely enters the sieve element through

plasmodesmata in symplastic loading, however it may enter the apoplast during unloading. Moreover, it is possible PLAFP binds a receptor or transporter on the outside of the cell or in target tissue, consistent with RFP signal in the apoplast of “sink” tissue.

From the microscopy data, it is unclear whether the protein, the transcript, or both are transported. Harvested tissue from these experiments will be used for Western blots to confirm the presence of protein in both treated and untreated leaves and for RT-PCR to test for the PLAFP-RFP-Flag transcript. If the transcript is detected only in the treated tissue, it is likely the protein is transported; however if the transcript is detected in both treated and untreated tissues, then either the mRNA is mobile and then transcribed in both source and distal leaves or both protein and mRNA are systemically translocated. While *PLAFP* mRNA was not found among transcripts known to be translocated into the SE, PLAFP protein has been identified in phloem sap, further supporting the hypothesis that the protein is the mobile signal [144, 181].

This novel method unveiled long-distance translocation of PLAFP, a protein identified in phloem sap but not previously shown, until now, to be phloem-mobile. The application of the PULSE system will be further validated as a tool for studying long-distance movement by applying it to proven mobile signals, like Flowering Locus T. These studies are currently underway, in collaboration with the Zurbriggen lab to establish stable transgenic lines of fluorescently tagged soybean FT under the regulation of the pOpto promoter. Overall, the PULSE system is a promising, targeted, and minimally invasive approach to investigate systemic signaling *in planta*. It is a method that now can be used by any phloem researcher to examine mobility of either protein or mRNA.

## **CHAPTER 5.**

### **Conclusions and Future Directions.**

## Summary

The complexity and multidimensionality of plant stress and development necessitates rapid and precise systemic coordination for efficient perception, communication, and response. In this dissertation, I characterized a novel phloem-mobile protein, Phloem Lipid-Associated Family Protein (PLAFP) involved in lipid-mediated long-distance signaling. Despite the hydrophilicity of the phloem, lipids and lipid-binding proteins (LBPs) have been identified in phloem exudates [13]. Here, I show that these predicted LBPs do bind phospholipids (Figure 2.1) and their expression fluctuates in response to osmotic, salt, and drought stress factors (Figure 2.2). The changes in LBP gene expression correlate with expression profiles of phospholipases that produce stress-responsive signaling lipids, like phosphatidic acid (PA). Phloem Lipid-Associated Family Protein (PLAFP) binds PA, and *PLAFP* expression increases in response to drought and abscisic acid (ABA). A PLAT/LH2 domain, predicted to function in lipid binding and protein-protein interaction, is the single domain of PLAFP. Experimental and computational data suggest that conserved basic residues Lys-42 and Arg-82 contribute to detection of the negatively charged phosphate headgroup in PA and adjacent tryptophan residues may play a role in lipid solubilization in a hydrophobic pocket of PLAFP (Figures 3.2-3.4). Although PLAFP was identified in phloem sap and its promoter is active in the plant vasculature [181], further study was needed to establish PLAFP as a phloem-mobile protein. I developed a novel optogenetics-based approach, implementing the recently engineered PULSE system [295], to investigate systemic movement. Application of this approach in transgenic *Arabidopsis* revealed that PLAFP-RFP-Flag was produced in red-light activated source tissue and subsequently detected

in distal tissue, where *pOpto::PLAFP* was repressed by white light conditions (Figure 4.8). These results indicate PLAFP as a phloem-mobile protein, translocated from source to sink tissue. Once unloaded out of the phloem and into distal tissue, PLAFP must be perceived by a receptor for the signal to be transmitted. Vascular Highway 1 Kinase (VH1K), a receptor-like kinase previously implicated in vascular development [248] and whose ligand is unknown [247], was found to interact with PLAFP *in vitro* (Figure 3.1). PLAFP and VH1K co-localize *in vivo*, affirming VH1K as a candidate for a PLAFP receptor (Figure 3.5). Finally, differentially expressed genes (DEGs) in *PLAFP* overexpression and knockdown lines are associated with endoplasmic reticulum-, abiotic-, and drought stress. DEGs include transcription factors, a predicted GTPase, and other regulatory proteins with possible roles in signaling.

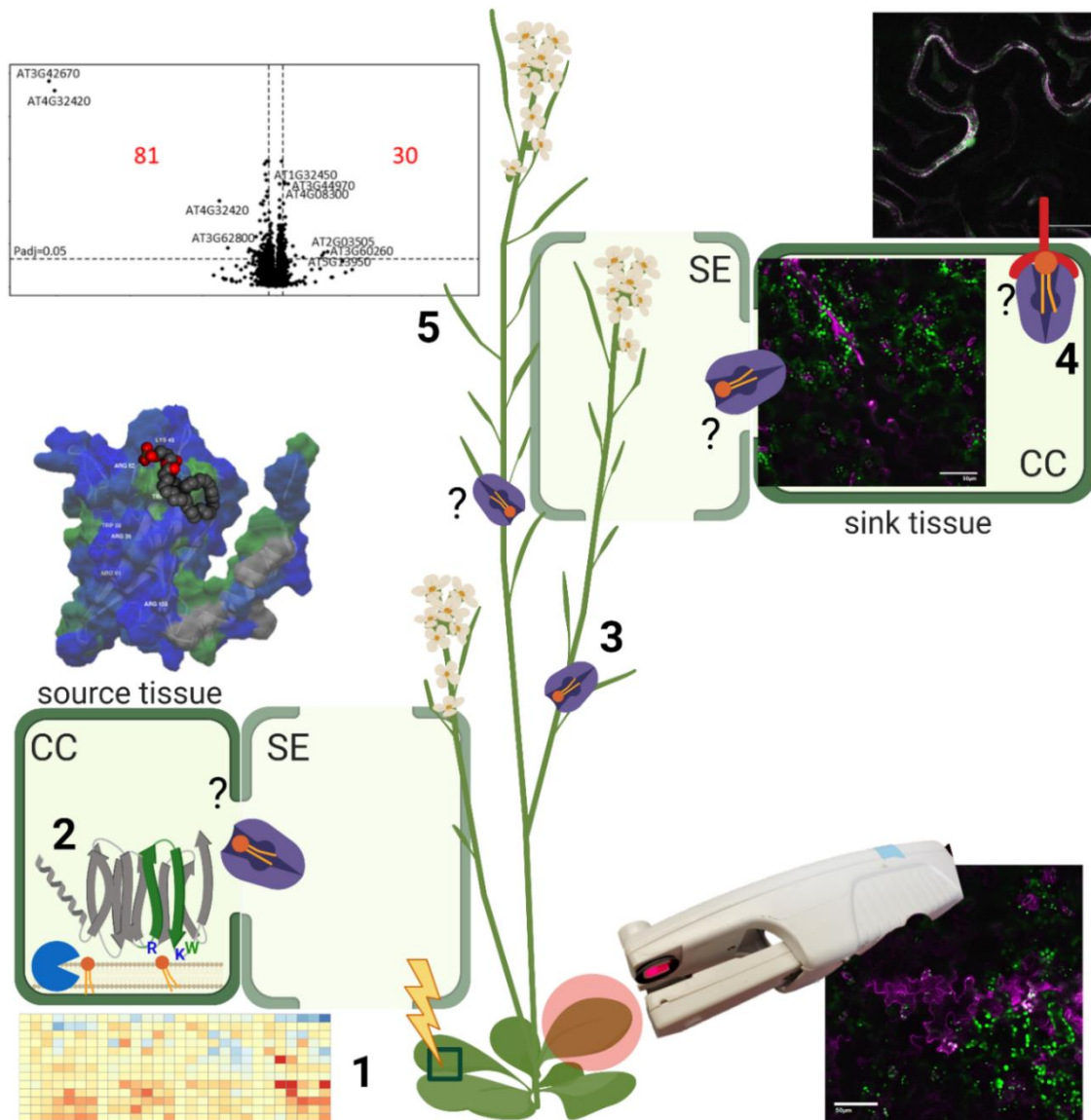


**Figure 5.1 Lipid-Mediated Systemic Signaling for Abiotic Stress Response.**

**(1)** Abiotic stress changes the expression of lipid-binding proteins (LBPs) identified in phloem sap. Some changes correlate with expression of phospholipases that generate phosphatidic acid (PA) (Chapter 2). **(2)** Phloem Lipid Associated-Family Protein (PLAFP), interacts with PA, facilitated, in part, by conserved basic residues Arg-82 and Lys-42 and hydrophobic regions enriched in tryptophans (Chapter 3). The mechanism by which PLAFP is loaded into the phloem and whether it moves in complex with PA is unknown. **(3)** A novel optogenetics approach revealed that PLAFP from source tissue is detected in distal tissue, indicative of systemic movement (Chapter 4). **(4)** PLAFP interacts with receptor-like kinase Vascular Highway 1 Kinase (VH1K), and they co-localize *in vivo* (Chapter 3). PA may facilitate this interaction. VH1K is a candidate for perception and transduction of the PLAFP mobile signal. **(5)** RNA-Seq suggests PLAFP as an activator of drought- and/or endoplasmic reticulum- stress mechanisms (Chapter 3). PLAFP is phloem-mobile and acts in PA-mediated systemic signaling for abiotic stress response. Created with [BioRender.com](https://www.biorender.com)

## Future Work

### ***Further Elucidation of the PLAFP Phosphatidic Acid-Binding Mechanism***

Although there is no universally defined PA binding domain, motifs composed of basic positively-charged residues with hydrophobic regions nearby are typical in proteins that bind PA [136, 241]. While single point mutations do not ablate PA-binding activity in PLAFP, multi-site mutations and quantitative assays that can detect subtle changes in binding affinity can further elucidate critical residues and regions for PLAFP-PA complex formation. The R82A single mutant was insufficient to reduce PLAFP interaction with PA, as observed in lipid overlay assays (Figure 3.4), however computational modelling places conserved Lys-42 in proximity to Arg-82 (Figure 3.3). A K42A/R82A double mutant may abolish PLAFP binding to the negatively charged phosphate headgroup. This can be investigated using lipid overlay assays, as described in this dissertation, coupled with liposome binding assays that allow for a quantitative approximation of binding and more closely mimic the membrane environment. Moreover, liposome binding assays obscure the acyl chains, requiring basic residues to work in conjunction with hydrophobic residues to first bind the headgroup and permit interaction with the buried fatty acid component. In overlay assays, the overt accessibility of the acyl chains may confound the effects of mutations.

Complementation can begin to clarify the role of PLAFP-PA interaction in plants. PA levels in phloem sap vary across *PLAFP* knockdown and overexpression lines (Hurlock *et al.*, in preparation). We can test whether PLAFP point or multi-site mutants complement the *PLAFP* knockdown line and restore phloem PA levels. If mutants that affect PA binding cannot restore the presence of phospholipids in the phloem, then

PLAFP interaction with PA is necessary for PA loading into the phloem. This would support the hypothesis that PLAFP solubilizes PA and they translocate as a complex in the phloem.

### ***Confirmation of PLAFP Systemic Movement***

The PULSE optogenetics tool is a revolutionary application for the study of systemic signaling. The method revealed long-distance movement of PLAFP using confocal microscopy. PLAFP translocated to distal tissue can be confirmed using Western blots and RT-PCR. It is unclear whether the protein itself moves or if its mRNA transcript is mobile and is subsequently translated in sink tissue. RT-PCR can probe for PLAFP-RFP-Flag transcripts in untreated tissue, where the pOpto promoter is repressed. Moreover, phloem sap can be extracted from plants in which a single leaf is activated by red light. The sap samples can be analyzed by RT-PCR, Western blot, and mass spectrometry to identify PLAFP-RFP-Flag protein and/or mRNA in exudates.

Other proteins, already established as phloem-mobile with grafting and other traditional approaches, can be evaluated with this novel method to further validate it as a reliable tool. Studies are currently underway to generate transgenic lines with PULSE-GmFT2a-mCerulean-HA. The *Glycine max* Flowering Locus T (GmFT2a) protein can be assessed for movement, and the transcript is distinct from native Arabidopsis *FT* which allows for detection and control of off-target effects.

PLAFP moves, however the role of PA in this mechanism remains unclear. PLAFP-PA may move as a complex. The PULSE system can be used in conjunction with fluorescently-labelled phosphatidic acid and FRET approaches can be implemented to probe source, phloem, and sink tissues for PLAFP, PA, and PLAFP-PA signals.

Moreover, radiolabeled PA can be applied to *PLAFP* knockdown and overexpression lines, and the amount of radiolabeled PA in the phloem and in distal tissue can be assessed compared to wild-type. If PLAFP contributes to PA mobility, *PLAFP* overexpression lines should enhance PA translocation and *PLAFP* knockdown lines should show reduced PA phloem localization and movement.

### ***Expansion of the PLAFP-Mediated Signal in Distal Tissue***

Future work to elucidate the PLAFP-PA-VH1K signaling cascade includes genetic approaches to investigate the role of VH1K in PLAFP-mediated processes. For example, *vh1k* knock-outs could be evaluated for response to drought and whether it phenocopies *PLAFP* knockdown lines. Additionally, we can test whether constitutively active VH1K rescues *PLAFP* knockdown phenotypes through complementation. The target(s) of VH1K is unknown, so PLAFP and VIK, and other putative VH1K-interactors, can be assessed for phosphorylation using Western blot and kinase activity assays. Levels of phosphorylation can be determined in VH1K overexpression lines compared to wild-type and/or knockouts. PA may be required for or facilitate protein-protein interaction in a mechanism similar to Frizzled/Wnt in mammals where palmitoylation is required for binding [106, 194]. This can be tested by mutating the PA binding domains to inhibit the PLAFP-VH1K interaction or, if PA is required for VH1K activation, the generation of PA can be modulated by overexpression or knockdown of phospholipases then VH1K activity can be measured.

*PLAFP* expression levels caused some genetic response, as uncovered by RNA-Seq (Figure 3.6). However, a more robust change in the transcriptome may require changes in modules up- or down- stream of PLAFP activity. To expand on the genetic

response to PLAFP signaling, *PLAFP* knockdown and overexpression lines can be subjected to drought stress or ABA treatment. The differentially expressed genes compared to Col-0 and among the expression lines can further identify likely genes and processes involved in PLAFP-mediated pathways.

## **Conclusion**

Overall, the work in this dissertation characterized PLAFP, among other phloem-localized LBPs, as a model systemic signal in PA-mediated long-distance signaling. The multilayered mechanism ensures specific, rapid, and targeted responses for coordination of stress response across the whole plant and expands the arsenal of translocated signaling macromolecules. This work pioneers a prospective field of mobile protein-lipid complexes in systemic signaling.

## REFERENCES

1. Muench, E., *Die Stoffbewegungen in der Pflanze*. 1930, Jena, Germany: Fischer.
2. Zhang, C. and R. Turgeon, *Mechanisms of phloem loading*. *Curr Opin Plant Biol*, 2018. **43**: p. 71-75.
3. Turgeon, R., *The role of phloem loading reconsidered*. *Plant Physiol*, 2010. **152**(4): p. 1817-23.
4. Turgeon, R. and S. Wolf, *Phloem transport: cellular pathways and molecular trafficking*. *Annu Rev Plant Biol*, 2009. **60**: p. 207-21.
5. Zhang, C., L. Han, T.L. Slewinski, J. Sun, J. Zhang, Z.Y. Wang, and R. Turgeon, *Symplastic phloem loading in poplar*. *Plant Physiol*, 2014. **166**(1): p. 306-13.
6. Ross-Elliott, T.J., K.H. Jensen, K.S. Haaning, B.M. Wager, J. Knoblauch, A.H. Howell, D.L. Mullendore, A.G. Monteith, D. Paultre, D. Yan, S. Otero, M. Bourdon, R. Sager, J.Y. Lee, Y. Helariutta, M. Knoblauch, and K.J. Oparka, *Phloem unloading in Arabidopsis roots is convective and regulated by the phloem-pole pericycle*. *Elife*, 2017. **6**.
7. Truernit, E., *Plant Physiology: Unveiling the Dark Side of Phloem Translocation*. *Curr Biol*, 2017. **27**(9): p. R348-R350.
8. Milne, R.J., C.P. Grof, and J.W. Patrick, *Mechanisms of phloem unloading: shaped by cellular pathways, their conductances and sink function*. *Curr Opin Plant Biol*, 2018. **43**: p. 8-15.
9. Tegeder, M. and U.Z. Hammes, *The way out and in: phloem loading and unloading of amino acids*. *Curr Opin Plant Biol*, 2018. **43**: p. 16-21.
10. Troncoso-Ponce, M.A., X. Cao, Z. Yang, and J.B. Ohlrogge, *Lipid turnover during senescence*. *Plant Sci*, 2013. **205-206**: p. 13-9.
11. Lucas, W.J., A. Groover, R. Lichtenberger, K. Furuta, S.R. Yadav, Y. Helariutta, X.Q. He, H. Fukuda, J. Kang, S.M. Brady, J.W. Patrick, J. Sperry, A. Yoshida, A.F. Lopez-Millan, M.A. Grusak, and P. Kachroo, *The plant vascular system: evolution, development and functions*. *J Integr Plant Biol*, 2013. **55**(4): p. 294-388.
12. Atkins, C.A., P.M. Smith, and C. Rodriguez-Medina, *Macromolecules in phloem exudates--a review*. *Protoplasma*, 2011. **248**(1): p. 165-72.
13. Guelette, B.S., U.F. Benning, and S. Hoffmann-Benning, *Identification of lipids and lipid-binding proteins in phloem exudates from Arabidopsis thaliana*. *J Exp Bot*, 2012. **63**(10): p. 3603-16.

14. Ham, B.K. and W.J. Lucas, *Phloem-Mobile RNAs as Systemic Signaling Agents*. *Annu Rev Plant Biol*, 2017. **68**: p. 173-195.
15. Liu, L. and X. Chen, *Intercellular and systemic trafficking of RNAs in plants*. *Nat Plants*, 2018. **4**(11): p. 869-878.
16. Kehr, J. and F. Kragler, *Long distance RNA movement*. *New Phytol*, 2018. **218**(1): p. 29-40.
17. Deeken, R., P. Ache, I. Kajahn, J. Klinkenberg, G. Bringmann, and R. Hedrich, *Identification of Arabidopsis thaliana phloem RNAs provides a search criterion for phloem-based transcripts hidden in complex datasets of microarray experiments*. *Plant J*, 2008. **55**(5): p. 746-59.
18. Sasaki, T., M. Chino, H. Hayashi, and T. Fujiwara, *Detection of several mRNA species in rice phloem sap*. *Plant Cell Physiol*, 1998. **39**(8): p. 895-7.
19. Doering-Saad, C., H.J. Newbury, J.S. Bale, and J. Pritchard, *Use of aphid stylectomy and RT-PCR for the detection of transporter mRNAs in sieve elements*. *J Exp Bot*, 2002. **53**(369): p. 631-7.
20. Gaupels, F., A. Buhtz, T. Knauer, S. Deshmukh, F. Waller, A.J. van Bel, K.H. Kogel, and J. Kehr, *Adaptation of aphid stylectomy for analyses of proteins and mRNAs in barley phloem sap*. *J Exp Bot*, 2008. **59**(12): p. 3297-306.
21. Ruiz-Medrano, R., B. Xoconostle-Cazares, and W.J. Lucas, *Phloem long-distance transport of CmNACP mRNA: implications for supracellular regulation in plants*. *Development*, 1999. **126**(20): p. 4405-19.
22. Omid, A., T. Keilin, A. Glass, D. Leshkowitz, and S. Wolf, *Characterization of phloem-sap transcription profile in melon plants*. *J Exp Bot*, 2007. **58**(13): p. 3645-56.
23. Doering-Saad, C., H.J. Newbury, C.E. Couldridge, J.S. Bale, and J. Pritchard, *A phloem-enriched cDNA library from Ricinus: insights into phloem function*. *J Exp Bot*, 2006. **57**(12): p. 3183-93.
24. Rodriguez-Medina, C., C.A. Atkins, A.J. Mann, M.E. Jordan, and P.M. Smith, *Macromolecular composition of phloem exudate from white lupin (Lupinus albus L.)*. *BMC Plant Biol*, 2011. **11**: p. 36.
25. Guo, S., J. Zhang, H. Sun, J. Salse, W.J. Lucas, H. Zhang, Y. Zheng, L. Mao, Y. Ren, Z. Wang, J. Min, X. Guo, F. Murat, B.K. Ham, Z. Zhang, S. Gao, M. Huang, Y. Xu, S. Zhong, A. Bombarely, L.A. Mueller, H. Zhao, H. He, Y. Zhang, S. Huang, T. Tan, E. Pang, K. Lin, Q. Hu, H. Kuang, P. Ni, B. Wang, J. Liu, Q. Kou, W. Hou, X. Zou, J. Jiang, G. Gong, K. Klee, H. Schoof, Y. Huang, X. Hu, S. Dong, D. Liang,

- J. Wang, K. Wu, Y. Xia, X. Zhao, Z. Zheng, M. Xing, X. Liang, B. Huang, T. Lv, Y. Yin, H. Yi, R. Li, M. Wu, A. Levi, X. Zhang, J.J. Giovannoni, Y. Li, and Z. Fei, *The draft genome of watermelon (Citrullus lanatus) and resequencing of 20 diverse accessions*. Nat Genet, 2013. **45**(1): p. 51-8.
26. Notaguchi, M., T. Higashiyama, and T. Suzuki, *Identification of mRNAs that move over long distances using an RNA-Seq analysis of Arabidopsis/Nicotiana benthamiana heterografts*. Plant Cell Physiol, 2015. **56**(2): p. 311-21.
  27. Thieme, C.J., M. Rojas-Triana, E. Stecyk, C. Schudoma, W. Zhang, L. Yang, M. Minambres, D. Walther, W.X. Schulze, J. Paz-Ares, W.R. Scheible, and F. Kragler, *Endogenous Arabidopsis messenger RNAs transported to distant tissues*. Nat Plants, 2015. **1**(4): p. 15025.
  28. Yoo, B.C., F. Kragler, E. Varkonyi-Gasic, V. Haywood, S. Archer-Evans, Y.M. Lee, T.J. Lough, and W.J. Lucas, *A systemic small RNA signaling system in plants*. Plant Cell, 2004. **16**(8): p. 1979-2000.
  29. Tolstyko, E., A. Lezzhov, and A. Solovyev, *Identification of miRNA precursors in the phloem of Cucurbita maxima*. PeerJ, 2019. **7**: p. e8269.
  30. Zhang, S., L. Sun, and F. Kragler, *The phloem-delivered RNA pool contains small noncoding RNAs and interferes with translation*. Plant Physiol, 2009. **150**(1): p. 378-87.
  31. Gai, Y.P., H.N. Zhao, Y.N. Zhao, B.S. Zhu, S.S. Yuan, S. Li, F.Y. Guo, and X.L. Ji, *MiRNA-seq-based profiles of miRNAs in mulberry phloem sap provide insight into the pathogenic mechanisms of mulberry yellow dwarf disease*. Sci Rep, 2018. **8**(1): p. 812.
  32. Zhang, Z., Y. Zheng, B.K. Ham, J. Chen, A. Yoshida, L.V. Kochian, Z. Fei, and W.J. Lucas, *Vascular-mediated signalling involved in early phosphate stress response in plants*. Nat Plants, 2016. **2**: p. 16033.
  33. Calderwood, A., S. Kopriva, and R.J. Morris, *Transcript Abundance Explains mRNA Mobility Data in Arabidopsis thaliana*. Plant Cell, 2016. **28**(3): p. 610-5.
  34. Banerjee, A.K., T. Lin, and D.J. Hannapel, *Untranslated regions of a mobile transcript mediate RNA metabolism*. Plant Physiol, 2009. **151**(4): p. 1831-43.
  35. Zhang, Z., Y. Zheng, B.K. Ham, S. Zhang, Z. Fei, and W.J. Lucas, *Plant lncRNAs are enriched in and move systemically through the phloem in response to phosphate deficiency*. J Integr Plant Biol, 2019. **61**(4): p. 492-508.
  36. Ham, B.K., J.L. Brandom, B. Xoconostle-Cazares, V. Ringgold, T.J. Lough, and W.J. Lucas, *A polypyrimidine tract binding protein, pumpkin RBP50, forms the*

- basis of a phloem-mobile ribonucleoprotein complex*. Plant Cell, 2009. **21**(1): p. 197-215.
37. Morris, R.J., *On the selectivity, specificity and signalling potential of the long-distance movement of messenger RNA*. Curr Opin Plant Biol, 2018. **43**: p. 1-7.
  38. Zhang, W., C.J. Thieme, G. Kollwig, F. Apelt, L. Yang, N. Winter, N. Andresen, D. Walther, and F. Kragler, *tRNA-Related Sequences Trigger Systemic mRNA Transport in Plants*. Plant Cell, 2016. **28**(6): p. 1237-49.
  39. Yan, Y., B.K. Ham, Y.H. Chong, S.D. Yeh, and W.J. Lucas, *A Plant SMALL RNA-BINDING PROTEIN 1 Family Mediates Cell-to-Cell Trafficking of RNAi Signals*. Mol Plant, 2020. **13**(2): p. 321-335.
  40. Bhogale, S., A.S. Mahajan, B. Natarajan, M. Rajabhoj, H.V. Thulasiram, and A.K. Banerjee, *MicroRNA156: a potential graft-transmissible microRNA that modulates plant architecture and tuberization in Solanum tuberosum ssp. andigena*. Plant Physiol, 2014. **164**(2): p. 1011-27.
  41. Martin, A., H. Adam, M. Diaz-Mendoza, M. Zurczak, N.D. Gonzalez-Schain, and P. Suarez-Lopez, *Graft-transmissible induction of potato tuberization by the microRNA miR172*. Development, 2009. **136**(17): p. 2873-81.
  42. Ghate, T.H., P. Sharma, K.R. Kondhare, D.J. Hannapel, and A.K. Banerjee, *The mobile RNAs, StBEL11 and StBEL29, suppress growth of tubers in potato*. Plant Mol Biol, 2017. **93**(6): p. 563-578.
  43. Banerjee, A.K., M. Chatterjee, Y. Yu, S.G. Suh, W.A. Miller, and D.J. Hannapel, *Dynamics of a mobile RNA of potato involved in a long-distance signaling pathway*. Plant Cell, 2006. **18**(12): p. 3443-57.
  44. Mahajan, A., S. Bhogale, I.H. Kang, D.J. Hannapel, and A.K. Banerjee, *The mRNA of a Knotted1-like transcription factor of potato is phloem mobile*. Plant Mol Biol, 2012. **79**(6): p. 595-608.
  45. Suarez-Lopez, P., *A critical appraisal of phloem-mobile signals involved in tuber induction*. Front Plant Sci, 2013. **4**: p. 253.
  46. Hannapel, D.J., P. Sharma, T. Lin, and A.K. Banerjee, *The Multiple Signals That Control Tuber Formation*. Plant Physiol, 2017. **174**(2): p. 845-856.
  47. Natarajan, B., K.R. Kondhare, D.J. Hannapel, and A.K. Banerjee, *Mobile RNAs and proteins: Prospects in storage organ development of tuber and root crops*. Plant Sci, 2019. **284**: p. 73-81.

48. Delhaize, E. and P.J. Randall, *Characterization of a Phosphate-Accumulator Mutant of Arabidopsis thaliana*. Plant Physiol, 1995. **107**(1): p. 207-213.
49. Aung, K., S.I. Lin, C.C. Wu, Y.T. Huang, C.L. Su, and T.J. Chiou, *pho2, a phosphate overaccumulator, is caused by a nonsense mutation in a microRNA399 target gene*. Plant Physiol, 2006. **141**(3): p. 1000-11.
50. Chiou, T.J., K. Aung, S.I. Lin, C.C. Wu, S.F. Chiang, and C. Su, *Regulation of Phosphate Homeostasis by MicroRNA in Arabidopsis*<sup>W</sup>, in *Plant Cell*. 2006. p. 412-21.
51. Bari, R., B. Datt Pant, M. Stitt, and W.R. Scheible, *PHO2, microRNA399, and PHR1 define a phosphate-signaling pathway in plants*. Plant Physiol, 2006. **141**(3): p. 988-99.
52. Lin, S.I., S.F. Chiang, W.Y. Lin, J.W. Chen, C.Y. Tseng, P.C. Wu, and T.J. Chiou, *Regulatory Network of MicroRNA399 and PHO2 by Systemic Signaling1*<sup>W</sup>[OA]. Plant Physiol, 2008. **147**(2): p. 732-46.
53. Pant, B.D., A. Buhtz, J. Kehr, and W.R. Scheible, *MicroRNA399 is a long-distance signal for the regulation of plant phosphate homeostasis*. Plant J, 2008. **53**(5): p. 731-8.
54. Sasaki, T., T. Suzaki, T. Soyano, M. Kojima, H. Sakakibara, and M. Kawaguchi, *Shoot-derived cytokinins systemically regulate root nodulation*. Nat Commun, 2014. **5**: p. 4983.
55. Tsikou, D., Z. Yan, D.B. Holt, N.B. Abel, D.E. Reid, L.H. Madsen, H. Bhasin, M. Sexauer, J. Stougaard, and K. Markmann, *Systemic control of legume susceptibility to rhizobial infection by a mobile microRNA*. Science, 2018. **362**(6411): p. 233-236.
56. Gautrat, P., V. Mortier, C. Laffont, A. De Keyser, J. Fromentin, F. Frugier, and S. Goormachtig, *Unraveling new molecular players involved in the autoregulation of nodulation in Medicago truncatula*. J Exp Bot, 2019. **70**(4): p. 1407-1417.
57. Giavalisco, P., K. Kapitza, A. Kolasa, A. Buhtz, and J. Kehr, *Towards the proteome of Brassica napus phloem sap*. Proteomics, 2006. **6**(3): p. 896-909.
58. Lin, M.K., Y.J. Lee, T.J. Lough, B.S. Phinney, and W.J. Lucas, *Analysis of the pumpkin phloem proteome provides insights into angiosperm sieve tube function*. Mol Cell Proteomics, 2009. **8**(2): p. 343-56.
59. Carella, P., D.C. Wilson, C.J. Kempthorne, and R.K. Cameron, *Vascular Sap Proteomics: Providing Insight into Long-Distance Signaling during Stress*. Front Plant Sci, 2016. **7**: p. 651.

60. Anstead, J.A., S.D. Hartson, and G.A. Thompson, *The broccoli (Brassica oleracea) phloem tissue proteome*. BMC Genomics, 2013. **14**: p. 764.
61. Lopez-Cobollo, R.M., I. Filippis, M.H. Bennett, and C.G. Turnbull, *Comparative proteomics of cucurbit phloem indicates both unique and shared sets of proteins*. Plant J, 2016. **88**(4): p. 633-647.
62. Oparka, K.J. and S.S. Cruz, *THE GREAT ESCAPE: Phloem Transport and Unloading of Macromolecules 1*. Annu Rev Plant Physiol Plant Mol Biol, 2000. **51**: p. 323-347.
63. Paultre, D.S.G., M.P. Gustin, A. Molnar, and K.J. Oparka, *Lost in Transit: Long-Distance Trafficking and Phloem Unloading of Protein Signals in Arabidopsis Homografts*. Plant Cell, 2016. **28**(9): p. 2016-2025.
64. Schulz, A., *Long-Distance Trafficking: Lost in Transit or Stopped at the Gate?* Plant Cell, 2017. **29**(3): p. 426-430.
65. Spiegelman, Z., G. Golan, and S. Wolf, *Don't kill the messenger: Long-distance trafficking of mRNA molecules*. Plant Sci, 2013. **213**: p. 1-8.
66. Lough, T.J. and W.J. Lucas, *Integrative plant biology: role of phloem long-distance macromolecular trafficking*. Annu Rev Plant Biol, 2006. **57**: p. 203-32.
67. Ohkubo, Y., M. Tanaka, R. Tabata, M. Ogawa-Ohnishi, and Y. Matsubayashi, *Shoot-to-root mobile polypeptides involved in systemic regulation of nitrogen acquisition*. Nat Plants, 2017. **3**: p. 17029.
68. Ota, R., Y. Ohkubo, Y. Yamashita, M. Ogawa-Ohnishi, and Y. Matsubayashi, *Shoot-to-root mobile CEPD-like 2 integrates shoot nitrogen status to systemically regulate nitrate uptake in Arabidopsis*. Nat Commun, 2020. **11**(1): p. 641.
69. Chen, X., Q. Yao, X. Gao, C. Jiang, N.P. Harberd, and X. Fu, *Shoot-to-Root Mobile Transcription Factor HY5 Coordinates Plant Carbon and Nitrogen Acquisition*. Curr Biol, 2016. **26**(5): p. 640-6.
70. Champigny, M.J., M. Isaacs, P. Carella, J. Faubert, P.R. Fobert, and R.K. Cameron, *Long distance movement of DIR1 and investigation of the role of DIR1-like during systemic acquired resistance in Arabidopsis*. Front Plant Sci, 2013. **4**: p. 230.
71. Isaacs, M., P. Carella, J. Faubert, J.K. Rose, and R.K. Cameron, *Orthology Analysis and In Vivo Complementation Studies to Elucidate the Role of DIR1 during Systemic Acquired Resistance in Arabidopsis thaliana and Cucumis sativus*. Front Plant Sci, 2016. **7**: p. 566.

72. Takahashi, F., T. Suzuki, Y. Osakabe, S. Betsuyaku, Y. Kondo, N. Dohmae, H. Fukuda, K. Yamaguchi-Shinozaki, and K. Shinozaki, *A small peptide modulates stomatal control via abscisic acid in long-distance signalling*. *Nature*, 2018. **556**(7700): p. 235-238.
73. McLachlan, D.H., A.J. Pridgeon, and A.M. Hetherington, *How Arabidopsis Talks to Itself about Its Water Supply*. *Mol Cell*, 2018. **70**(6): p. 991-992.
74. Mathieu, J., N. Warthmann, F. Kuttner, and M. Schmid, *Export of FT protein from phloem companion cells is sufficient for floral induction in Arabidopsis*. *Curr Biol*, 2007. **17**(12): p. 1055-60.
75. Turck, F., F. Fornara, and G. Coupland, *Regulation and identity of florigen: FLOWERING LOCUS T moves center stage*. *Annu Rev Plant Biol*, 2008. **59**: p. 573-94.
76. Corbesier, L., C. Vincent, S. Jang, F. Fornara, Q. Fan, I. Searle, A. Giakountis, S. Farrona, L. Gissot, C. Turnbull, and G. Coupland, *FT protein movement contributes to long-distance signaling in floral induction of Arabidopsis*. *Science*, 2007. **316**(5827): p. 1030-3.
77. Jaeger, K.E. and P.A. Wigge, *FT protein acts as a long-range signal in Arabidopsis*. *Curr Biol*, 2007. **17**(12): p. 1050-4.
78. Lin, M.K., H. Belanger, Y.J. Lee, E. Varkonyi-Gasic, K. Taoka, E. Miura, B. Xoconostle-Cazares, K. Gendler, R.A. Jorgensen, B. Phinney, T.J. Lough, and W.J. Lucas, *FLOWERING LOCUS T protein may act as the long-distance florigenic signal in the cucurbits*. *Plant Cell*, 2007. **19**(5): p. 1488-506.
79. Tamaki, S., S. Matsuo, H.L. Wong, S. Yokoi, and K. Shimamoto, *Hd3a protein is a mobile flowering signal in rice*. *Science*, 2007. **316**(5827): p. 1033-6.
80. Lifschitz, E. and Y. Eshed, *Universal florigenic signals triggered by FT homologues regulate growth and flowering cycles in perennial day-neutral tomato*. *J Exp Bot*, 2006. **57**(13): p. 3405-14.
81. Lifschitz, E., T. Eviatar, A. Rozman, A. Shalit, A. Goldshmidt, Z. Amsellem, J.P. Alvarez, and Y. Eshed, *The tomato FT ortholog triggers systemic signals that regulate growth and flowering and substitute for diverse environmental stimuli*. *Proc Natl Acad Sci U S A*, 2006. **103**(16): p. 6398-403.
82. Meng, X., M.G. Muszynski, and O.N. Danilevskaya, *The FT-like ZCN8 Gene Functions as a Floral Activator and Is Involved in Photoperiod Sensitivity in Maize*. *Plant Cell*, 2011. **23**(3): p. 942-60.

83. Kong, F., B. Liu, Z. Xia, S. Sato, B.M. Kim, S. Watanabe, T. Yamada, S. Tabata, A. Kanazawa, K. Harada, and J. Abe, *Two coordinately regulated homologs of FLOWERING LOCUS T are involved in the control of photoperiodic flowering in soybean*. *Plant Physiol*, 2010. **154**(3): p. 1220-31.
84. Sun, H., Z. Jia, D. Cao, B. Jiang, C. Wu, W. Hou, Y. Liu, Z. Fei, D. Zhao, and T. Han, *GmFT2a, a soybean homolog of FLOWERING LOCUS T, is involved in flowering transition and maintenance*. *PLoS One*, 2011. **6**(12): p. e29238.
85. Harig, L., F.A. Beinecke, J. Oltmanns, J. Muth, O. Muller, B. Ruping, R.M. Twyman, R. Fischer, D. Pruffer, and G.A. Noll, *Proteins from the FLOWERING LOCUS T-like subclade of the PEBP family act antagonistically to regulate floral initiation in tobacco*. *Plant J*, 2012. **72**(6): p. 908-21.
86. Li, C., Y. Zhang, K. Zhang, D. Guo, B. Cui, X. Wang, and X. Huang, *Promoting flowering, lateral shoot outgrowth, leaf development, and flower abscission in tobacco plants overexpressing cotton FLOWERING LOCUS T (FT)-like gene GhFT1*. *Front Plant Sci*, 2015. **6**: p. 454.
87. Notaguchi, M., M. Abe, T. Kimura, Y. Daimon, T. Kobayashi, A. Yamaguchi, Y. Tomita, K. Dohi, M. Mori, and T. Araki, *Long-distance, graft-transmissible action of Arabidopsis FLOWERING LOCUS T protein to promote flowering*. *Plant Cell Physiol*, 2008. **49**(11): p. 1645-58.
88. Koenig, A.M. and S. Hoffmann-Benning, *The interplay of phloem-mobile signals in plant development and stress response*. *Biosci Rep*, 2020. **40**(10).
89. Andres, F. and G. Coupland, *The genetic basis of flowering responses to seasonal cues*. *Nat Rev Genet*, 2012. **13**(9): p. 627-39.
90. Abe, M., Y. Kobayashi, S. Yamamoto, Y. Daimon, A. Yamaguchi, Y. Ikeda, H. Ichinoki, M. Notaguchi, K. Goto, and T. Araki, *FD, a bZIP protein mediating signals from the floral pathway integrator FT at the shoot apex*. *Science*, 2005. **309**(5737): p. 1052-6.
91. Nakamura, Y., F. Andres, K. Kanehara, Y.C. Liu, P. Dormann, and G. Coupland, *Arabidopsis florigen FT binds to diurnally oscillating phospholipids that accelerate flowering*. *Nat Commun*, 2014. **5**: p. 3553.
92. Nakamura, Y., Y.C. Lin, S. Watanabe, Y.C. Liu, K. Katsuyama, K. Kanehara, and K. Inaba, *High-Resolution Crystal Structure of Arabidopsis FLOWERING LOCUS T Illuminates Its Phospholipid-Binding Site in Flowering*. *iScience*, 2019. **21**: p. 577-586.
93. Susila, H., S. Juric, L. Liu, K. Gawarecka, K.S. Chung, S. Jin, S.J. Kim, Z. Nasim, G. Youn, M.C. Suh, H. Yu, and J.H. Ahn, *Florigen sequestration in cellular*

- membranes modulates temperature-responsive flowering.* Science, 2021. **373**(6559): p. 1137-1142.
94. Moellering, E.R., B. Muthan, and C. Benning, *Freezing tolerance in plants requires lipid remodeling at the outer chloroplast membrane.* Science, 2010. **330**(6001): p. 226-8.
  95. Barnes, A.C., C. Benning, and R.L. Roston, *Chloroplast Membrane Remodeling during Freezing Stress Is Accompanied by Cytoplasmic Acidification Activating SENSITIVE TO FREEZING2.* Plant Physiol, 2016. **171**(3): p. 2140-9.
  96. Roston, R.L., K. Wang, L.A. Kuhn, and C. Benning, *Structural determinants allowing transferase activity in SENSITIVE TO FREEZING 2, classified as a family I glycosyl hydrolase.* J Biol Chem, 2014. **289**(38): p. 26089-106.
  97. Siebers, M.D., P. Hölzl, G., *Membrane remodelling in phosphorus-deficient plants,* in *Phosphorus Metabolism in Plants*, W.C.L. Plaxton, H, Editor. 2015. p. 237-263.
  98. Barbaglia, A.M. and S. Hoffmann-Benning, *Long-Distance Lipid Signaling and its Role in Plant Development and Stress Response.* Subcell Biochem, 2016. **86**: p. 339-61.
  99. Huby, E., J.A. Napier, F. Baillieux, L.V. Michaelson, and S. Dhondt-Cordelier, *Sphingolipids: towards an integrated view of metabolism during the plant stress response.* New Phytol, 2019. **225**(2): p. 659-670.
  100. Dong, W., H. Lv, G. Xia, and M. Wang, *Does diacylglycerol serve as a signaling molecule in plants?,* in *Plant Signal Behav.* 2012. p. 472-5.
  101. Tontonoz, P., E. Hu, and B.M. Spiegelman, *Stimulation of adipogenesis in fibroblasts by PPAR gamma 2, a lipid-activated transcription factor.* Cell, 1994. **79**(7): p. 1147-56.
  102. Wahli, W. and L. Michalik, *PPARs at the crossroads of lipid signaling and inflammation.* Trends Endocrinol Metab, 2012. **23**(7): p. 351-63.
  103. Nagy, L. and A. Szanto, *Roles for lipid-activated transcription factors in atherosclerosis.* Mol Nutr Food Res, 2005. **49**(11): p. 1072-4.
  104. Musille, P.M., J.A. Kohn, and E.A. Ortlund, *Phospholipid--Driven gene regulation.* FEBS Lett, 2013. **587**(8): p. 1238-46.
  105. Musille, P.M., M. Pathak, J.L. Lauer, W.H. Hudson, P.R. Griffin, and E.A. Ortlund, *Antidiabetic phospholipid-nuclear receptor complex reveals the mechanism for phospholipid-driven gene regulation.* Nat Struct Mol Biol, 2012. **19**(5): p. 532-S2.

106. Janda, C.Y., D. Waghray, A.M. Levin, C. Thomas, and K.C. Garcia, *Structural basis of Wnt recognition by Frizzled*. Science, 2012. **337**(6090): p. 59-64.
107. Kim, S.C., D.A. Nusinow, M.L. Sorkin, J. Pruneda-Paz, and X. Wang, *Interaction and Regulation Between Lipid Mediator Phosphatidic Acid and Circadian Clock Regulators*. Plant Cell, 2019. **31**(2): p. 399-416.
108. Yao, H., G. Wang, L. Guo, and X. Wang, *Phosphatidic Acid Interacts with a MYB Transcription Factor and Regulates Its Nuclear Localization and Function in Arabidopsis*. Plant Cell, 2013. **25**(12): p. 5030-42.
109. Cai, G., S.C. Kim, J. Li, Y. Zhou, and X. Wang, *Transcriptional Regulation of Lipid Catabolism during Seedling Establishment*. Mol Plant, 2020. **13**(7): p. 984-1000.
110. Munnik, T. and C. Testerink, *Plant phospholipid signaling: "in a nutshell"*. J Lipid Res, 2009. **50** Suppl: p. S260-5.
111. Xue, H.W., X. Chen, and Y. Mei, *Function and regulation of phospholipid signalling in plants*. Biochem J, 2009. **421**(2): p. 145-56.
112. Hong, Y., W. Zhang, and X. Wang, *Phospholipase D and phosphatidic acid signalling in plant response to drought and salinity*. Plant Cell Environ, 2010. **33**(4): p. 627-35.
113. Testerink, C. and T. Munnik, *Molecular, cellular, and physiological responses to phosphatidic acid formation in plants*. J Exp Bot, 2011. **62**(7): p. 2349-61.
114. Julkowska, M.M. and C. Testerink, *Tuning plant signaling and growth to survive salt*. Trends Plant Sci, 2015. **20**(9): p. 586-94.
115. Bargmann, B.O. and T. Munnik, *The role of phospholipase D in plant stress responses*. Curr Opin Plant Biol, 2006. **9**(5): p. 515-22.
116. Yao, H.Y. and H.W. Xue, *Phosphatidic acid plays key roles regulating plant development and stress responses*. J Integr Plant Biol, 2018. **60**(9): p. 851-863.
117. Wang, X., Y. Su, Y. Liu, S. Kim, and B. Fanella, *Phosphatidic Acid as Lipid Messenger and Growth Regulators in Plants*, in *Phospholipases in Plant Signaling*, X. Wang, Editor. 2014, Springer, Berlin, Heidelberg: Signaling and Communication in Plants. p. 69-92.
118. Arisz, S.A., R. van Wijk, W. Roels, J.K. Zhu, M.A. Haring, and T. Munnik, *Rapid phosphatidic acid accumulation in response to low temperature stress in Arabidopsis is generated through diacylglycerol kinase*. Front Plant Sci, 2013. **4**.

119. Uraji, M., T. Katagiri, E. Okuma, W. Ye, M.A. Hossain, C. Masuda, A. Miura, Y. Nakamura, I.C. Mori, K. Shinozaki, and Y. Murata, *Cooperative function of PLDdelta and PLDalpha1 in abscisic acid-induced stomatal closure in Arabidopsis*. *Plant Physiol*, 2012. **159**(1): p. 450-60.
120. Hong, Y., J. Zhao, L. Guo, S.C. Kim, X. Deng, G. Wang, G. Zhang, M. Li, and X. Wang, *Plant phospholipases D and C and their diverse functions in stress responses*. *Prog Lipid Res*, 2016. **62**: p. 55-74.
121. Wang, G., S. Ryu, and X. Wang, *Plant phospholipases: an overview*. *Methods Mol Biol*, 2012. **861**: p. 123-37.
122. Wang, X., *Plant Phospholipases*. *Annu Rev Plant Physiol Plant Mol Biol*, 2001. **52**: p. 211-231.
123. Thomashow, M.F., *Role of Cold-Responsive Genes in Plant Freezing Tolerance*. *Plant Physiol*, 1998. **118**(1): p. 1-8.
124. Welti, R., W. Li, M. Li, Y. Sang, H. Biesiada, H.E. Zhou, C.B. Rajashekar, T.D. Williams, and X. Wang, *Profiling membrane lipids in plant stress responses. Role of phospholipase D alpha in freezing-induced lipid changes in Arabidopsis*. *J Biol Chem*, 2002. **277**(35): p. 31994-2002.
125. Rajashekar, C.B., H.E. Zhou, Y. Zhang, W. Li, and X. Wang, *Suppression of phospholipase Dalpha1 induces freezing tolerance in Arabidopsis: response of cold-responsive genes and osmolyte accumulation*. *J Plant Physiol*, 2006. **163**(9): p. 916-26.
126. Kooijman, E.E., V. Chupin, B. de Kruijff, and K.N. Burger, *Modulation of membrane curvature by phosphatidic acid and lysophosphatidic acid*. *Traffic*, 2003. **4**(3): p. 162-74.
127. Putta, P., J. Rankenberg, R.A. Korver, R. van Wijk, T. Munnik, C. Testerink, and E.E. Kooijman, *Phosphatidic acid binding proteins display differential binding as a function of membrane curvature stress and chemical properties*. *Biochim Biophys Acta*, 2016. **1858**(11): p. 2709-2716.
128. Iuchi, S., M. Kobayashi, T. Taji, M. Naramoto, M. Seki, T. Kato, S. Tabata, Y. Kakubari, K. Yamaguchi-Shinozaki, and K. Shinozaki, *Regulation of drought tolerance by gene manipulation of 9-cis-epoxycarotenoid dioxygenase, a key enzyme in abscisic acid biosynthesis in Arabidopsis*. *Plant J*, 2001. **27**(4): p. 325-33.
129. Endo, A., Y. Sawada, H. Takahashi, M. Okamoto, K. Ikegami, H. Koiwai, M. Seo, T. Toyomasu, W. Mitsuhashi, K. Shinozaki, M. Nakazono, Y. Kamiya, T. Koshiba, and E. Nambara, *Drought induction of Arabidopsis 9-cis-epoxycarotenoid*

- dioxygenase occurs in vascular parenchyma cells*. Plant Physiol, 2008. **147**(4): p. 1984-93.
130. Zhang, W., C. Qin, J. Zhao, and X. Wang, *Phospholipase D alpha 1-derived phosphatidic acid interacts with ABI1 phosphatase 2C and regulates abscisic acid signaling*. Proc Natl Acad Sci U S A, 2004. **101**(25): p. 9508-13.
  131. Cutler, S.R., P.L. Rodriguez, R.R. Finkelstein, and S.R. Abrams, *Abscisic acid: emergence of a core signaling network*. Annu Rev Plant Biol, 2010. **61**: p. 651-79.
  132. Yu, L., J. Nie, C. Cao, Y. Jin, M. Yan, F. Wang, J. Liu, Y. Xiao, Y. Liang, and W. Zhang, *Phosphatidic acid mediates salt stress response by regulation of MPK6 in Arabidopsis thaliana*. New Phytol, 2010. **188**(3): p. 762-73.
  133. Yang, Y. and Y. Guo, *Unraveling salt stress signaling in plants*. J Integr Plant Biol, 2018. **60**(9): p. 796-804.
  134. Wang, P., L. Shen, J. Guo, W. Jing, Y. Qu, W. Li, R. Bi, W. Xuan, Q. Zhang, and W. Zhang, *Phosphatidic Acid Directly Regulates PINOID-Dependent Phosphorylation and Activation of the PIN-FORMED2 Auxin Efflux Transporter in Response to Salt Stress*. Plant Cell, 2019. **31**(1): p. 250-271.
  135. Gao, H.B., Y.J. Chu, and H.W. Xue, *Phosphatidic acid (PA) binds PP2AA1 to regulate PP2A activity and PIN1 polar localization*. Mol Plant, 2013. **6**(5): p. 1692-702.
  136. Testerink, C., P.B. Larsen, D. van der Does, J.A. van Himbergen, and T. Munnik, *Phosphatidic acid binds to and inhibits the activity of Arabidopsis CTR1*. J Exp Bot, 2007. **58**(14): p. 3905-14.
  137. Testerink, C., P.B. Larsen, F. McLoughlin, D. van der Does, J.A. van Himbergen, and T. Munnik, *PA, a stress-induced short cut to switch-on ethylene signalling by switching-off CTR1?*, in *Plant Signal Behav*. 2008. p. 681-3.
  138. Kalachova, T., O. Iakovenko, S. Kretinin, and V. Kravets, *Involvement of phospholipase D and NADPH-oxidase in salicylic acid signaling cascade*. Plant Physiol Biochem, 2013. **66**: p. 127-33.
  139. Janda, M., V. Šašek, H. Chmelařová, J. Andrejch, M. Nováková, J. Hajšlová, L. Burketová, and O. Valentová, *Phospholipase D affects translocation of NPR1 to the nucleus in Arabidopsis thaliana*. Front Plant Sci, 2015. **6**.
  140. Hoad, G.V., *Transport of hormones in the phloem of higher plants*. Plant Growth Regulation, 1995. **16**: p. 173-182.
  141. Hoffmann-Benning, S., *Transport and function of lipids in the plant phloem*. AOCS Lipid Library, 2015.

142. Hirose, N., K. Takei, T. Kuroha, T. Kamada-Nobusada, H. Hayashi, and H. Sakakibara, *Regulation of cytokinin biosynthesis, compartmentalization and translocation*. J Exp Bot, 2008. **59**(1): p. 75-83.
143. Kudo, T., T. Kiba, and H. Sakakibara, *Metabolism and long-distance translocation of cytokinins*. J Integr Plant Biol, 2010. **52**(1): p. 53-60.
144. Benning, U., B. Tamot, B. Guelette, and S. Hoffmann-Benning, *New aspects of phloem-mediated long-distance lipid signaling in plants*. Frontiers in Plant Science, 2012. **3**: p. 53.
145. Valim, M.F. and N. Killiny, *Occurrence of free fatty acids in the phloem sap of different citrus varieties*. Plant Signal Behav, 2017. **12**(6): p. e1327497.
146. Eckardt, N.A., *Oxylipin Signaling in Plant Stress Responses*. Plant Cell, 2008. **20**(3): p. 495-7.
147. Wasternack, C. and I. Feussner, *The Oxylipin Pathways: Biochemistry and Function*. Annu Rev Plant Biol, 2018. **69**: p. 363-386.
148. Howe, G.A., I.T. Major, and A.J. Koo, *Modularity in Jasmonate Signaling for Multistress Resilience*. Annu Rev Plant Biol, 2018. **69**: p. 387-415.
149. Koo, A.J., X. Gao, A.D. Jones, and G.A. Howe, *A rapid wound signal activates the systemic synthesis of bioactive jasmonates in Arabidopsis*. Plant J, 2009. **59**(6): p. 974-86.
150. Ruan, J., Y. Zhou, M. Zhou, J. Yan, M. Khurshid, W. Weng, J. Cheng, and K. Zhang, *Jasmonic Acid Signaling Pathway in Plants*. Int J Mol Sci, 2019. **20**(10).
151. Glatz, J.F., T. Borchers, F. Spener, and G.J. van der Vusse, *Fatty acids in cell signalling: modulation by lipid binding proteins*. Prostaglandins Leukot Essent Fatty Acids, 1995. **52**(2-3): p. 121-7.
152. Charbonneau, D., M. Beauregard, and H.A. Tajmir-Riahi, *Structural analysis of human serum albumin complexes with cationic lipids*. J Phys Chem B, 2009. **113**(6): p. 1777-84.
153. Blaner, W.S., *Retinol-binding protein: the serum transport protein for vitamin A*. Endocr Rev, 1989. **10**(3): p. 308-16.
154. Natanson, A.O. and I. Kon, *[Vitamin A transport in the blood: retinol-binding serum protein and its biological role]*. Vopr Pitan, 1979(3): p. 3-12.

155. Chaturvedi, R., B. Venables, R.A. Petros, V. Nalam, M. Li, X. Wang, L.J. Takemoto, and J. Shah, *An abietane diterpenoid is a potent activator of systemic acquired resistance*. *Plant J*, 2012. **71**(1): p. 161-72.
156. Chanda, B., Y. Xia, M.K. Mandal, K. Yu, K.T. Sekine, Q.M. Gao, D. Selote, Y. Hu, A. Stromberg, D. Navarre, A. Kachroo, and P. Kachroo, *Glycerol-3-phosphate is a critical mobile inducer of systemic immunity in plants*. *Nat Genet*, 2011. **43**(5): p. 421-7.
157. Yu, K., J.M. Soares, M.K. Mandal, C. Wang, B. Chanda, A.N. Gifford, J.S. Fowler, D. Navarre, A. Kachroo, and P. Kachroo, *A feedback regulatory loop between G3P and lipid transfer proteins DIR1 and AZI1 mediates azelaic-acid-induced systemic immunity*. *Cell Rep*, 2013. **3**(4): p. 1266-78.
158. Jung, H.W., T.J. Tschaplinski, L. Wang, J. Glazebrook, and J.T. Greenberg, *Priming in systemic plant immunity*. *Science*, 2009. **324**(5923): p. 89-91.
159. Shah, J., R. Chaturvedi, Z. Chowdhury, B. Venables, and R.A. Petros, *Signaling by small metabolites in systemic acquired resistance*. *Plant J*, 2014. **79**(4): p. 645-58.
160. Cecchini, N.M., K. Steffes, M.R. Schlappi, A.N. Gifford, and J.T. Greenberg, *Arabidopsis AZI1 family proteins mediate signal mobilization for systemic defence priming*. *Nat Commun*, 2015. **6**: p. 7658.
161. Ye, Z.W., S.C. Lung, T.H. Hu, Q.F. Chen, Y.L. Suen, M. Wang, S. Hoffmann-Benning, E. Yeung, and M.L. Chye, *Arabidopsis acyl-CoA-binding protein ACBP6 localizes in the phloem and affects jasmonate composition*. *Plant Mol Biol*, 2016. **92**(6): p. 717-730.
162. Hu, T.H., S.C. Lung, Z.W. Ye, and M.L. Chye, *Depletion of Arabidopsis ACYL-COA-BINDING PROTEIN3 Affects Fatty Acid Composition in the Phloem*. *Front Plant Sci*, 2018. **9**: p. 2.
163. Gasperini, D., A. Chauvin, I.F. Acosta, A. Kurenda, S. Stolz, A. Chetelat, J.L. Wolfender, and E.E. Farmer, *Axial and Radial Oxylipin Transport*. *Plant Physiol*, 2015. **169**(3): p. 2244-54.
164. Thorpe, M.R., A.P. Ferrieri, M.M. Herth, and R.A. Ferrieri, *11C-imaging: methyl jasmonate moves in both phloem and xylem, promotes transport of jasmonate, and of photoassimilate even after proton transport is decoupled*. *Planta*, 2007. **226**(2): p. 541-51.
165. Sato, C., K. Aikawa, S. Sugiyama, K. Nabeta, C. Masuta, and H. Matsuura, *Distal transport of exogenously applied jasmonoyl-isoleucine with wounding stress*. *Plant Cell Physiol*, 2011. **52**(3): p. 509-17.

166. Jimenez-Aleman, G.H., S.S. Scholz, M. Heyer, M. Reichelt, A. Mithofer, and W. Boland, *Synthesis, metabolism and systemic transport of a fluorinated mimic of the endogenous jasmonate precursor OPC-8:0*. *Biochim Biophys Acta*, 2015. **1851**(12): p. 1545-53.
167. Koo, A.J. and G.A. Howe, *The wound hormone jasmonate*. *Phytochemistry*, 2009. **70**(13-14): p. 1571-80.
168. Schulze, A., M. Zimmer, S. Mielke, H. Stellmach, C.W. Melnyk, B. Hause, and D. Gasperini, *Wound-Induced Shoot-to-Root Relocation of JA-Ile Precursors Coordinates Arabidopsis Growth*. *Mol Plant*, 2019. **12**(10): p. 1383-1394.
169. Scharwies, J.D. and J.R. Dinneny, *Water transport, perception, and response in plants*. *J Plant Res*, 2019. **132**(3): p. 311-324.
170. Schachtman, D.P. and J.Q. Goodger, *Chemical root to shoot signaling under drought*. *Trends Plant Sci*, 2008. **13**(6): p. 281-7.
171. Davies, W.J. and J. Zhang, *Root Signals and the Regulation of Growth and Development of Plants in Drying Soil*. *Annu. Rev. Plan Physiol. Plant Mol. Biol.*, 1991. **42**: p. 55-76.
172. Zhang, J., *Control of Stomatal Behaviour by Abscisic Acid which Apparently Originates in the Roots*. *Journal of Experimental Botany*, 1987. **38**(7): p. 1174-1181.
173. Jiang, F. and W. Hartung, *Long-distance signalling of abscisic acid (ABA): the factors regulating the intensity of the ABA signal*. *J Exp Bot*, 2008. **59**(1): p. 37-43.
174. Setter, T.L., W.A. Brun, and M.L. Brenner, *Effect of obstructed translocation on leaf abscisic Acid, and associated stomatal closure and photosynthesis decline*. *Plant Physiol*, 1980. **65**(6): p. 1111-5.
175. Zeevaart, J.A. and G.L. Boyer, *Accumulation and transport of abscisic Acid and its metabolites in ricinus and xanthium*. *Plant Physiol*, 1984. **74**(4): p. 934-9.
176. Setter, T.L. and W.A. Brun, *Abscisic Acid Translocation and Metabolism in Soybeans following Depodding and Petiole Girdling Treatments*. *Plant Physiol*, 1981. **67**(4): p. 774-9.
177. Zhong, W., W. Hartung, E. Komor, and C. Schobert, *Phloem transport of abscisic acid in Ricinus communis L seedlings*. *Plant Cell Environ*, 1996. **19**(4): p. 471-477.
178. Manzi, M., J. Lado, M.J. Rodrigo, L. Zacarias, V. Arbona, and A. Gomez-Cadenas, *Root ABA Accumulation in Long-Term Water-Stressed Plants is Sustained by*

- Hormone Transport from Aerial Organs*. Plant Cell Physiol, 2015. **56**(12): p. 2457-66.
179. McAdam, S.A.M., M. Manzi, J.J. Ross, T.J. Brodribb, and A. Gómez-Cadenas, *Uprooting an abscisic acid paradigm: Shoots are the primary source*, in *Plant Signal Behav.* 2016.
  180. Hartung, W., A. Sauter, and E. Hose, *Abscisic acid in the xylem: where does it come from, where does it go to?* J Exp Bot, 2002. **53**(366): p. 27-32.
  181. Barbaglia, A.M., B. Tamot, V. Greve, and S. Hoffmann-Benning, *Phloem Proteomics Reveals New Lipid-Binding Proteins with a Putative Role in Lipid-Mediated Signaling*. Front Plant Sci, 2016. **7**: p. 563.
  182. Mishra, G., W. Zhang, F. Deng, J. Zhao, and X. Wang, *A bifurcating pathway directs abscisic acid effects on stomatal closure and opening in Arabidopsis*. Science, 2006. **312**(5771): p. 264-6.
  183. Zhang, Y., H. Zhu, Q. Zhang, M. Li, M. Yan, R. Wang, L. Wang, R. Welti, W. Zhang, and X. Wang, *Phospholipase  $\alpha$ 1 and phosphatidic acid regulate NADPH oxidase activity and production of reactive oxygen species in ABA-mediated stomatal closure in Arabidopsis*. Plant Cell, 2009. **21**(8): p. 2357-77.
  184. Testerink, C. and T. Munnik, *Phosphatidic acid: a multifunctional stress signaling lipid in plants*. Trends Plant Sci, 2005. **10**(8): p. 368-75.
  185. Koenig, A.M., C. Benning, and S. Hoffmann-Benning, *Lipid trafficking and signaling in plants*, in *Lipid Signaling and Metabolism*, J.M. Ntambi, Editor. 2020, Elsevier.
  186. Zierer, W., D. Ruscher, U. Sonnewald, and S. Sonnewald, *Tuber and Tuberous Root Development*. Annu Rev Plant Biol, 2021. **72**: p. 551-580.
  187. Fu, Z.Q. and X. Dong, *Systemic acquired resistance: turning local infection into global defense*. Annu Rev Plant Biol, 2013. **64**: p. 839-63.
  188. Yu, L., C. Zhou, J. Fan, J. Shanklin, and C. Xu, *Mechanisms and functions of membrane lipid remodeling in plants*. Plant J, 2021. **107**(1): p. 37-53.
  189. Guo, Q., L. Liu, and B.J. Barkla, *Membrane Lipid Remodeling in Response to Salinity*. Int J Mol Sci, 2019. **20**(17).
  190. Lu, J., Y. Xu, J. Wang, S.D. Singer, and G. Chen, *The Role of Triacylglycerol in Plant Stress Response*. Plants (Basel), 2020. **9**(4).
  191. Wang, X., S.P. Devaiah, W. Zhang, and R. Welti, *Signaling functions of phosphatidic acid*. Prog Lipid Res, 2006. **45**(3): p. 250-78.

192. Zhou, Y., D.M. Zhou, W.W. Yu, L.L. Shi, Y. Zhang, Y.X. Lai, L.P. Huang, H. Qi, Q.F. Chen, N. Yao, J.F. Li, L.J. Xie, and S. Xiao, *Phosphatidic acid modulates MPK3- and MPK6-mediated hypoxia signaling in Arabidopsis*. *Plant Cell*, 2022. **34**(2): p. 889-909.
193. Kim, S.C., L. Guo, and X. Wang, *Nuclear moonlighting of cytosolic glyceraldehyde-3-phosphate dehydrogenase regulates Arabidopsis response to heat stress*. *Nat Commun*, 2020. **11**(1): p. 3439.
194. Janda, C.Y. and K.C. Garcia, *Wnt acylation and its functional implication in Wnt signalling regulation*. *Biochem Soc Trans*, 2015. **43**(2): p. 211-6.
195. Laohavisit, A. and J.M. Davies, *Annexins*. *New Phytol*, 2011. **189**(1): p. 40-53.
196. Wang, Y., L. Yang, X. Chen, T. Ye, B. Zhong, R. Liu, Y. Wu, and Z. Chan, *Major latex protein-like protein 43 (MLP43) functions as a positive regulator during abscisic acid responses and confers drought tolerance in Arabidopsis thaliana*. *J Exp Bot*, 2016. **67**(1): p. 421-34.
197. Radauer, C., P. Lackner, and H. Breiteneder, *The Bet v 1 fold: an ancient, versatile scaffold for binding of large, hydrophobic ligands*. *BMC Evol Biol*, 2008. **8**: p. 286.
198. Iyer, L.M., E.V. Koonin, and L. Aravind, *Adaptations of the helix-grip fold for ligand binding and catalysis in the START domain superfamily*. *Proteins*, 2001. **43**(2): p. 134-44.
199. Earley, K.W., J.R. Haag, O. Pontes, K. Opper, T. Juehne, K. Song, and C.S. Pikaard, *Gateway-compatible vectors for plant functional genomics and proteomics*. *Plant J*, 2006. **45**(4): p. 616-29.
200. Awai, K., C. Xu, B. Tamot, and C. Benning, *A phosphatidic acid-binding protein of the chloroplast inner envelope membrane involved in lipid trafficking*. *Proc Natl Acad Sci U S A*, 2006. **103**(28): p. 10817-22.
201. Che, P., S. Lall, D. Nettleton, and S.H. Howell, *Gene expression programs during shoot, root, and callus development in Arabidopsis tissue culture*. *Plant Physiol*, 2006. **141**(2): p. 620-37.
202. Krishnaswamy, S.S., S. Srivastava, M. Mohammadi, M.H. Rahman, M.K. Deyholos, and N.N. Kav, *Transcriptional profiling of pea ABR17 mediated changes in gene expression in Arabidopsis thaliana*. *BMC Plant Biol*, 2008. **8**: p. 91.
203. Laohavisit, A., S.L. Richards, L. Shabala, C. Chen, R.D. Colaco, S.M. Swarbreck, E. Shaw, A. Dark, S. Shabala, Z. Shang, and J.M. Davies, *Salinity-induced calcium signaling and root adaptation in Arabidopsis require the calcium regulatory protein annexin1*. *Plant Physiol*, 2013. **163**(1): p. 253-62.

204. Laohavisit, A., Z. Shang, L. Rubio, T.A. Cuin, A.A. Very, A. Wang, J.C. Mortimer, N. Macpherson, K.M. Coxon, N.H. Battey, C. Brownlee, O.K. Park, H. Sentenac, S. Shabala, A.A. Webb, and J.M. Davies, *Arabidopsis annexin1 mediates the radical-activated plasma membrane Ca<sup>2+</sup>- and K<sup>+</sup>-permeable conductance in root cells*. *Plant Cell*, 2012. **24**(4): p. 1522-33.
205. Richards, S.L., A. Laohavisit, J.C. Mortimer, L. Shabala, S.M. Swarbreck, S. Shabala, and J.M. Davies, *Annexin 1 regulates the H<sub>2</sub>O<sub>2</sub>-induced calcium signature in Arabidopsis thaliana roots*. *Plant J*, 2014. **77**(1): p. 136-45.
206. Nakamura, Y., *Plant Phospholipid Diversity: Emerging Functions in Metabolism and Protein-Lipid Interactions*. *Trends Plant Sci*, 2017. **22**(12): p. 1027-1040.
207. Schrick, K., M. Bruno, A. Khosla, P.N. Cox, S.A. Marlatt, R.A. Roque, H.C. Nguyen, C. He, M.P. Snyder, D. Singh, and G. Yadav, *Shared functions of plant and mammalian StAR-related lipid transfer (START) domains in modulating transcription factor activity*. *BMC Biol*, 2014. **12**: p. 70.
208. Mogensen, J.E., R. Wimmer, J.N. Larsen, M.D. Spangfort, and D.E. Otzen, *The major birch allergen, Bet v 1, shows affinity for a broad spectrum of physiological ligands*. *J Biol Chem*, 2002. **277**(26): p. 23684-92.
209. Konopka-Postupolska, D., G. Clark, G. Goch, J. Debski, K. Floras, A. Cantero, B. Fijolek, S. Roux, and J. Hennig, *The role of annexin 1 in drought stress in Arabidopsis*. *Plant Physiol*, 2009. **150**(3): p. 1394-410.
210. Malabarba, J., A.K. Meents, M. Reichelt, S.S. Scholz, E. Peiter, J. Rachowka, D. Konopka-Postupolska, K.A. Wilkins, J.M. Davies, R. Oelmüller, and A. Mithöfer, *ANNEXIN1 mediates calcium-dependent systemic defense in Arabidopsis plants upon herbivory and wounding*. *New Phytol*, 2021. **231**(1): p. 243-254.
211. Cantero, A., S. Barthakur, T.J. Bushart, S. Chou, R.O. Morgan, M.P. Fernandez, G.B. Clark, and S.J. Roux, *Expression profiling of the Arabidopsis annexin gene family during germination, de-etiolation and abiotic stress*. *Plant Physiol Biochem*, 2006. **44**(1): p. 13-24.
212. Abercrombie, J.M., M.D. Halfhill, P. Ranjan, M.R. Rao, A.M. Saxton, J.S. Yuan, and C.N. Stewart, Jr., *Transcriptional responses of Arabidopsis thaliana plants to As (V) stress*. *BMC Plant Biol*, 2008. **8**: p. 87.
213. Berr, A., L. Xu, J. Gao, V. Cognat, A. Steinmetz, A. Dong, and W.H. Shen, *SET DOMAIN GROUP25 encodes a histone methyltransferase and is involved in FLOWERING LOCUS C activation and repression of flowering*. *Plant Physiol*, 2009. **151**(3): p. 1476-85.

214. Jakoby, M.J., D. Falkenhan, M.T. Mader, G. Brininstool, E. Wischnitzki, N. Platz, A. Hudson, M. Hulskamp, J. Larkin, and A. Schnittger, *Transcriptional profiling of mature Arabidopsis trichomes reveals that NOECK encodes the MIXTA-like transcriptional regulator MYB106*. Plant Physiol, 2008. **148**(3): p. 1583-602.
215. Cornah, J.E., V. Germain, J.L. Ward, M.H. Beale, and S.M. Smith, *Lipid utilization, gluconeogenesis, and seedling growth in Arabidopsis mutants lacking the glyoxylate cycle enzyme malate synthase*. J Biol Chem, 2004. **279**(41): p. 42916-23.
216. Brenner, W.G., G.A. Romanov, I. Kollmer, L. Burkle, and T. Schmulling, *Immediate-early and delayed cytokinin response genes of Arabidopsis thaliana identified by genome-wide expression profiling reveal novel cytokinin-sensitive processes and suggest cytokinin action through transcriptional cascades*. Plant J, 2005. **44**(2): p. 314-33.
217. Wu, W., K. Du, X. Kang, and H. Wei, *The diverse roles of cytokinins in regulating leaf development*. Hortic Res, 2021. **8**(1): p. 118.
218. Hu, W. and H. Ma, *Characterization of a novel putative zinc finger gene MIF1: involvement in multiple hormonal regulation of Arabidopsis development*. Plant J, 2006. **45**(3): p. 399-422.
219. Ali, U., S. Lu, T. Fadlalla, S. Iqbal, H. Yue, B. Yang, Y. Hong, X. Wang, and L. Guo, *The functions of phospholipases and their hydrolysis products in plant growth, development and stress responses*. Prog Lipid Res, 2022. **86**: p. 101158.
220. Litholdo, C.G., Jr., B.L. Parker, A.L. Eamens, M.R. Larsen, S.J. Cordwell, and P.M. Waterhouse, *Proteomic Identification of Putative MicroRNA394 Target Genes in Arabidopsis thaliana Identifies Major Latex Protein Family Members Critical for Normal Development*. Mol Cell Proteomics, 2016. **15**(6): p. 2033-47.
221. Ticha, M., H. Richter, M. Ovecka, N. Maghelli, M. Hrbackova, P. Dvorak, J. Samaj, and O. Samajova, *Advanced Microscopy Reveals Complex Developmental and Subcellular Localization Patterns of ANNEXIN 1 in Arabidopsis*. Front Plant Sci, 2020. **11**: p. 1153.
222. Lee, S., E.J. Lee, E.J. Yang, J.E. Lee, A.R. Park, W.H. Song, and O.K. Park, *Proteomic identification of annexins, calcium-dependent membrane binding proteins that mediate osmotic stress and abscisic acid signal transduction in Arabidopsis*. Plant Cell, 2004. **16**(6): p. 1378-91.
223. Bindschedler, L.V., M. Palmblad, and R. Cramer, *Hydroponic isotope labelling of entire plants (HILEP) for quantitative plant proteomics; an oxidative stress case study*. Phytochemistry, 2008. **69**(10): p. 1962-72.

224. Clark, G.B., A. Sessions, D.J. Eastburn, and S.J. Roux, *Differential expression of members of the annexin multigene family in Arabidopsis*. Plant Physiol, 2001. **126**(3): p. 1072-84.
225. Clark, G.B., D. Lee, M. Dauwalder, and S.J. Roux, *Immunolocalization and histochemical evidence for the association of two different Arabidopsis annexins with secretion during early seedling growth and development*. Planta, 2005. **220**(4): p. 621-31.
226. Bateman, A. and R. Sandford, *The PLAT domain: a new piece in the PKD1 puzzle*. Curr Biol, 1999. **9**(16): p. R588-90.
227. Walther, M., K. Hofheinz, R. Vogel, J. Roffeis, and H. Kuhn, *The N-terminal beta-barrel domain of mammalian lipoxygenases including mouse 5-lipoxygenase is not essential for catalytic activity and membrane binding but exhibits regulatory functions*. Arch Biochem Biophys, 2011. **516**(1): p. 1-9.
228. Kulkarni, S., S. Das, C.D. Funk, D. Murray, and W. Cho, *Molecular basis of the specific subcellular localization of the C2-like domain of 5-lipoxygenase*. J Biol Chem, 2002. **277**(15): p. 13167-74.
229. Hammarberg, T., P. Provost, B. Persson, and O. Radmark, *The N-terminal domain of 5-lipoxygenase binds calcium and mediates calcium stimulation of enzyme activity*. J Biol Chem, 2000. **275**(49): p. 38787-93.
230. Xu, Y., A.J. Streets, A.M. Hounslow, U. Tran, F. Jean-Alphonse, A.J. Needham, J.P. Vilardaga, O. Wessely, M.P. Williamson, and A.C. Ong, *The Polycystin-1, Lipoxygenase, and alpha-Toxin Domain Regulates Polycystin-1 Trafficking*. J Am Soc Nephrol, 2016. **27**(4): p. 1159-73.
231. Eek, P., R. Jarving, I. Jarving, N.C. Gilbert, M.E. Newcomer, and N. Samel, *Structure of a calcium-dependent 11R-lipoxygenase suggests a mechanism for Ca<sup>2+</sup> regulation*. J Biol Chem, 2012. **287**(26): p. 22377-86.
232. Ivanov, I., A. Di Venere, T. Horn, P. Scheerer, E. Nicolai, S. Stehling, C. Richter, E. Skrzypczak-Jankun, G. Mei, M. Maccarrone, and H. Kuhn, *Tight association of N-terminal and catalytic subunits of rabbit 12/15-lipoxygenase is important for protein stability and catalytic activity*. Biochim Biophys Acta, 2011. **1811**(12): p. 1001-10.
233. Burghardt, L.T., D.I. Trujillo, B. Epstein, P. Tiffin, and N.D. Young, *A Select and Resequencing Approach Reveals Strain-Specific Effects of Medicago Nodule-Specific PLAT-Domain Genes*. Plant Physiol, 2020. **182**(1): p. 463-471.

234. Trujillo, D.I., K.A.T. Silverstein, and N.D. Young, *Nodule-specific PLAT domain proteins are expanded in the Medicago lineage and required for nodulation*. *New Phytol*, 2019. **222**(3): p. 1538-1550.
235. Pislariu, C.I., S. Sinharoy, I. Torres-Jerez, J. Nakashima, E.B. Blancaflor, and M.K. Udvardi, *The Nodule-Specific PLAT Domain Protein NPD1 Is Required for Nitrogen-Fixing Symbiosis*. *Plant Physiol*, 2019. **180**(3): p. 1480-1497.
236. Savadogo, E.H., Y. Shiomi, J. Yasuda, T. Akino, M. Yamaguchi, H. Yoshida, T. Umegawachi, R. Tanaka, D.N.A. Suong, K. Miura, K. Yazaki, and S. Kitajima, *Gene expression of PLAT and ATS3 proteins increases plant resistance to insects*. *Planta*, 2021. **253**(2): p. 37.
237. Hyun, T.K., A. Albacete, E. van der Graaff, S.H. Eom, D.K. Grosskinsky, H. Bohm, U. Janschek, Y. Rim, W.W. Ali, S.Y. Kim, and T. Roitsch, *The Arabidopsis PLAT domain protein1 promotes abiotic stress tolerance and growth in tobacco*. *Transgenic Res*, 2015. **24**(4): p. 651-63.
238. Hyun, T.K., E. van der Graaff, A. Albacete, S.H. Eom, D.K. Grosskinsky, H. Bohm, U. Janschek, Y. Rim, W.W. Ali, S.Y. Kim, and T. Roitsch, *The Arabidopsis PLAT domain protein1 is critically involved in abiotic stress tolerance*. *PLoS One*, 2014. **9**(11): p. e112946.
239. Liu, Y., Y. Su, and X. Wang, *Phosphatidic acid-mediated signaling*. *Adv Exp Med Biol*, 2013. **991**: p. 159-76.
240. Tanguy, E., N. Kassas, and N. Vitale, *Protein(-)Phospholipid Interaction Motifs: A Focus on Phosphatidic Acid*. *Biomolecules*, 2018. **8**(2).
241. Wang, Z., N.S. Anderson, and C. Benning, *The phosphatidic acid binding site of the Arabidopsis trigalactosyldiacylglycerol 4 (TGD4) protein required for lipid import into chloroplasts*. *J Biol Chem*, 2013. **288**(7): p. 4763-71.
242. Ghosh, S., J.C. Strum, V.A. Sciorra, L. Daniel, and R.M. Bell, *Raf-1 kinase possesses distinct binding domains for phosphatidylserine and phosphatidic acid. Phosphatidic acid regulates the translocation of Raf-1 in 12-O-tetradecanoylphorbol-13-acetate-stimulated Madin-Darby canine kidney cells*. *J Biol Chem*, 1996. **271**(14): p. 8472-80.
243. Mott, H.R., J.W. Carpenter, S. Zhong, S. Ghosh, R.M. Bell, and S.L. Campbell, *The solution structure of the Raf-1 cysteine-rich domain: a novel ras and phospholipid binding site*. *Proc Natl Acad Sci U S A*, 1996. **93**(16): p. 8312-7.
244. Jones, J.A., R. Rawles, and Y.A. Hannun, *Identification of a novel phosphatidic acid binding domain in protein phosphatase-1*. *Biochemistry*, 2005. **44**(40): p. 13235-45.

245. Baillie, G.S., E. Huston, G. Scotland, M. Hodgkin, I. Gall, A.H. Peden, C. MacKenzie, E.S. Houslay, R. Currie, T.R. Pettitt, A.R. Walmsley, M.J. Wakelam, J. Warwicker, and M.D. Houslay, *TAPAS-1, a novel microdomain within the unique N-terminal region of the PDE4A1 cAMP-specific phosphodiesterase that allows rapid, Ca<sup>2+</sup>-triggered membrane association with selectivity for interaction with phosphatidic acid*. J Biol Chem, 2002. **277**(31): p. 28298-309.
246. Clay, N.K. and T. Nelson, *VH1, a provascular cell-specific receptor kinase that influences leaf cell patterns in Arabidopsis*. Plant Cell, 2002. **14**(11): p. 2707-22.
247. Cano-Delgado, A., Y. Yin, C. Yu, D. Vafeados, S. Mora-Garcia, J.C. Cheng, K.H. Nam, J. Li, and J. Chory, *BRL1 and BRL3 are novel brassinosteroid receptors that function in vascular differentiation in Arabidopsis*. Development, 2004. **131**(21): p. 5341-51.
248. Ceserani, T., A. Trofka, N. Gandotra, and T. Nelson, *VH1/BRL2 receptor-like kinase interacts with vascular-specific adaptor proteins VIT and VIK to influence leaf venation*. Plant J, 2009. **57**(6): p. 1000-14.
249. Wingenter, K., O. Trentmann, I. Wanschuh, Hormiller, II, A.G. Heyer, J. Reinders, A. Schulz, D. Geiger, R. Hedrich, and H.E. Neuhaus, *A member of the mitogen-activated protein 3-kinase family is involved in the regulation of plant vacuolar glucose uptake*. Plant J, 2011. **68**(5): p. 890-900.
250. Baek, M., F. DiMaio, I. Anishchenko, J. Dauparas, S. Ovchinnikov, G.R. Lee, J. Wang, Q. Cong, L.N. Kinch, R.D. Schaeffer, C. Millan, H. Park, C. Adams, C.R. Glassman, A. DeGiovanni, J.H. Pereira, A.V. Rodrigues, A.A. van Dijk, A.C. Ebrecht, D.J. Opperman, T. Sagmeister, C. Buhlheller, T. Pavkov-Keller, M.K. Rathinaswamy, U. Dalwadi, C.K. Yip, J.E. Burke, K.C. Garcia, N.V. Grishin, P.D. Adams, R.J. Read, and D. Baker, *Accurate prediction of protein structures and interactions using a three-track neural network*. Science, 2021. **373**(6557): p. 871-876.
251. Hiranuma, N., H. Park, M. Baek, I. Anishchenko, J. Dauparas, and D. Baker, *Improved protein structure refinement guided by deep learning based accuracy estimation*. Nat Commun, 2021. **12**(1): p. 1340.
252. Yang, J., I. Anishchenko, H. Park, Z. Peng, S. Ovchinnikov, and D. Baker, *Improved protein structure prediction using predicted interresidue orientations*. Proc Natl Acad Sci U S A, 2020. **117**(3): p. 1496-1503.
253. Song, Y., F. DiMaio, R.Y. Wang, D. Kim, C. Miles, T. Brunette, J. Thompson, and D. Baker, *High-resolution comparative modeling with RosettaCM*. Structure, 2013. **21**(10): p. 1735-42.

254. Raman, S., R. Vernon, J. Thompson, M. Tyka, R. Sadreyev, J. Pei, D. Kim, E. Kellogg, F. DiMaio, O. Lange, L. Kinch, W. Sheffler, B.H. Kim, R. Das, N.V. Grishin, and D. Baker, *Structure prediction for CASP8 with all-atom refinement using Rosetta*. Proteins, 2009. **77 Suppl 9**: p. 89-99.
255. Kallberg, M., H. Wang, S. Wang, J. Peng, Z. Wang, H. Lu, and J. Xu, *Template-based protein structure modeling using the RaptorX web server*. Nat Protoc, 2012. **7(8)**: p. 1511-22.
256. Gilbert, N.C., S.G. Bartlett, M.T. Waight, D.B. Neau, W.E. Boeglin, A.R. Brash, and M.E. Newcomer, *The structure of human 5-lipoxygenase*. Science, 2011. **331(6014)**: p. 217-9.
257. Pettersen, E.F., T.D. Goddard, C.C. Huang, G.S. Couch, D.M. Greenblatt, E.C. Meng, and T.E. Ferrin, *UCSF Chimera--a visualization system for exploratory research and analysis*. J Comput Chem, 2004. **25(13)**: p. 1605-12.
258. Bolger, A.M., M. Lohse, and B. Usadel, *Trimmomatic: a flexible trimmer for Illumina sequence data*. Bioinformatics, 2014. **30(15)**: p. 2114-20.
259. Cheng, C.Y., V. Krishnakumar, A.P. Chan, F. Thibaud-Nissen, S. Schobel, and C.D. Town, *Araport11: a complete reannotation of the Arabidopsis thaliana reference genome*. Plant J, 2017. **89(4)**: p. 789-804.
260. Patro, R., G. Duggal, M.I. Love, R.A. Irizarry, and C. Kingsford, *Salmon provides fast and bias-aware quantification of transcript expression*. Nat Methods, 2017. **14(4)**: p. 417-419.
261. Raudvere, U., L. Kolberg, I. Kuzmin, T. Arak, P. Adler, H. Peterson, and J. Vilo, *g:Profiler: a web server for functional enrichment analysis and conversions of gene lists (2019 update)*. Nucleic Acids Res, 2019. **47(W1)**: p. W191-W198.
262. Kim, J.S., H.J. Jung, H.J. Lee, K.A. Kim, C.H. Goh, Y. Woo, S.H. Oh, Y.S. Han, and H. Kang, *Glycine-rich RNA-binding protein 7 affects abiotic stress responses by regulating stomata opening and closing in Arabidopsis thaliana*. Plant J, 2008. **55(3)**: p. 455-66.
263. Ascenzi, R. and J.S. Gantt, *A drought-stress-inducible histone gene in Arabidopsis thaliana is a member of a distinct class of plant linker histone variants*. Plant Mol Biol, 1997. **34(4)**: p. 629-41.
264. Wu, X., J. Xu, X. Meng, X. Fang, M. Xia, J. Zhang, S. Cao, and T. Fan, *Linker histone variant HIS1-3 and WRKY1 oppositely regulate salt stress tolerance in Arabidopsis*. Plant Physiol, 2022. **189(3)**: p. 1833-1847.

265. Bogamuwa, S. and J.C. Jang, *The Arabidopsis tandem CCCH zinc finger proteins AtTZF4, 5 and 6 are involved in light-, abscisic acid- and gibberellic acid-mediated regulation of seed germination*. Plant Cell Environ, 2013. **36**(8): p. 1507-19.
266. Bogamuwa, S. and J.C. Jang, *Plant Tandem CCCH Zinc Finger Proteins Interact with ABA, Drought, and Stress Response Regulators in Processing-Bodies and Stress Granules*. PLoS One, 2016. **11**(3): p. e0151574.
267. Lu, B. and C. Benning, *A 25-amino acid sequence of the Arabidopsis TGD2 protein is sufficient for specific binding of phosphatidic acid*. J Biol Chem, 2009. **284**(26): p. 17420-7.
268. Kobe, B. and J. Deisenhofer, *The leucine-rich repeat: a versatile binding motif*. Trends Biochem Sci, 1994. **19**(10): p. 415-21.
269. Murphy, F., Q. He, M. Armstrong, L.M. Giuliani, P.C. Boevink, W. Zhang, Z. Tian, P.R.J. Birch, and E.M. Gilroy, *The Potato MAP3K StVIK Is Required for the Phytophthora infestans RXLR Effector Pi17316 to Promote Disease*. Plant Physiol, 2018. **177**(1): p. 398-410.
270. Al-Harrasi, I., H.V. Patankar, R. Al-Yahyai, R. Sunkar, P. Krishnamurthy, P.P. Kumar, and M.W. Yaish, *Molecular Characterization of a Date Palm Vascular Highway 1-Interacting Kinase (PdVIK) Under Abiotic Stresses*. Genes (Basel), 2020. **11**(5).
271. Ohyama, K., M. Ogawa, and Y. Matsubayashi, *Identification of a biologically active, small, secreted peptide in Arabidopsis by in silico gene screening, followed by LC-MS-based structure analysis*. Plant J, 2008. **55**(1): p. 152-60.
272. Tabata, R., K. Sumida, T. Yoshii, K. Ohyama, H. Shinohara, and Y. Matsubayashi, *Perception of root-derived peptides by shoot LRR-RKs mediates systemic N-demand signaling*. Science, 2014. **346**(6207): p. 343-6.
273. Okamoto, S., H. Shinohara, T. Mori, Y. Matsubayashi, and M. Kawaguchi, *Root-derived CLE glycopeptides control nodulation by direct binding to HAR1 receptor kinase*. Nat Commun, 2013. **4**: p. 2191.
274. Fujita, K. and H. Inui, *Review: Biological functions of major latex-like proteins in plants*. Plant Sci, 2021. **306**: p. 110856.
275. Sakakibara, H., *Cytokinin biosynthesis and transport for systemic nitrogen signaling*. Plant J, 2021. **105**(2): p. 421-430.
276. Li, C., M. Gu, N. Shi, H. Zhang, X. Yang, T. Osman, Y. Liu, H. Wang, M. Vatish, S. Jackson, and Y. Hong, *Mobile FT mRNA contributes to the systemic florigen signalling in floral induction*. Sci Rep, 2011. **1**: p. 73.

277. Amsbury, S., P. Kirk, and Y. Benitez-Alfonso, *Emerging models on the regulation of intercellular transport by plasmodesmata-associated callose*. J Exp Bot, 2017. **69**(1): p. 105-115.
278. Azim, M.F. and T.M. Burch-Smith, *Organelles-nucleus-plasmodesmata signaling (ONPS): an update on its roles in plant physiology, metabolism and stress responses*. Curr Opin Plant Biol, 2020. **58**: p. 48-59.
279. Kirk, P. and Y. Benitez-Alfonso, *Plasmodesmata Structural Components and Their Role in Signaling and Plant Development*. Methods Mol Biol, 2022. **2457**: p. 3-22.
280. Han, X., L.J. Huang, D. Feng, W. Jiang, W. Miu, and N. Li, *Plasmodesmata-Related Structural and Functional Proteins: The Long Sought-After Secrets of a Cytoplasmic Channel in Plant Cell Walls*. Int J Mol Sci, 2019. **20**(12).
281. Lu, K.J., F.R. Danila, Y. Cho, and C. Faulkner, *Peeking at a plant through the holes in the wall - exploring the roles of plasmodesmata*. New Phytol, 2018. **218**(4): p. 1310-1314.
282. Lee, J.Y. and M. Frank, *Plasmodesmata in phloem: different gateways for different cargoes*. Curr Opin Plant Biol, 2018. **43**: p. 119-124.
283. Zhang, Y., S. Wang, L. Wang, X. Chang, Y. Fan, M. He, and D. Yan, *Sphingolipids at Plasmodesmata: Structural Components and Functional Modulators*. Int J Mol Sci, 2022. **23**(10).
284. Liu, L., C. Liu, X. Hou, W. Xi, L. Shen, Z. Tao, Y. Wang, and H. Yu, *FTIP1 is an essential regulator required for florigen transport*. PLoS Biol, 2012. **10**(4): p. e1001313.
285. Turnbull, C., *Long-distance regulation of flowering time*. J Exp Bot, 2011. **62**(13): p. 4399-4413.
286. Goldschmidt, E.E., *Plant grafting: new mechanisms, evolutionary implications*. Front Plant Sci, 2014. **5**: p. 727.
287. Mudge, K.J., J. Scofield, S. Goldschmidt, E.E., *A History of Grafting*, in *Horticultural Reviews*, J. Janick, Editor. 2009. p. 437-493.
288. Tsutsui, H. and M. Notaguchi, *The Use of Grafting to Study Systemic Signaling in Plants*. Plant Cell Physiol, 2017. **58**(8): p. 1291-1301.
289. Turnbull, C.G., J.P. Booker, and H.M. Leyser, *Micrografting techniques for testing long-distance signalling in Arabidopsis*. Plant J, 2002. **32**(2): p. 255-62.

290. Notaguchi, M., Y. Daimon, M. Abe, and T. Araki, *Adaptation of a seedling micro-grafting technique to the study of long-distance signaling in flowering of Arabidopsis thaliana*. J Plant Res, 2009. **122**(2): p. 201-14.
291. Marsch-Martinez, N., J. Franken, K.L. Gonzalez-Aguilera, S. de Folter, G. Angenent, and E.R. Alvarez-Buylla, *An efficient flat-surface collar-free grafting method for Arabidopsis thaliana seedlings*. Plant Methods, 2013. **9**(1): p. 14.
292. Huang, N.C. and T.S. Yu, *A pin-fasten grafting method provides a non-sterile and highly efficient method for grafting Arabidopsis at diverse developmental stages*. Plant Methods, 2015. **11**: p. 38.
293. Tsutsui, H., N. Yanagisawa, Y. Kawakatsu, S. Ikematsu, Y. Sawai, R. Tabata, H. Arata, T. Higashiyama, and M. Notaguchi, *Micrografting device for testing systemic signaling in Arabidopsis*. Plant J, 2020. **103**(2): p. 918-929.
294. Padidam, M., *Chemically regulated gene expression in plants*. Curr Opin Plant Biol, 2003. **6**(2): p. 169-77.
295. Ochoa-Fernandez, R., N.B. Abel, F.G. Wieland, J. Schlegel, L.A. Koch, J.B. Miller, R. Engesser, G. Giuriani, S.M. Brandl, J. Timmer, W. Weber, T. Ott, R. Simon, and M.D. Zurbriggen, *Optogenetic control of gene expression in plants in the presence of ambient white light*. Nat Methods, 2020. **17**(7): p. 717-725.
296. Sarrion-Perdigones, A., E.E. Falconi, S.I. Zandalinas, P. Juarez, A. Fernandez-del-Carmen, A. Granell, and D. Orzaez, *GoldenBraid: an iterative cloning system for standardized assembly of reusable genetic modules*. PLoS One, 2011. **6**(7): p. e21622.
297. Sarrion-Perdigones, A., M. Vazquez-Vilar, J. Palaci, B. Castelijns, J. Forment, P. Ziarsolo, J. Blanca, A. Granell, and D. Orzaez, *GoldenBraid 2.0: a comprehensive DNA assembly framework for plant synthetic biology*. Plant Physiol, 2013. **162**(3): p. 1618-31.
298. Vazquez-Vilar, M., A. Quijano-Rubio, A. Fernandez-Del-Carmen, A. Sarrion-Perdigones, R. Ochoa-Fernandez, P. Ziarsolo, J. Blanca, A. Granell, and D. Orzaez, *GB3.0: a platform for plant bio-design that connects functional DNA elements with associated biological data*. Nucleic Acids Res, 2017. **45**(4): p. 2196-2209.
299. Yoo, S.D., Y.H. Cho, and J. Sheen, *Arabidopsis mesophyll protoplasts: a versatile cell system for transient gene expression analysis*. Nat Protoc, 2007. **2**(7): p. 1565-72.

300. Muller, K., D. Siegel, F. Rodriguez Jahnke, K. Gerrer, S. Wend, E.L. Decker, R. Reski, W. Weber, and M.D. Zurbriggen, *A red light-controlled synthetic gene expression switch for plant systems*. *Mol Biosyst*, 2014. **10**(7): p. 1679-88.
301. Zhang, X., R. Henriques, S.S. Lin, Q.W. Niu, and N.H. Chua, *Agrobacterium-mediated transformation of Arabidopsis thaliana using the floral dip method*. *Nat Protoc*, 2006. **1**(2): p. 641-6.
302. Davis, A.M., A. Hall, A.J. Millar, C. Darrah, and S.J. Davis, *Protocol: Streamlined sub-protocols for floral-dip transformation and selection of transformants in Arabidopsis thaliana*. *Plant Methods*, 2009. **5**: p. 3.
303. Kuhlert, S., G. Austic, R. Zegarac, I. Osei-Bonsu, D. Hoh, M.I. Chilvers, M.G. Roth, K. Bi, D. TerAvest, P. Weebadde, and D.M. Kramer, *MultispeQ Beta: a tool for large-scale plant phenotyping connected to the open PhotosynQ network*. *R Soc Open Sci*, 2016. **3**(10): p. 160592.
304. Windt, C.W., F.J. Vergeldt, P.A. de Jager, and H. van As, *MRI of long-distance water transport: a comparison of the phloem and xylem flow characteristics and dynamics in poplar, castor bean, tomato and tobacco*. *Plant Cell Environ*, 2006. **29**(9): p. 1715-29.
305. Savage, J.A., M.A. Zwieniecki, and N.M. Holbrook, *Phloem transport velocity varies over time and among vascular bundles during early cucumber seedling development*. *Plant Physiol*, 2013. **163**(3): p. 1409-18.
306. Schmidt, L., G.M. Hummel, B. Thiele, U. Schurr, and M.R. Thorpe, *Leaf wounding or simulated herbivory in young N. attenuata plants reduces carbon delivery to roots and root tips*. *Planta*, 2015. **241**(4): p. 917-28.
307. Goeschl, J.D. and L. Han, *A Proposed Drought Response Equation Added to the Munch-Horwitz Theory of Phloem Transport*. *Front Plant Sci*, 2020. **11**: p. 505153.
308. Braun, D.M., *Phloem Loading and Unloading of Sucrose: What a Long, Strange Trip from Source to Sink*. *Annu Rev Plant Biol*, 2022. **73**: p. 553-584.
309. Paniagua, C., B. Sinanaj, and Y. Benitez-Alfonso, *Plasmodesmata and their role in the regulation of phloem unloading during fruit development*. *Curr Opin Plant Biol*, 2021. **64**: p. 102145.
310. Zhao, J., B. Ding, E. Zhu, X. Deng, M. Zhang, P. Zhang, L. Wang, Y. Dai, S. Xiao, C. Zhang, C.J. Liu, and K. Zhang, *Phloem unloading via the apoplastic pathway is essential for shoot distribution of root-synthesized cytokinins*. *Plant Physiol*, 2021. **186**(4): p. 2111-2123.

## **Appendix A.**

### **Supplemental Data for Chapter 2**

**Table A.1: RT-qPCR Primers for Phloem-Localized Predicted Lipid Binding Proteins**

Gene Name	Primer Sequences	Size (bp)	Annealing Temp (°C)	Accession Number
Actin 8 (ACT8)	F: 5'-CCT ATC TAC GAG GGT TTC-3' R: 5'-CTC TCG GTA AGG ATC TTC-3'	98	56.5	AT1G49240
Annexin 1 (ANN1)	F: 5'-GAA CAG AGG AAA GTC ATC-3' R: 5'-GAG TCC ACA ACA AGA TAG-3'	115	55	AT1G35720
Major Latex-like Protein 43 (MLP-43)	F: 5'-GGG AAG AAT AAG ATC GAG-3' R: 5'-CTC ATT CAT CAG ATC ACC-3'	81	55	AT1G70890
Major Latex-like Protein 423 (MLP-423)	F: 5'- GAG GTT GAG GTT AAG TCT-3' R: 5'-TGT AGT CGT TAG GGA AAG-3'	91	56	AT1G24020
Bet v1 Allergen	F: 5'-TAG TGC TCA GGG TAA TAG-3' R: 5'-GAC ACT TAA CCA CAC TTC-3'	108	56	AT1G23130
Phloem Lipid-Associated Family Protein (PLAFP) [181]	F: 5'-GGT GAC TAC ATC GGA ATC-3' R: 5'-CAG ATC GGA CTA GGT AAA C-3'	128	57	AT4G39730
Phospholipase D $\alpha$ 1 (PLD $\alpha$ 1)	F: 5'-ATT GGA GCT ACC CTT ATC-3' R: 5'-TTG ATC CTC CCT GAA TAG-3'	121	56	AT3G15730
Phospholipase D $\alpha$ 2 (PLD $\alpha$ 2)	F: 5'-GGT CTA TGT TGT TGT TCC-3' R: 5'-CTC TAA GTG CCT TGA TTA C-3'	125	56	AT1G52570
Phospholipase D $\delta$ (PLD $\delta$ )	F: 5'-GGA TAG GGC GTA TAT CAT-3' R: 5'-CTC TGG ATC ATC TTC TTT AG-3'	116	56	AT4G35790
Phospholipase C 3 (PLC3)	F: 5'-ATC CAG AGA AGC CTA TAC-3' R: 5'-GAT TCC TCT GTG TAA ACC-3'	99	55.5	AT4G38530
Sec 14-like protein (Sec14)	F: 5'-CTA CCA CTC TCG TTA CAC-3' R: 5'-CTC CAG AGT TTC TGT CTC-3'	107	51	AT1G72160
14-3-3	F: 5'-CCC ACA CAT CCA GTT AG-3' R: 5'-CAT CGA ATG CTT GCT TAG-3'	109	51	AT1G22300
GDSL-lipase [181]	F: 5'-TCG GCC AAC CGA ATC TTC AA-3' R: 5'-CCT TCC AAT TCC GCA ACA CG-3'	173	52	AT1G29660
PIG-P-like protein [181]	F: 5'-GAC GAA TTC GGA AGA TGC TC-3' R: 5'-TCA GGG TTT CCA GCT GAT TC-3'	247	50	AT2G39445

**Table A.2 Primers for Cloning LBPs in Expression Vectors**

Gene Name	Forward	Reverse	Annealing Temp (°C)	Accession Number
Gateway Cloning				
Annexin 1 (ANN1)	5'-GGGGACAAGTTT GTACAAAAAAGCAG GCTATGGCGACTCT TAAGGTTTC-3'	5'-GGGGACCAC TTTGTACAAGAAA GCTGGGTCAGCA TCATCTTCACCGA GAAG-3'	60	AT1G35720
Major Latex-like Protein 43 (MLP-43)	5'-GGGGACAAGTTT GTACAAAAAAGCAG GCTATGGCAGAAG CGTCTAGTTTG-3'	5'-GGGGACCAC TTTGTACAAGAAA GCTGGGTCTTCC TCGGCCAAGAGA TG-3'	68	AT1G70890
Major Latex-like Protein 423 (MLP-423)	5'-GGGGACAAGTTT GTACAAAAAAGCAG GCTATGGGGTTGA GTGGTGTTCTTC-3'	5'-GGGGACCAC TTTGTACAAGAAA GCTGGGTCGGCA CTAGTTTGCTTAA GAAGATAC-3'	55	AT1G24020
Bet v1 Allergen	5'-GGGGACAAGTTT GTACAAAAAAGCAG GCTATGGCACAAGC TACGCGTC-3'	5'-GGGGACCAC TTTGTACAAGAAA GCTGGGTCTGACT TCGGACAAAAGC ATTTCGTCC-3'	60	AT1G23130
In-Fusion Cloning				
Annexin 1 (ANN1)	5'-CGCGCGGCA GCCATATGGCGACT CTTAAGGTTTCTGA TT-3'	5'-GGATCCTCG AGCATATGCTAA GCATCATCTTCAC CGAGAAGTG-3'	60	AT1G35720
Major Latex-like Protein 43 (MLP-43)	5'-CGCGCGGCA GCCATATGGCAGAA GCGTCTAGTTTGG- 3'	5'-GGATCCTCG AGCATATGCTATT CCTCGGCCAAGA GATGTTTCG-3'	60	AT1G70890
Major Latex-like Protein 423 (MLP-423)	5'-CGCGCGGCA GCCATATGGGGTTG AGTGGTGTTCTT-3'	5'-GGATCCTCG AGCATATGCTAG GCACTAGTTTGC TTAAGAAGATACT CATCT-3'	60	AT1G24020
Bet v1 Allergen	5'-CGCGCGGCA GCCATATGGCACAA GCTACGCG-3'	5'-GGATCCTCG AGCATATGCTAG ACTTCGGACAAA AGCATTTCGTCC- 3'	60	AT1G23130

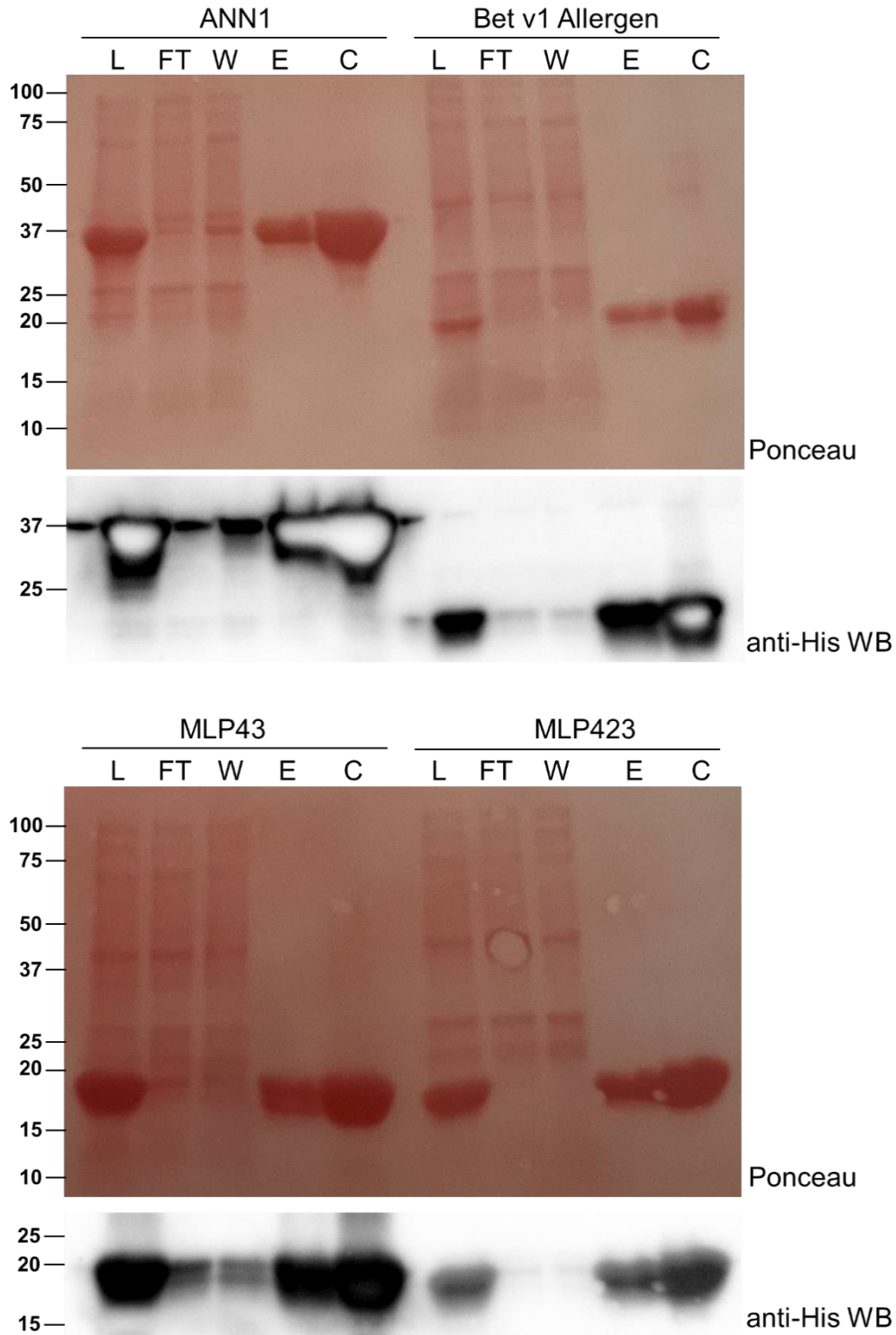


**Figure A.1 Validation of His-tagged LBPs with SDS-PAGE and Western Blot.** Top: Annexin 1 (ANN1, 36 kDa) and Bet v1 Allergen (18 kDa); Bottom: Major Latex Protein-like Protein 43 (MLP43, 18 kDa) and Major Latex Protein-like Protein 423 (MLP423, 17 kDa). L, Lysate; FT, Flow-through; W, Wash; E, Elution; C, Concentrated fraction; WB, Western Blot. Ladder sizes are denoted on the left in kDa.

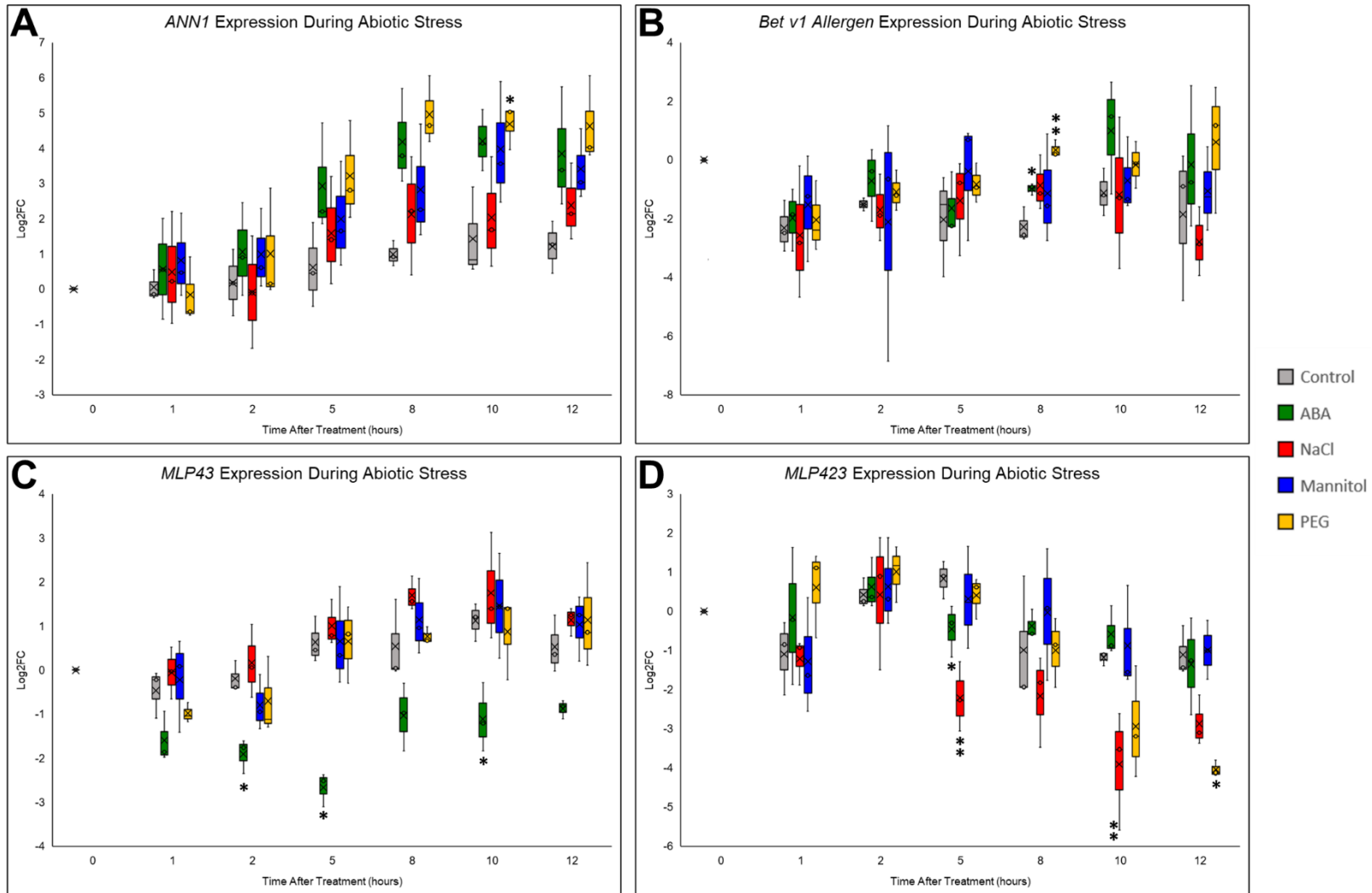


**Figure A.2 Gene Expression of Lipid Binding Proteins during Abiotic Stress.** The gene expression of *ANN1* (A), *Bet v1 Allergen* (B), *MLP43* (C), and *MLP423* (D) across 12 hours of abiotic stresses is shown. The X in the boxplot represents the average Log<sub>2</sub>Fold-Change (Log<sub>2</sub>FC). A paired student's t-test was used to determine the statistical significance between the stress-treated sample and the control at the corresponding timepoint, \* p≤0.05, \*\* p≤0.01, \*\*\* p≤0.001, \*\*\*\* p≤0.0001

**Appendix B.**

**Supplemental Data for Chapter 3**

**Table B.1 Primers for Mutagenesis and Expression Constructs**

Name	Primer Sequences	Annealing Temp (°C)
Q5 Site-Directed Mutagenesis		
R36A	F: 5'-ATTCTACCTCgcAACCGGATCG-3' R: 5'-GTGTATACACAGTCTGGATC-3'	57
W41A	F: 5'-CGGATCGATCgcGAAAGCCGGAAC-3' R: 5'-GTTCTGAGGTAGAATGTG-3'	57
K42A	F: 5'-ATCGATCTGGgcAGCCGGAACC-3' R: 5'-CCGGTTCTGAGGTAGAATG-3'	63
W69A	F: 5'-CCTTCAAGCTgcGGCTGGATTAATG-3' R: 5'-TTTTTGATTCCGATGTAGTC-3'	58
R82A	F: 5'-TACTTCGAGgcGGTAATCTCGAC-3' R: 5'-TTGTAATCAGGTCCCATTAATC-3'	59
R91A	F: 5'-TTTCAGTGGAgcAGCACCGTGTTTAC-3' R: 5'-ATGTCGAGATTACCCCTC-3'	61
W115A	F: 5'-TCACCATGGTgcGTACGTTA ATTACGTTGAGATCACG-3' R: 5'-TCGCCGGAGCCATCGGAG-3'	69
W141A	F: 5'-GATTGAGCAAgcGCTCGCTACTG-3' R: 5'-TCAAATCCTGCGTCGAG-3'	58
R155A	F: 5'-CACCGCCGTAgcGAACAATTGTC-3' R: 5'-AGCTCATAAGGAGAAGTATC-3'	57
Cloning Primers		
PLAFP-RFP	Gateway F: 5'-GGGGACAAGTTTGTACAAAAAAGCAGGCTATGG CTCGTCGCGATGTTTC-3' R: 5'-GGGGACCACTTTGTACAAGAAAGCTGGGTtcaa ttaagtttgccccagtttgc-3'	65
	InFusion F: 5'-AGAGGACACGCTCGAATGGCTCGTCGCGATGT- 3' R: 5'-GATCTACCATCTCGAattaagtttgccccagtttgct-3'	66
VIK-GFP	TOPO F: 5'-CACCATGAGCTCCGATTCACCGG--3' R: 5'-TGAAGTGAATAAGCCCCAATGGTG-3'	
VH1K-GFP	InFusion F: 5'-CACCATGACTACTTCACCAATCCGGG-3' R: 5'-CAAGCTGTTACTGTGACTGTGAC-3' F: 5'-AGAGGACACGCTCGAGATGACTACTTCACCAAT CCGGGT-3' R: 5'-GATCTACCATCTCGAGCAAGCTGTTACTGTGAC TGTGACTAT-3'	60

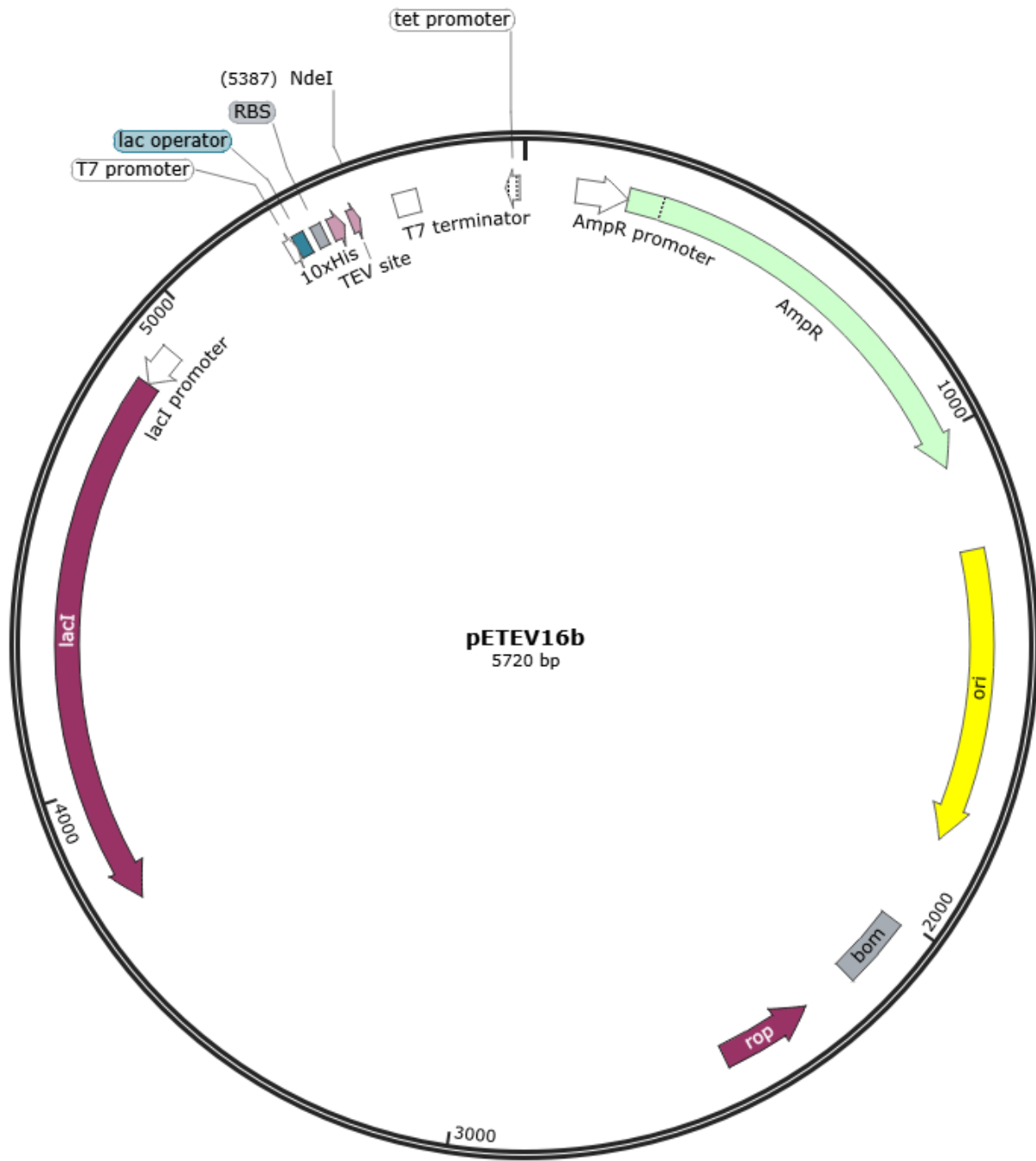
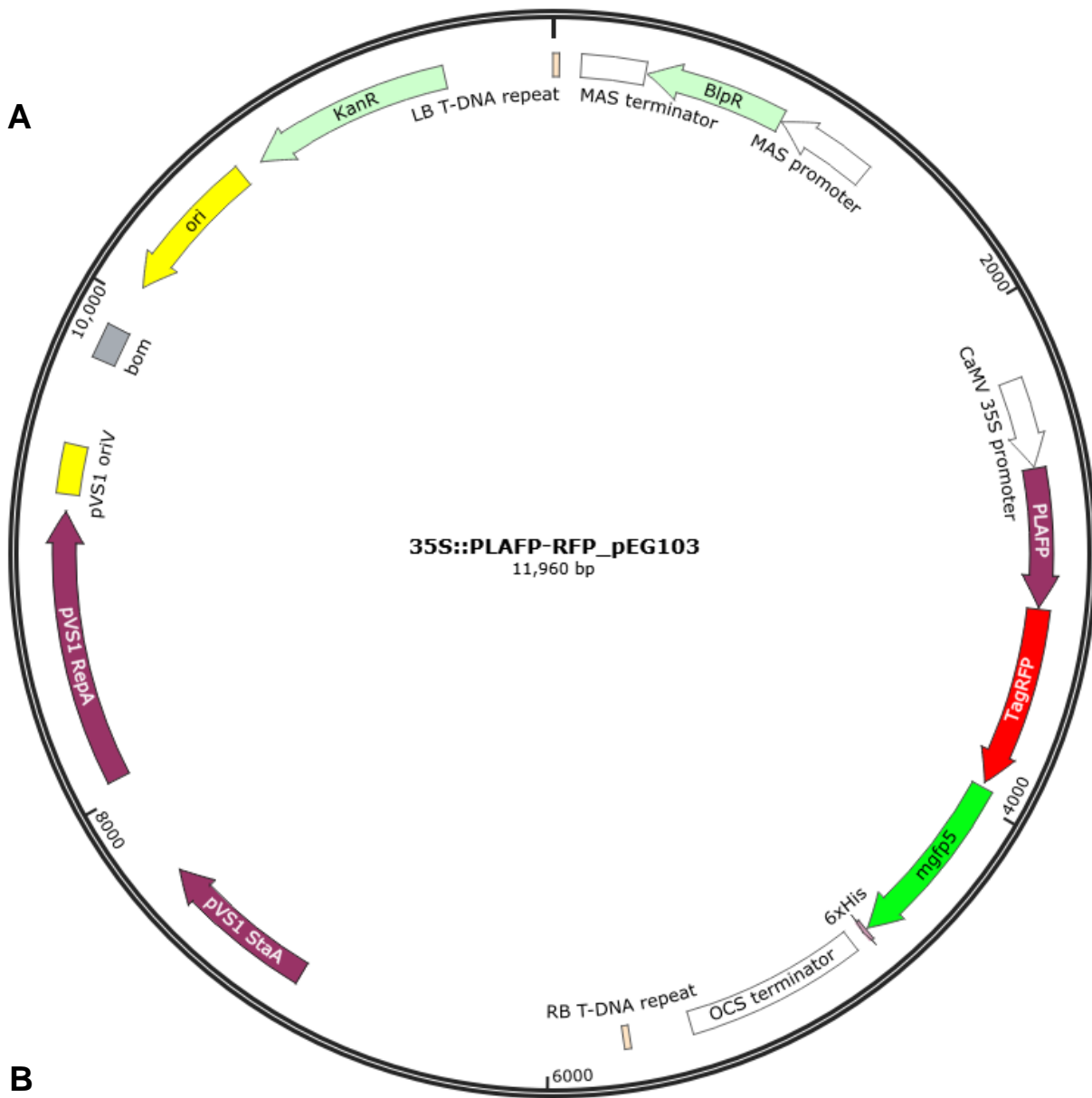


Figure B.1 Construct Map of pETEVE16b Vector.



```

tcgagcagcagcaggggtgctgtggccagatactgcgacctccctagcaaacctggggcacaaccttaatTCGAGATGGTAGATCTGACTAGTAAAGGAGAAGAACTTTTCA
agctcgtcgtgctccaccgacaccgggtctatgacgctggagggatcggttgaccctgtttgaattaAGCTCTACCATCTAGACTGATCATTTCCTTCTTGAAAAGT
215  V E Q H E V A V A R Y C D L P S K L G H K L N S R W S K G E E L F
TagRFP mgfp5
    
```

**Figure B.2 Construct Map of 35S::PLAFP-RFP in the pEarleyGate 103 vector.** (A) PLAFP-RFP fusion was amplified and ligated into the pEarleyGate 103 backbone using XhoI and In-Fusion (Takara) cloning. The stop codon in TagRFP was retained (B) so GFP is not translated.

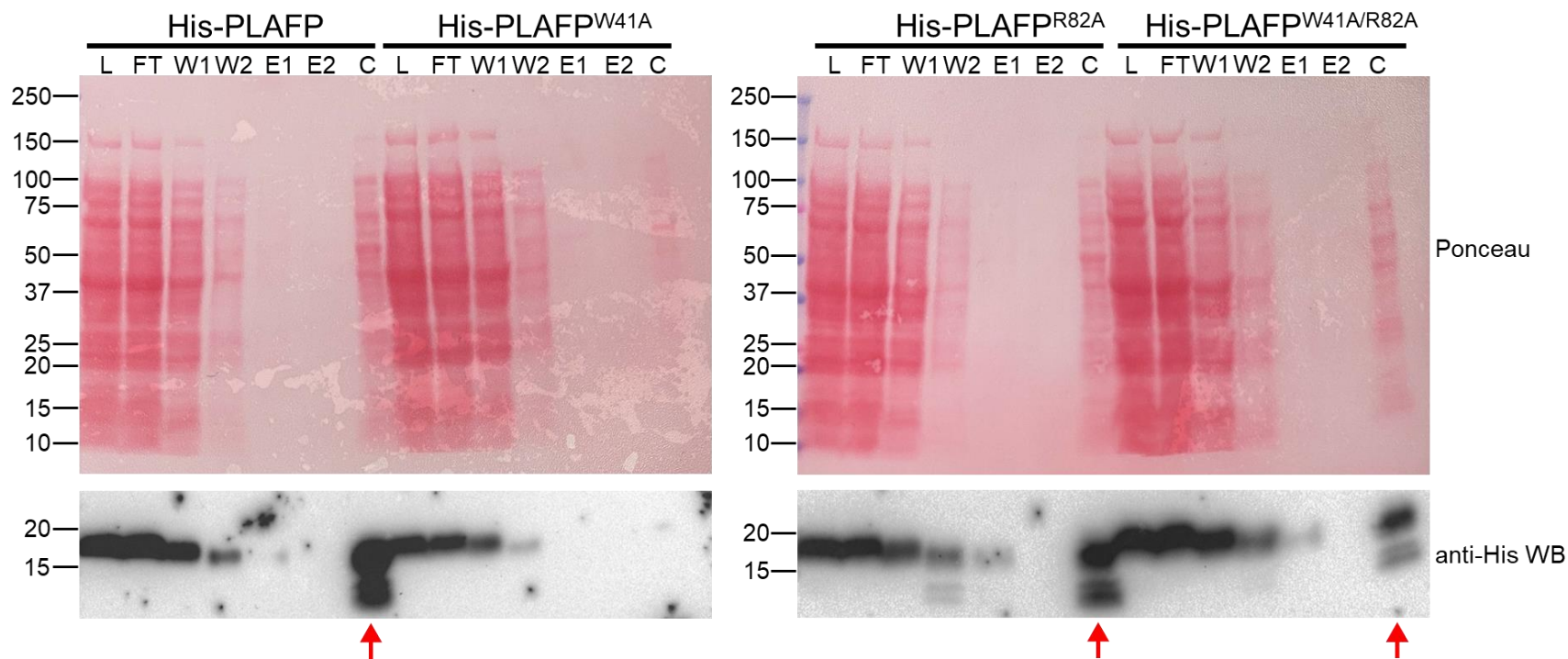


**Figure B.3 Validation of PLAFP Mutant Purifications with SDS-PAGE and Western Blot.** N-terminally His-tagged native PLAFP and point mutants were purified by gravity affinity column. Fractions were collected and run on 4-20% gradient protein gel by SDS-PAGE (Ponceau, top) and validated with anti-His Western Blot (bottom). Native His-PLAFP, R82A single mutant, and the W41A/R82A double mutant were recovered in the elution fraction and concentrated, indicated by the red arrows. The W41A mutant was resistant to purification and was lost in the lysate, flow-through, and wash steps. Lipid overlays (Figure 3.3) were carried out for native PLAFP, R82A single mutant, and W41A/R82A double mutant.

L, Lysate; FT, Flow-through; W1, 100 mM imidazole Wash; W2, 250 mM imidazole Wash; E1, first 500 mM imidazole Elution; E2, second 500 mM imidazole Elution; C, Concentrated fraction

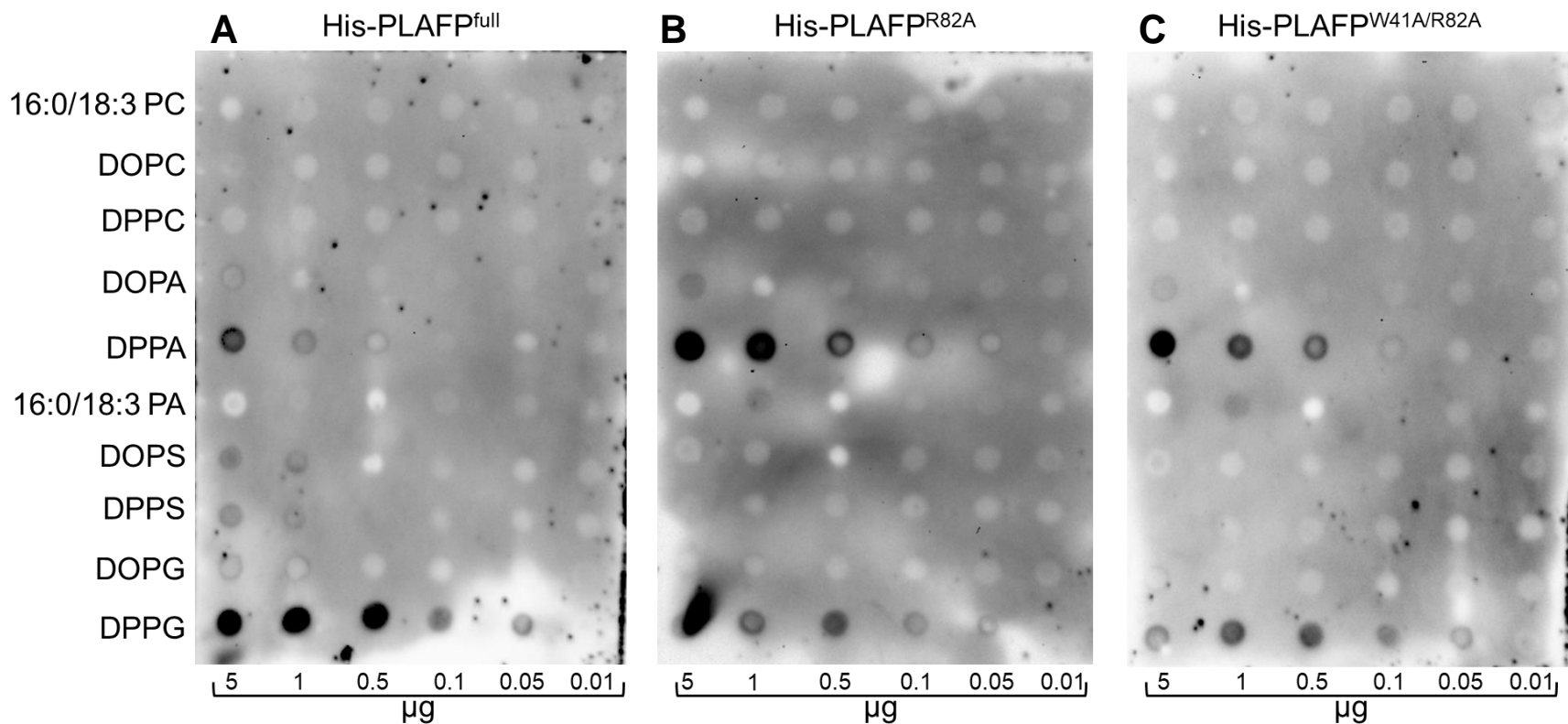


**Figure B.4 Lipid Overlays to Detect Phospholipid Binding Activity of PLAFP and PLAFP Mutants.** Representative PLAFP (A), PLAFP R82A single mutant (B), and PLAFP W41A/R82A double mutant (C) lipid overlays are shown. A dilution series of various phospholipids was employed to estimate binding affinity. Similar results were obtained in triplicate.

PC, phosphatidylcholine; DOPC, dioleoyl (18:1/18:1) phosphatidylcholine; DPPC, dipalmitoyl (16:0/16:0) phosphatidylcholine; DOPA, dioleoyl phosphatidic acid; DPPA, dipalmitoyl phosphatidic acid; PA, phosphatidic acid; DOPS, dioleoyl phosphatidylserine; DPPS, dipalmitoyl phosphatidylserine; DOPG, dioleoyl phosphatidylglycerol; DPPG, dipalmitoyl phosphatidylglycerol; PLAFP, Phloem Lipid-Associated Family Protein; R82A, Arginine-82 mutated to Alanine; W41A, Tryptophan-41 mutated to Alanine.

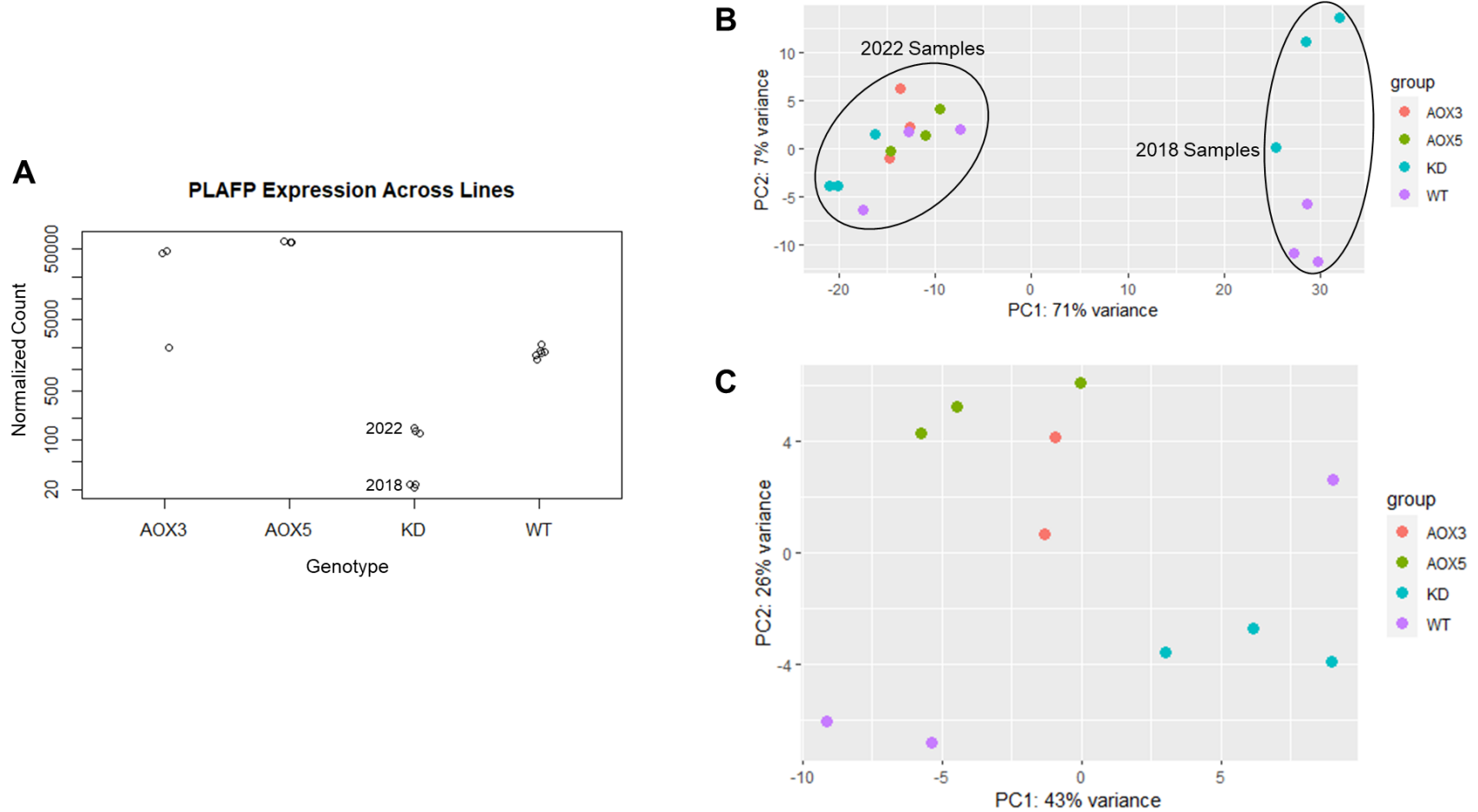


**Figure B.5 Dot Plot and Principal Component Analysis for *PLAFP* RNA-Seq Samples.** (A) *PLAFP* expression levels for each biological replicate within genotypes are represented by dots. The AOX3 sample with wild-type (WT) expression level was discarded from differential expression analysis. (B) Samples collected in 2018 and 2022 were compared using Principal Component Analysis. The sample year was the predominant contributing factor to clustering, so 2018 knockdown (KD) and wild-type samples were not grouped with the 2022 samples for further analysis to minimize confounding variables. (C) The AOX3 and AOX5 samples cluster away from the KD and WT samples within the 2022 samples.

**Table B.2 Differentially Expressed Genes in *PLAFP* Expression Lines**  
(FDR  $\leq$  0.05;  $-1 \geq \text{Log}_2\text{FC} \geq 1$ ) Differentially expressed genes identified in both knockdown experiments are highlighted in yellow.

Accession Number	Log <sub>2</sub> Fold-Change	FDR p <sub>adj</sub>
<b>Knockdown Compared to Wild-Type (2018)</b>		
<i>Up-Regulated</i>		
AT3G09940	3.254	6.78E-34
AT2G24850	3.384	4.92E-30
AT2G29350	2.259	5.25E-30
AT3G21230	2.202	1.11E-17
AT2G40460	1.311	9.16E-16
AT4G29740	2.317	3.81E-15
AT5G57150	1.232	1.17E-14
AT5G01900	3.345	1.73E-13
AT1G22410	1.100	4.58E-13
AT2G39050	1.053	5.79E-13
AT3G01060	2.212	1.44E-12
AT1G10370	2.918	6.89E-12
AT3G24982	2.223	1.43E-11
AT1G61120	3.875	1.90E-11
AT2G37970	1.672	2.29E-10
AT3G25760	3.063	4.87E-10
AT4G31870	3.240	1.18E-09
AT2G40230	1.289	1.76E-09
AT5G17000	1.085	2.70E-09
AT5G38710	2.168	3.49E-09
AT5G28630	1.963	5.21E-09
AT5G27060	2.070	5.22E-09
AT1G51805	1.156	5.42E-09
AT4G21830	4.262	5.93E-09
AT2G39420	1.913	9.87E-09
AT3G54500	1.095	1.22E-08
AT4G18250	1.272	1.72E-08
AT1G74590	1.597	2.25E-08
AT5G65870	1.456	2.79E-08
AT2G23600	1.259	3.13E-08
AT5G07460	1.089	3.32E-08
AT3G12320	1.230	4.97E-08
AT4G29110	2.076	1.18E-07
AT4G23200	1.377	1.29E-07
AT1G11670	2.222	1.37E-07
AT3G02870	1.218	2.45E-07
AT4G30530	1.156	3.54E-07
AT2G44940	1.206	6.53E-07

**Table B.2 (cont'd)**

AT3G51450	1.971	6.74E-07
AT5G55050	1.522	6.74E-07
AT2G39330	2.754	7.05E-07
AT5G42650	1.716	8.02E-07
AT1G77760	2.303	1.21E-06
AT5G17220	3.611	1.21E-06
AT4G14090	2.175	1.30E-06
AT4G04020	1.362	1.61E-06
AT4G39950	1.387	1.84E-06
AT1G26560	1.028	2.97E-06
AT2G20340	1.297	3.11E-06
AT2G23010	2.045	3.62E-06
AT2G30770	1.774	3.62E-06
AT2G40100	1.303	3.84E-06
AT4G36950	4.105	4.76E-06
AT1G54575	1.259	7.04E-06
AT1G74010	1.555	7.04E-06
AT1G20510	1.007	7.23E-06
AT5G24530	1.033	7.67E-06
AT1G77960	1.906	8.20E-06
AT5G59580	2.264	8.80E-06
AT5G01820	1.181	9.16E-06
AT3G25770	1.875	9.74E-06
AT1G32900	1.437	1.01E-05
AT3G25180	3.590	1.10E-05
AT3G44860	2.590	1.20E-05
AT3G48460	1.527	1.22E-05
AT3G57460	1.322	1.42E-05
AT4G19380	1.857	1.61E-05
AT1G06620	1.657	1.62E-05
AT5G40390	1.396	1.77E-05
AT2G31380	1.374	1.78E-05
AT5G52390	2.885	2.07E-05
AT1G72520	2.946	2.22E-05
AT3G03780	1.007	2.31E-05
AT1G65610	2.188	2.52E-05
AT4G00970	1.170	2.55E-05
AT5G45820	1.697	3.00E-05
AT4G13410	3.061	3.08E-05
AT2G29650	1.068	3.38E-05
AT2G30100	1.075	3.39E-05
AT1G61800	1.986	4.09E-05
AT1G45145	1.103	5.10E-05
AT3G21500	5.514	5.21E-05

**Table B.2 (cont'd)**

AT5G61270	1.281	5.44E-05
AT4G36030	1.011	6.56E-05
AT1G23740	1.297	6.66E-05
AT1G56650	2.400	7.35E-05
AT2G05940	1.051	7.50E-05
AT4G04610	1.012	8.00E-05
AT1G09080	2.308	8.48E-05
AT3G44550	2.351	8.91E-05
AT3G44970	3.449	9.04E-05
AT3G60160	1.286	9.04E-05
AT1G28600	1.113	9.17E-05
AT1G72770	3.862	0.000101328
AT2G36590	3.278	0.000101328
AT5G13930	2.174	0.000102464
AT3G09520	2.361	0.000106333
AT3G11480	7.989	0.000112143
AT4G10390	1.639	0.00011954
AT1G17380	2.385	0.00012798
AT4G11460	2.557	0.000140035
AT1G09932	1.642	0.000141694
AT5G48540	1.054	0.000174176
AT3G01550	1.276	0.00017425
AT1G65390	3.031	0.000194207
AT2G40330	1.767	0.000203244
AT1G65690	1.196	0.000204395
AT2G46830	1.555	0.000204722
AT5G60890	2.012	0.000204722
AT2G28510	1.182	0.000226984
AT4G21870	2.438	0.000237493
AT5G66640	1.038	0.000238351
AT5G06730	4.492	0.000241007
AT4G28140	2.869	0.000286856
AT1G19640	2.605	0.000287497
AT4G37150	2.736	0.00028761
AT1G58420	1.622	0.000298802
AT1G21110	1.280	0.000316914
AT1G51760	1.043	0.00032816
AT2G37240	1.249	0.000333072
AT3G55970	2.436	0.000340131
AT1G10470	1.333	0.000411368
AT2G38240	2.941	0.000427123
AT4G18220	1.048	0.000457801
AT5G19240	1.516	0.000457801
AT2G39250	1.169	0.000474998

**Table B.2 (cont'd)**

AT2G46650	1.109	0.000474998
AT5G63450	2.915	0.000525507
AT3G21670	1.384	0.000526502
AT5G56980	1.986	0.000530773
AT5G64850	1.792	0.000547005
AT5G64750	2.882	0.00055464
AT5G65140	1.441	0.00056213
AT1G45201	1.296	0.000580932
AT3G27400	2.832	0.000580932
AT4G21940	1.029	0.000595661
AT5G22930	1.796	0.000611796
AT2G16890	1.282	0.00063127
AT1G06000	1.054	0.000670182
AT1G60470	4.137	0.000748307
AT3G26290	1.045	0.00077491
AT5G67210	1.492	0.00077491
AT1G24575	1.112	0.000803409
AT5G57800	1.055	0.000832469
AT3G51660	1.098	0.000833518
AT3G50770	1.339	0.000848958
AT1G76240	1.337	0.000860846
AT2G41800	3.790	0.000868992
AT4G35110	1.160	0.000929088
AT1G19050	1.827	0.000990461
AT3G02380	1.521	0.001020252
AT3G28070	1.083	0.001026374
AT2G42760	1.886	0.001035911
AT1G69610	1.146	0.001037679
AT5G57345	1.013	0.001043573
AT4G35160	3.754	0.001053037
AT1G76130	1.238	0.001073924
AT1G17420	3.574	0.001102964
AT2G42360	1.486	0.001116349
AT2G04039	1.321	0.001122718
AT3G22275	5.408	0.001179609
AT5G59130	1.792	0.001187892
AT3G47960	1.537	0.001196106
AT5G49480	1.399	0.001216922
AT3G47780	1.057	0.001240027
AT3G19450	1.152	0.001265441
AT1G73325	3.960	0.001278582
AT5G52050	2.928	0.001305936
AT2G34810	1.674	0.001325678
AT4G37990	2.201	0.001346386

**Table B.2 (cont'd)**

AT3G47420	1.110	0.001392741
AT1G07180	1.244	0.001519275
AT4G15210	2.642	0.001539777
AT1G80820	2.207	0.00157688
AT3G59140	1.183	0.001584216
AT3G25780	2.285	0.001607732
AT5G66650	2.039	0.001654525
AT5G06320	1.069	0.001693817
AT2G06050	1.813	0.001703038
AT1G71140	1.178	0.001714073
AT3G51240	1.577	0.001759104
AT4G33010	1.124	0.001783081
AT3G22620	1.157	0.001923407
AT1G72450	1.026	0.00192842
AT5G15950	1.521	0.00192842
AT5G54160	1.228	0.00192842
AT5G58310	2.029	0.001931406
AT1G62540	1.185	0.001972332
AT2G38750	1.608	0.001972332
AT2G20880	2.824	0.002105603
AT5G14700	1.016	0.002132991
AT1G12110	1.389	0.002178812
AT5G46350	1.511	0.002235594
AT2G27690	2.782	0.002302779
AT4G11480	3.175	0.002317242
AT5G37600	1.069	0.00232631
AT1G62262	2.203	0.00235845
AT2G05100	1.224	0.00235845
AT2G15020	3.247	0.002366508
AT5G59730	1.214	0.00243348
AT5G07690	1.030	0.002434373
AT5G10300	1.298	0.002444842
AT3G12990	4.815	0.002489263
AT3G22600	1.537	0.002546127
AT1G32960	1.647	0.002574232
AT1G73600	2.203	0.002620654
AT3G48520	4.895	0.002666714
AT1G55210	1.259	0.002764496
AT5G28237	2.581	0.002840134
AT4G13890	2.175	0.002990589
AT2G30830	4.231	0.003123006
AT5G06570	1.294	0.003126549
AT3G22840	3.452	0.003167619
AT1G31550	1.073	0.003271257

**Table B.2 (cont'd)**

AT4G26070	3.722	0.003366571
AT5G26220	1.692	0.003524712
AT4G01080	1.558	0.003601594
AT1G68600	1.213	0.00360665
AT3G56260	1.787	0.003617713
AT4G24570	1.533	0.003719839
AT4G24190	1.003	0.003867241
AT1G04600	1.092	0.003928462
AT1G52800	1.184	0.00396932
AT5G47240	1.392	0.004120366
AT5G08030	3.041	0.004199643
AT4G18440	2.013	0.004227583
AT4G25470	1.153	0.004362858
AT5G45340	1.031	0.004667375
AT2G29450	1.477	0.004753899
AT2G33380	1.643	0.004886267
AT1G24070	1.559	0.004913673
AT5G54710	1.169	0.004917947
AT4G05020	1.088	0.005100768
AT1G61610	2.102	0.005115034
AT1G03820	1.845	0.005185159
AT1G66160	2.046	0.00534552
AT2G35980	1.725	0.005358005
AT3G44450	1.606	0.00542229
AT1G21120	1.195	0.005449362
AT3G03910	2.496	0.005509925
AT3G57260	1.610	0.005697505
AT4G15230	1.344	0.005757859
AT2G28210	2.082	0.005794418
AT3G50760	1.106	0.005923595
AT3G53260	1.045	0.005923595
AT4G29690	1.980	0.005923595
AT5G47330	1.514	0.005923595
AT3G48350	1.429	0.005949836
AT5G43420	1.370	0.006035398
AT1G73260	2.147	0.00615221
AT5G54720	1.519	0.006245856
AT1G13650	2.433	0.006330972
AT1G28480	1.643	0.006420996
AT3G46900	3.048	0.006438458
AT1G15520	1.698	0.006683096
AT4G24780	1.076	0.006683096
AT5G05340	2.468	0.00678864
AT1G79680	1.566	0.007068082

**Table B.2 (cont'd)**

AT5G67620	2.258	0.007284284
AT3G50280	1.350	0.007310739
AT1G33260	1.523	0.007610402
AT2G41250	1.126	0.007642673
AT1G77510	1.169	0.007781532
AT2G25440	2.143	0.007832789
AT1G04220	1.121	0.007854693
AT4G23260	1.004	0.007877253
AT4G16730	4.488	0.007999895
AT5G67370	1.023	0.00820528
AT4G21850	1.837	0.008230192
AT5G53760	1.017	0.008405444
AT2G23000	1.889	0.008460896
AT1G20070	1.882	0.008470084
AT1G18590	1.039	0.00854031
AT5G16570	2.281	0.008995234
AT4G31800	1.275	0.009130084
AT1G28370	1.622	0.009382369
AT3G04010	1.427	0.009382369
AT5G38900	1.030	0.009385898
AT4G23290	1.527	0.009409858
AT1G14430	1.275	0.009461599
AT3G56290	1.302	0.009477672
AT2G02010	1.047	0.009722424
AT4G24380	1.479	0.009994111
AT5G10625	1.213	0.01030095
AT5G44050	2.280	0.010355785
AT2G46790	1.083	0.010537457
AT5G62430	1.015	0.010714118
AT3G44990	1.821	0.010994145
AT1G65890	1.942	0.011250647
AT2G22200	2.280	0.011442683
AT4G13860	2.612	0.011976283
AT2G42350	1.487	0.012151721
AT4G27860	1.145	0.012543474
AT2G22770	1.555	0.012924329
AT2G27660	1.139	0.012924329
AT5G65020	1.059	0.013137645
AT5G53750	1.224	0.013319997
AT2G25735	1.058	0.013329768
AT1G72280	1.103	0.013621537
AT1G66280	4.315	0.013633344
AT2G04100	1.303	0.01373612
AT3G09270	1.585	0.013908395

**Table B.2 (cont'd)**

AT4G11650	1.401	0.013908395
AT4G39250	5.647	0.013908395
AT1G26730	1.161	0.013917766
AT4G10290	5.310	0.014085639
AT1G78860	1.185	0.014275595
AT5G40210	2.707	0.01450539
AT1G60190	2.037	0.014562823
AT5G05440	1.109	0.014800565
AT3G16410	1.424	0.015273302
AT4G17340	1.383	0.015616381
AT3G45140	1.479	0.015815418
AT5G44390	1.572	0.015825577
AT5G14730	1.075	0.015943531
AT5G12340	2.490	0.016314762
AT3G16400	1.234	0.016426221
AT2G43530	1.349	0.016573931
AT5G62920	2.100	0.016595652
AT2G04090	3.856	0.017339726
AT3G27415	4.201	0.017348461
AT1G26770	1.114	0.017858793
AT1G79400	2.226	0.017863755
AT5G41590	2.344	0.018183103
AT1G65490	1.197	0.018323812
AT1G52040	1.109	0.018324108
AT5G06720	2.480	0.018407643
AT1G69720	1.061	0.018900208
AT1G17750	1.276	0.019758966
AT1G64200	1.350	0.019758966
AT4G15100	3.727	0.019758966
AT5G48400	1.066	0.020382223
AT4G25070	1.000	0.020438299
AT1G71390	1.457	0.020479293
AT4G01895	1.351	0.020581249
AT2G32190	1.578	0.020625041
AT4G11470	2.317	0.021005063
AT5G07990	1.361	0.021005063
AT1G26761	1.030	0.021010615
AT3G04640	1.148	0.021113121
AT1G09070	1.096	0.021179723
AT5G59820	1.824	0.021642588
AT1G32910	4.166	0.021898413
AT1G02460	1.408	0.02218346
AT1G71400	1.040	0.02229969
AT1G47510	2.346	0.02232793

**Table B.2 (cont'd)**

AT5G24150	1.886	0.022358604
AT1G74930	1.979	0.022436626
AT1G74430	1.517	0.02332351
AT2G29110	1.261	0.02386714
AT2G02990	1.781	0.023903939
AT5G26260	2.375	0.024425043
AT2G46660	1.383	0.024465549
AT3G43250	3.230	0.024475245
AT5G02780	1.221	0.024603792
AT5G43890	1.775	0.024753364
AT2G34960	1.621	0.02482811
AT4G38420	1.257	0.02505058
AT1G61560	1.342	0.025507464
AT5G64510	1.681	0.025507464
AT5G14760	1.031	0.025587569
AT4G18630	1.384	0.025824186
AT1G21550	1.699	0.025884338
AT4G09750	1.185	0.027590227
AT4G04840	1.452	0.027590536
AT1G54020	1.955	0.028650351
AT3G61990	1.062	0.028886744
AT5G13220	2.071	0.029154052
AT3G46660	2.385	0.029163382
AT4G08870	2.255	0.029452164
AT1G73540	1.228	0.029477841
AT2G15220	1.408	0.030136348
AT5G01100	1.696	0.030470925
AT3G23250	1.958	0.030871281
AT2G37040	1.280	0.031227732
AT3G46700	2.072	0.031227732
AT1G61110	4.671	0.031272639
AT5G01380	2.249	0.031276579
AT4G27030	1.384	0.032204858
AT1G26390	1.180	0.032256511
AT2G38995	1.054	0.032256511
AT1G75000	1.231	0.033051559
AT2G29170	1.442	0.033200064
AT5G17350	3.334	0.033798518
AT4G05100	1.850	0.033847513
AT4G03610	1.485	0.034096645
AT5G21280	1.243	0.034329906
AT4G23310	1.133	0.034511512
AT1G66465	1.380	0.034801591
AT4G30450	1.556	0.034801591

**Table B.2 (cont'd)**

AT5G01550	1.349	0.034808017
AT2G47550	1.930	0.035927395
AT5G05580	1.168	0.036149668
AT4G29780	1.721	0.036189168
AT1G52410	1.100	0.036203404
AT3G27690	1.300	0.036447155
AT3G28540	1.128	0.036449784
AT4G24010	1.499	0.036489541
AT3G09960	1.246	0.036757543
AT5G45630	2.568	0.03676456
AT1G67000	1.162	0.037216663
AT3G46650	2.300	0.037798987
AT1G52400	6.799	0.038045982
AT5G39090	1.046	0.038168774
AT3G20370	2.134	0.038848318
AT3G53830	1.165	0.039185221
AT4G17660	1.678	0.039185221
AT4G23600	1.394	0.039783533
AT1G77520	1.911	0.039878094
AT4G30460	1.025	0.040164065
AT4G24340	2.336	0.040931675
AT2G30020	1.265	0.041203854
AT2G22500	1.227	0.041488048
AT5G43170	1.117	0.041626512
AT1G33960	1.379	0.041747013
AT4G24130	1.057	0.041885481
AT5G24770	2.807	0.042557202
AT4G37400	1.349	0.042890695
AT4G39030	1.226	0.042890695
AT1G68620	1.121	0.04410613
AT2G43510	1.438	0.044526605
AT1G11580	1.273	0.044736322
AT1G44130	1.533	0.046285383
AT4G39320	1.954	0.046545461
AT1G66700	1.240	0.046770224
AT5G51465	1.292	0.046878928
AT4G23680	1.909	0.04726966
AT5G11920	1.245	0.04751087
AT1G32350	1.281	0.047772193
AT1G45191	1.161	0.048568193
AT2G46400	1.164	0.048671733
AT3G49340	1.371	0.04891709
AT2G21650	1.402	0.048996152
AT1G45616	2.346	0.049332487

**Table B.2 (cont'd)**

<i>Down-Regulated</i>		
AT4G39730	-6.174	1.77E-124
AT3G20810	-3.306	1.21E-45
AT5G23050	-1.360	1.91E-26
AT1G78970	-1.096	8.53E-22
AT4G33980	-3.146	2.81E-20
AT2G40080	-2.731	8.59E-19
<b>AT2G21660</b>	-1.411	1.28E-17
AT3G09390	-1.157	1.31E-16
AT4G27130	-1.094	1.55E-16
AT1G04620	-1.902	4.39E-15
AT1G17665	-2.224	1.17E-14
AT1G68050	-1.653	5.23E-14
AT3G46640	-2.092	5.93E-14
AT3G47860	-1.152	1.53E-13
AT3G05880	-1.428	5.79E-13
AT5G24580	-1.429	8.18E-13
AT2G15890	-1.254	1.60E-11
<b>AT1G28330</b>	-1.924	2.18E-11
AT4G12520	-3.723	2.75E-11
AT5G61380	-1.441	2.75E-11
AT5G23240	-1.252	1.83E-10
AT2G33830	-2.081	5.01E-10
AT2G05540	-2.234	5.84E-10
AT5G48250	-1.498	2.18E-09
AT1G75750	-3.305	2.53E-09
AT4G14130	-5.425	2.63E-09
AT2G23910	-3.356	8.45E-09
AT1G12710	-1.075	1.61E-08
AT3G50120	-1.856	9.37E-08
<b>AT3G29370</b>	-1.711	1.29E-07
AT1G77210	-8.172	3.39E-07
AT1G76490	-1.031	5.37E-07
<b>AT2G05380</b>	-1.715	6.28E-07
AT1G26665	-1.085	6.58E-07
AT1G22740	-1.535	6.90E-07
AT4G32340	-1.248	9.63E-07
AT1G06080	-3.595	1.21E-06
AT1G12080	-1.846	3.62E-06
AT1G67265	-2.013	4.63E-06
AT1G02340	-1.294	5.41E-06
AT1G64660	-1.443	7.59E-06
AT1G11545	-1.125	9.07E-06
AT2G44130	-1.223	9.96E-06

**Table B.2 (cont'd)**

AT5G14920	-1.137	3.08E-05
AT2G02100	-1.417	3.10E-05
AT5G66052	-1.353	3.29E-05
AT1G12010	-1.186	4.13E-05
AT5G44260	-1.218	5.09E-05
AT3G60530	-1.071	6.16E-05
AT1G49210	-1.645	0.000122363
AT2G38465	-1.349	0.000149297
AT3G61160	-1.460	0.000150266
AT2G22980	-1.042	0.000155372
AT2G47780	-1.725	0.00017139
AT5G63810	-1.164	0.00017425
AT4G35770	-2.168	0.000179471
AT5G21940	-1.256	0.000179471
AT1G12730	-1.128	0.000181361
AT2G40340	-1.757	0.000233163
AT3G61260	-1.007	0.000235874
AT1G04310	-1.034	0.000340366
AT1G08500	-1.483	0.000485179
AT5G56550	-1.463	0.000489645
AT5G49450	-1.148	0.000713278
AT1G49130	-1.489	0.000748307
AT5G62670	-1.126	0.000824656
AT1G07050	-1.950	0.000937867
AT1G54740	-1.651	0.001256042
AT5G02540	-2.043	0.001287103
AT3G45300	-1.385	0.001336269
AT3G21260	-1.408	0.001635921
AT4G39070	-1.720	0.002095562
AT4G01335	-2.331	0.002105603
AT2G33810	-1.164	0.002138841
AT5G03120	-1.186	0.002244365
AT3G02040	-1.117	0.00243329
AT5G53980	-3.346	0.002543645
AT1G68110	-1.056	0.00257413
AT3G62570	-1.165	0.00257413
AT5G25475	-1.059	0.002814338
AT3G51400	-1.119	0.003253182
AT1G80420	-1.507	0.003255557
AT1G11740	-2.552	0.003376161
AT1G32170	-1.274	0.00346816
AT4G15760	-1.091	0.003839812
AT1G22990	-2.215	0.004120366
AT4G31290	-1.235	0.005243703

**Table B.2 (cont'd)**

AT3G62090	-1.619	0.005358005
AT2G36270	-1.544	0.005449362
AT5G39240	-1.846	0.005672331
AT5G05890	-1.138	0.005923595
AT3G11020	-1.004	0.005949836
AT1G09980	-1.109	0.006035398
AT4G34138	-1.082	0.006165906
AT1G49200	-1.009	0.007046994
AT3G15620	-1.161	0.007134272
AT5G49360	-1.256	0.007311618
AT5G65730	-1.346	0.007373045
AT5G25240	-1.185	0.008254183
AT5G67480	-1.053	0.008860617
AT3G14360	-1.143	0.008880259
AT2G42170	-2.125	0.009149592
AT5G57550	-2.024	0.00929084
AT1G03010	-1.244	0.009661437
AT1G62770	-1.661	0.009865753
AT3G18530	-1.451	0.010994145
AT3G53530	-1.045	0.011698745
AT3G15450	-1.444	0.01235363
AT3G30720	-1.889	0.012977538
AT1G73830	-1.056	0.013908395
AT5G42200	-1.249	0.014983969
AT2G47270	-1.728	0.015616381
AT1G03090	-1.250	0.015900275
AT5G22500	-1.554	0.016426221
AT1G62480	-1.222	0.016725191
AT2G03640	-2.005	0.017596271
AT4G36450	-1.219	0.017858793
AT1G79700	-1.071	0.018688716
AT5G57655	-1.021	0.018941714
AT5G64190	-1.062	0.019487396
AT1G62510	-1.518	0.019758966
AT3G02410	-2.059	0.021005063
AT2G15880	-1.323	0.021504746
AT4G24050	-1.348	0.022837201
AT1G77330	-1.479	0.02386714
AT2G28200	-1.397	0.023898725
AT3G63470	-1.384	0.024475181
AT2G02930	-1.239	0.02505058
AT5G47590	-1.568	0.02505058
AT3G62950	-1.304	0.02546296
AT4G04630	-1.073	0.026048384

**Table B.2 (cont'd)**

AT2G15830	-1.136	0.026700656
AT4G27620	-2.844	0.027136384
AT1G27670	-2.766	0.027210269
AT2G40085	-1.326	0.028633801
AT3G15440	-2.973	0.030015138
AT3G26890	-1.138	0.030136348
AT5G57760	-1.211	0.031701808
AT3G13450	-1.068	0.032432464
AT3G26760	-1.101	0.033057097
<b>AT2G18050</b>	-1.395	0.033537052
AT1G62880	-1.046	0.033847513
AT5G06470	-1.128	0.034096645
AT2G17880	-1.112	0.037585224
AT1G74390	-6.571	0.038186242
AT5G44440	-5.097	0.039185221
AT4G36110	-1.004	0.039536869
AT1G52750	-1.356	0.039817697
AT1G44830	-1.269	0.040447459
AT5G20630	-1.444	0.040566263
AT5G51670	-1.021	0.040900641
AT1G07985	-1.697	0.041829323
AT1G28960	-1.425	0.047123989
AT4G21500	-1.177	0.048262378
<b>Knockdown Compared to Wild-Type (2022)</b>		
<i>Up-Regulated</i>		
AT1G32450	1.224	1.26E-05
<b>AT3G44970</b>	1.702	1.59E-05
AT4G08300	1.249	1.59E-05
AT3G16670	1.049	0.000140647
AT5G48850	1.385	0.000584005
AT5G24150	1.341	0.001252414
AT5G24660	1.230	0.002081373
AT1G06830	1.084	0.002264041
AT4G21990	1.026	0.003779422
AT1G09240	1.043	0.005555076
<b>AT3G22840</b>	1.331	0.006390589
AT4G01080	1.435	0.008569993
AT5G02230	1.002	0.009620538
AT1G62180	1.120	0.009682691
AT1G02820	1.243	0.012697899
AT5G62730	2.348	0.012697899
AT2G18210	1.281	0.012710739
AT3G23510	1.259	0.018444225
AT3G60260	7.133	0.023533331

**Table B.2 (cont'd)**

AT2G03505	6.636	0.02664438
AT1G16400	1.193	0.028827612
AT5G65080	2.712	0.03712315
AT5G13950	6.389	0.037660008
AT4G15680	1.312	0.038810658
AT5G65070	1.284	0.038833714
AT3G18710	1.028	0.039088501
AT1G78990	1.147	0.044590547
AT3G28840	1.325	0.045563488
AT5G13170	3.847	0.045637452
AT2G36790	1.149	0.049997186
<i>Down-Regulated</i>		
AT3G42670	-31.070	2.44E-10
AT4G32420	-30.308	6.56E-10
AT4G28830	-7.696	9.72E-05
AT3G62800	-6.536	0.016603835
AT4G39730	-3.853	3.52E-163
AT2G26020	-3.722	0.023618873
AT5G61160	-3.565	0.017678169
AT5G52390	-3.212	0.021238008
AT5G64750	-3.070	0.040742566
AT5G51465	-2.766	0.023482703
AT1G65510	-2.764	0.037089458
AT3G54730	-2.759	0.030329555
AT5G15960	-2.604	0.004950857
AT5G10100	-2.395	0.031041891
AT4G28140	-2.391	0.034379805
AT1G06160	-2.313	0.031041891
AT1G16850	-2.285	0.023533331
AT4G05100	-2.253	0.044185943
AT5G57010	-2.208	0.048514005
AT5G50335	-2.176	0.000843656
AT1G73810	-2.120	0.03409979
AT1G14870	-2.084	0.027507371
AT2G26400	-2.076	0.000140647
AT4G22470	-2.073	0.012697899
AT3G55500	-2.056	0.049598026
AT3G47340	-2.055	0.04981762
AT5G26690	-2.022	0.003286377
AT5G25110	-1.938	0.016958867
AT2G18050	-1.859	0.012272611
AT4G04500	-1.855	0.032985724
AT1G18710	-1.810	0.006350811
AT1G10070	-1.754	0.031132377

**Table B.2 (cont'd)**

AT3G50970	-1.751	0.030879173
AT5G08240	-1.742	0.046747452
AT2G19800	-1.720	0.000147797
AT5G52760	-1.711	0.006237069
AT3G29370	-1.679	0.011100116
AT3G20395	-1.640	0.049145819
AT3G05660	-1.613	0.01850543
AT5G54190	-1.572	9.72E-05
AT1G12160	-1.550	0.000430806
AT4G12850	-1.537	0.021117344
AT5G44260	-1.530	0.027507371
AT1G08890	-1.524	0.005130525
AT4G22517	-1.521	1.93E-06
AT5G63580	-1.514	0.004925143
AT1G34420	-1.489	0.039848026
AT1G28330	-1.411	0.011900566
AT1G03010	-1.399	0.027507371
AT1G09350	-1.389	5.94E-06
AT3G16565	-1.347	0.025118109
AT1G20440	-1.330	0.042176503
AT1G22250	-1.328	0.00084792
AT5G23980	-1.321	0.02985818
AT1G13670	-1.291	0.034390112
AT4G22513	-1.269	6.00E-05
AT3G25020	-1.268	1.09E-05
AT2G37130	-1.267	0.004049243
AT2G43620	-1.247	0.038178195
AT4G10500	-1.229	0.038833714
AT4G21850	-1.227	0.031132377
AT3G05727	-1.207	0.010903561
AT2G44790	-1.206	0.011143242
AT4G38530	-1.195	0.013335546
AT2G42870	-1.194	0.038178195
AT5G64110	-1.191	0.016658813
AT2G05380	-1.188	1.38E-06
AT1G14170	-1.181	0.003807072
AT2G21660	-1.179	3.51E-05
AT4G27260	-1.176	0.044955613
AT4G32280	-1.169	0.022471724
AT5G55450	-1.162	6.65E-05
AT1G76970	-1.152	0.010208383
AT1G01010	-1.077	0.023156826
AT1G45145	-1.058	0.041196258
AT5G64000	-1.055	0.044551219

**Table B.2 (cont'd)**

AT3G26200	-1.046	0.00799152
AT5G09440	-1.042	0.034626527
AT5G44568	-1.033	0.030509909
AT4G18253	-1.007	0.044590547
AT3G23010	-1.000	0.039878121
<b>AOX3 Compared to Wild-Type</b>		
<i>Up-Regulated</i>		
AT4G39730	4.564	4.22E-261
AT2G20890	1.261	2.62E-25
AT1G14360	1.056	5.75E-14
AT3G30720	2.839	6.44E-08
AT1G53480	6.122	1.29E-07
AT4G03157	7.564	0.000128279
AT4G03156	6.883	0.000283038
AT5G64510	1.559	0.000283038
AT4G08300	1.135	0.002381342
AT1G04980	1.082	0.002384818
AT1G26390	3.090	0.017461513
AT3G44970	1.341	0.02509929
AT5G18937	1.620	0.030234535
<i>Down-Regulated</i>		
AT5G39040	-7.326	6.59E-48
AT1G75945	-4.938	1.18E-13
AT1G64795	-7.104	5.39E-12
AT4G02660	-9.099	1.49E-05
AT4G32420	-21.287	0.002384818
AT2G19800	-1.576	0.009808098
AT3G42670	-18.826	0.020283725
AT4G22513	-1.019	0.036093331
AT5G41080	-1.191	0.04092085
<b>AOX5 Compared to Wild-Type</b>		
<i>Up-Regulated</i>		
AT4G03157	7.452	2.83E-05
AT4G03156	7.040	3.68E-05
AT4G04601	6.520	0.013261736
AT1G53480	6.331	1.77E-10
AT4G39730	5.032	0
AT3G45290	4.831	3.04E-78
AT5G65080	3.766	0.000773524
AT3G63380	3.357	0.017568397
AT3G30720	3.208	1.05E-13
AT1G26390	2.846	0.007780671
AT5G64510	2.388	8.02E-16

**Table B.2 (cont'd)**

AT4G12490	2.386	0.000254435
AT1G66700	2.240	0.021862002
AT3G28510	2.122	0.026860113
AT1G04980	1.722	1.34E-13
AT1G14360	1.671	6.04E-49
AT5G18937	1.567	0.006870704
AT2G02810	1.436	1.68E-14
AT3G23510	1.390	0.008926661
AT1G65040	1.331	2.03E-48
AT1G51820	1.317	0.01587942
AT5G42020	1.297	3.61E-14
AT3G29631	1.258	0.000266542
AT5G61790	1.237	4.90E-13
AT5G28540	1.176	1.57E-11
AT5G03160	1.155	3.94E-19
AT3G16670	1.138	9.03E-06
AT4G29520	1.091	1.01E-07
AT3G62600	1.075	4.29E-30
AT1G56340	1.008	4.90E-13
AT2G25110	1.001	2.66E-14
<i>Down-Regulated</i>		
AT1G75945	-5.002	6.13E-20
AT1G64795	-7.218	2.01E-17
AT4G22517	-1.440	4.17E-06
AT4G22513	-1.210	0.000109429
AT1G08940	-1.261	0.001771274
AT4G08950	-1.279	0.00331178
AT1G18710	-1.827	0.007780671
AT5G49280	-1.019	0.008583773
AT5G38940	-1.349	0.010199932
AT1G34580	-1.640	0.012720047
AT2G02790	-5.970	0.022571534
AT1G65310	-1.261	0.02982813
AT2G42170	-1.496	0.040572096
AT3G05140	-1.538	0.04146869

**Appendix C.**

**Supplemental Data for Chapter 4**

**Table C.1: GoldenBraid Cloning Primers for Optogenetics Constructs**

Gene Name	Primer Sequences	Amplicon Size (bp)	Annealing Temp (°C)
Level 0			
tagRFP-Flag	F: 5'-ttgaagacttaggtatggtgtctaagggcga-3' R: 5'-ttgaagacttaagcttactgtcatcgatccttgaatcattaagttgtg-3'	766	62
eYFP-His	F: 5'-ttgaagacttaggtatggtgagcaagggc-3' R: 5'- ttgaagacttaagctaGTGATGATGATGATGATG ctgtacagctcgccat-3'	766	66
eYFP-HA	F: 5'-ttgaagacttaggtatggtgagcaagggc-3' R: 5'- ttgaagacttaagctaagcgtaatctg gaacatcgatgggtactgtacagctcgccat-3'	775	66
mCerulean-HA	F: 5'-ttgaagacttaggtatggtgagcaagggc-3' R: 5'-ttgaagacttaagctaagcgtaatctggaac atcgatgggtactgtacagctcgccat-3'	775	66
Phloem Lipid-Associated Family Protein (PLAFP, AT4G39730)	F: 5'-ttgaagacttaatggctcgctcgca-3' R: 5'- ttgaagacttacctccaacgaccaagaaagctt-3'	570	62
GRIP1, AT1G09310	F: 5'-ttgaagacttaatgggttggttacagagg-3' R: 5'-ttgaagacttacctccggccgcctcttgac-3'	564	55
Rhomboid Like Protein 10 (RBL10, AT1G25290.2)	F: 5'-ttgaagacttaatggtatcagtgtcattatctc-3' R: 5'-ttgaagacttacctccaagccgtcgctgttc-3'	1035	66
<i>Glycine max</i> Flowering Locus T 2a (GmFT2a)	F: 5'-TTGAAGACTTAATGCCTAGTGGAAGTAGG-3' R: 5'-ttgaagacttacctccgtataacctcctccacca-3'	555	51
Q5 Site-Directed Mutagenesis			
PLAFP (pDGB1α1)	F: 5'- GAGGTTTAAACGATTGAATAT-3' R: 5'-CTGAGACGAAGCTTGTTAC-3'	-	59
Arabidopsis Genotyping Primers			
PLAFP_F/Flag_R	F: 5'-ccttaaactaacctccgatgg-3' / R: 5'-cttgtcatcgatccttgaatc-3'	983	51
VP16_F/RFP_F	F: 5'-cagatcggactaggtaaa-3' / R: 5'-ggcttcacatgggagagag-3'	1439	51
SDRX_F/EL222_R	F: 5'-atgacaacaatgccccgcc-3' / R: 5'-agattccggcttcgac-3'	682	51

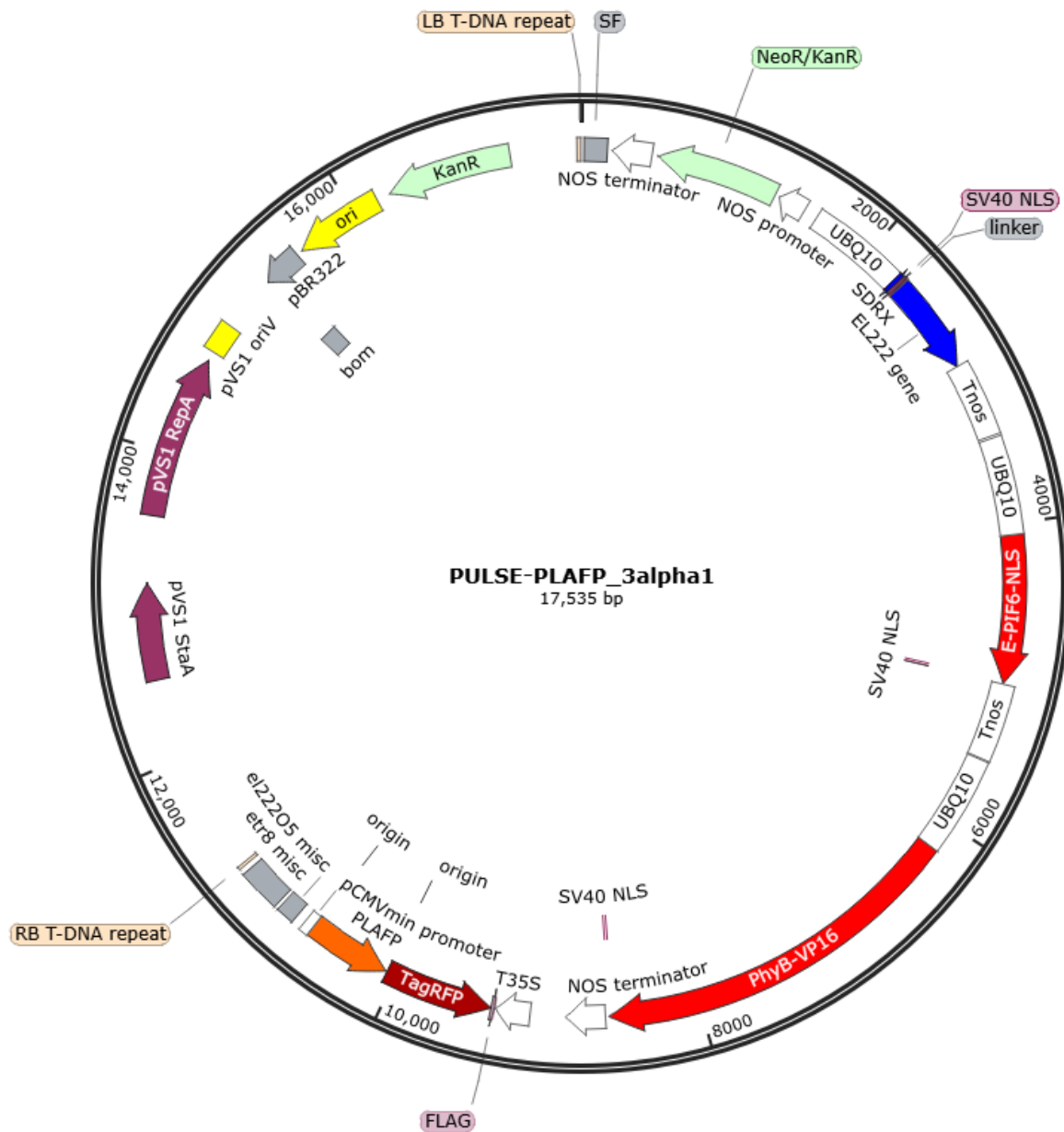


**Figure C.1 Plasmid Map of Final PULSE-PLAFP Construct in GB3 $\alpha$ 1 Vector.** Phloem Lipid Associated Family Protein (PLAFP, orange) fused to TagRFP-Flag (dark red) is downstream of the pOpto promoter (etr8, el22205, pCMVmin). The activator modules (red), E-PIF6-NLS and PhyB-VP16, and the repressor module (blue), NLS-SDRX-EL222, are constitutively expressed by a UBQ10 promoters.

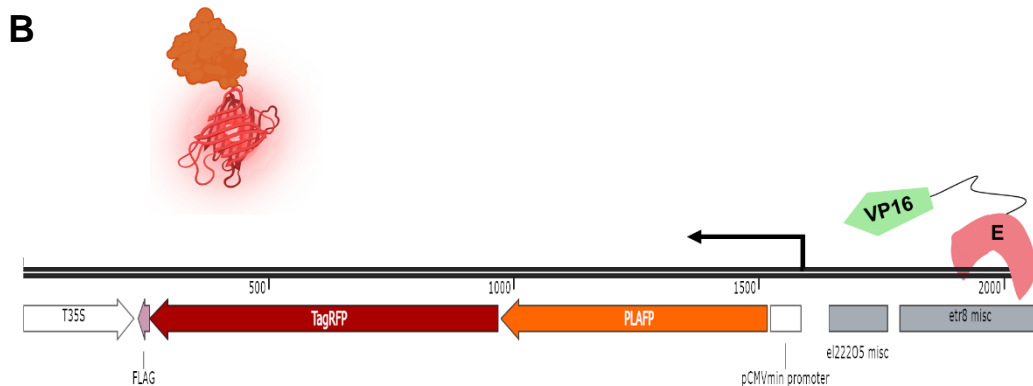
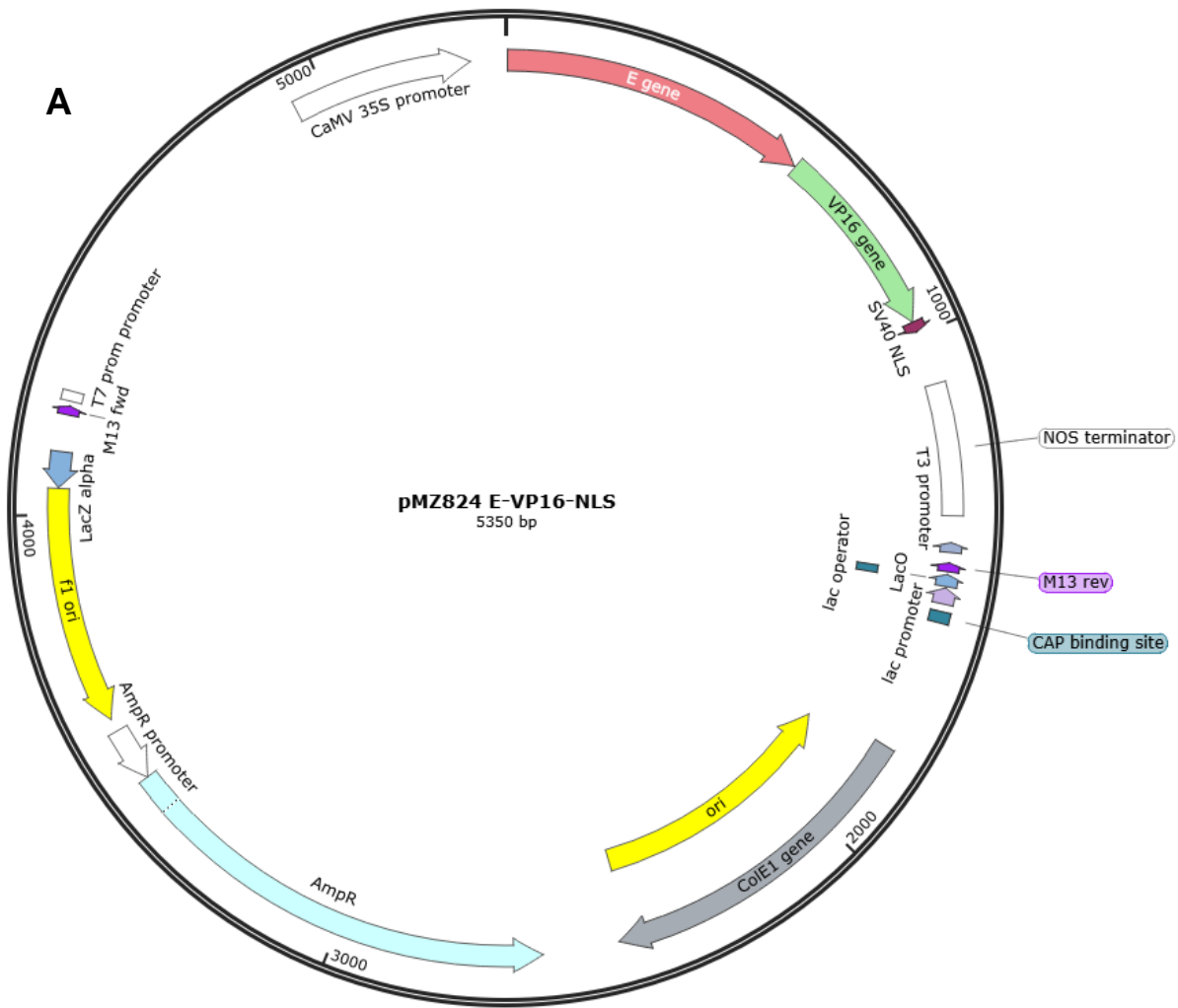


**Figure C.2 Constitutive Activation of pOpto Promoter in Protoplasts.** To test the functionality of the pOpto promoter, pMZ824 (A) is co-transfected with pOpto constructs into protoplasts. The DNA-binding component E protein (pink) is fused to the transactivator VP16 (green), so the experiment is light independent. The activator interacts with the *etr8* component of the pOpto promoter, and PLAFP-RFP fluorescence is detected (B). Created, in part, with [BioRender.com](https://www.biorender.com).

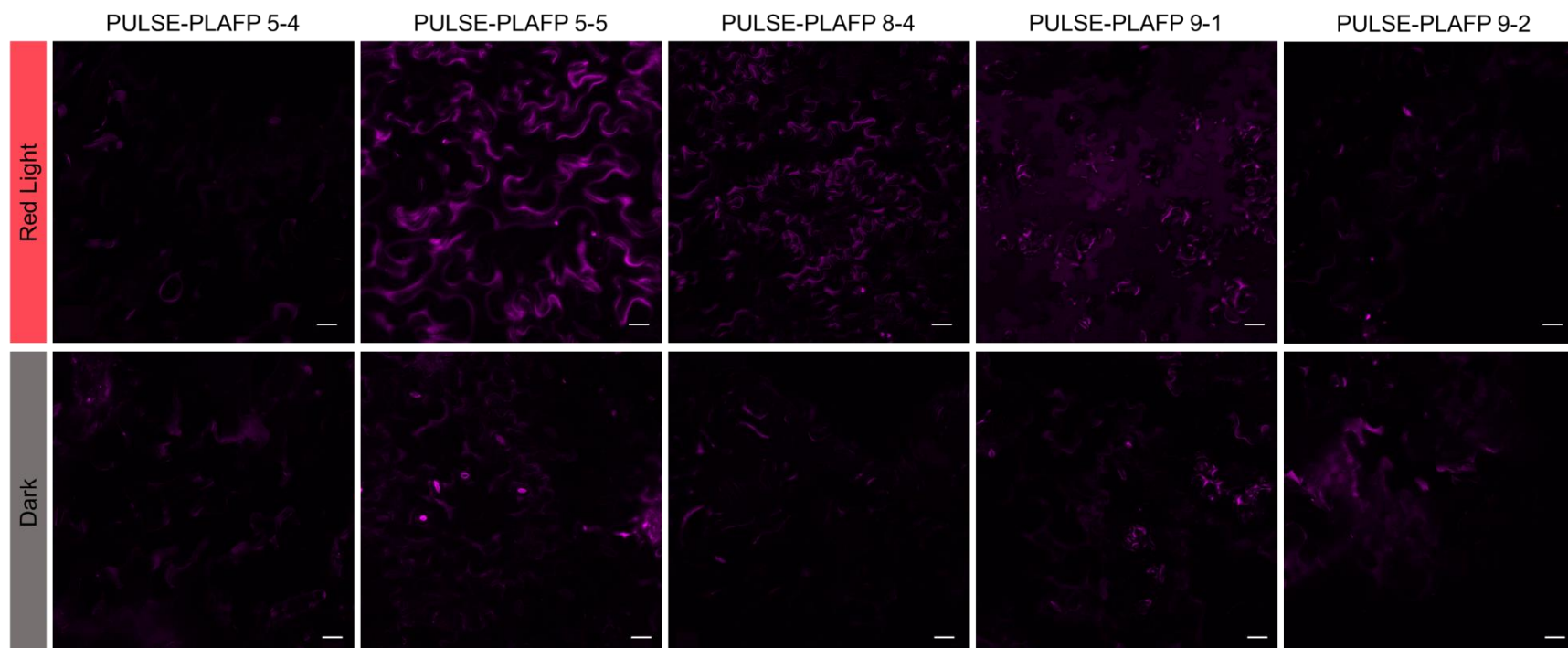


**Figure C.3 Assessment of PULSE-PLAFP Expression in Transgenic Arabidopsis Lines.** PULSE-PLAFP transgenic plants (T2, confirmed by genotyping) were left in the dark or exposed to red light ( $40\mu\text{mol m}^{-2} \text{s}^{-1}$ ) in Trichromatic Percival chambers for 2 hours. Confocal microscopy was used to assess PLAFP-RFP production. Independent lines 5-5 and 8-4 were selected as the most efficiently activated. Scale bar represents 20  $\mu\text{m}$ .